Establishment of interaction partners of *Plasmodium falciparum* heat shock protein 70-x (PfHsp70-x)

A thesis submitted in fulfilment of the requirements for the degree of

MASTER OF SCIENCE IN BIOCHEMISTRY

SCHOOL OF MATHEMATICS AND NATURAL SCIENCES

UNIVERSITY OF VENDA

by

MONYAI FLORINA SEMAKALENG

11594736

Supervisor: Prof. A. SHONHAI

Co-supervisor: Dr T. ZININGA

February 2018

Abstract

Plasmodium falciparum is a unicellular protozoan parasite that causes malaria in humans. The parasite is passed to humans through mosquito bites and migrates to the liver before it infects host erythrocytes. It is at the erythrocytic stage of development that the parasite causes malaria pathology. Malaria is characterized by the modification of host erythrocytes making them cytoadherent. This is as a result of formation of protein complexes (knobs) on the surface of the erythrocyte. The knobs that develop on the surface of the erythrocyte are constituted by proteins of host origin as well as some proteins that the parasite 'exports' to the host cell surface. Nearly 550 parasite proteins are thought to be exported to the infected erythrocyte. Amongst the exported proteins is *P. falciparum* heat shock protein 70-x (PfHsp70-x). Hsp70 proteins are known to maintain protein homeostasis. Thus, the export of PfHsp70-x may be important for maintaining protein homeostasis in the host cell. PfHsp70-x is not essential for parasite survival although is implicated in the development of parasite virulence. This is possibly through its role in facilitating the trafficking of parasite proteins to the erythrocyte as well as supporting the formation of protein complexes that constitute the knobs that develop on the surface of the infected erythrocyte. The main objective of the current study was to investigate protein interaction partners of PfHsp70-x. It is generally believed that PfHsp70-x interacts with various proteins of human and parasite origin. Potential candidate interactors include its protein substrates, Hsp70 co-chaperones such as Hsp40 members, and human Hsp70-Hsp90 organizing protein (hHop). The establishment of the PfHsp70-x interactome would highlight the possible role of PfHsp70-x in the development of malaria pathogenicity. Based on bioinformatics analysis, PfHsp70-x was predicted to interact with some exported *P. falciparum* Hsp40s, hHop and human Hsp90 (hHsp90). Recombinant forms of PfHsp70-x (full length and a truncated form that lacks the C-terminal EEVN motif implicated in co-chaperone binding) were expressed in *E. coli* BL21 Star (DE3) cells. Recombinant hHop and hHsp70 were expressed in *E. coli* JM109 (DE3) cells. The proteins were successfully purified using nickel affinity chromatography. Co-affinity chromatography using recombinant PfHsp70-x and immuno-affinity chromatography using PfHsp70-x specific antibody did not confirm the direct interaction of PfHsp70-x with human Hop. However, the direct interaction of hHop and PfHsp70-x has previously been validated *in vitro* and the current bioinformatics data support

the existence of such a complex. PfHsp70-x was not stable in the cell lysate that was prepared and this could explain why its interaction with hHop could not be ascertained. However, taken together the evidence from a previous independent study, and the predicted interaction of PfHsp70-x with human chaperones suggests cooperation of chaperone systems which possibly facilitates the folding and function of parasite proteins that are exported to the infected erythrocyte.

Key words: Malaria, *P. falciparum*, PfHsp70-x, human chaperones, human Hop, chaperone networks, interaction partners, protein-protein interactions.

Declaration

I, Florina Smakaleng Monyai, declare that this thesis submitted to the University of Venda for a Master of Science degree in Biochemistry under the department of Biochemistry in the School of Mathematics and Natural Sciences is my own unaided work, with the exception of citations, and that this work has not been submitted to any other institution for award of any degree.

Signature: …….

Date: .....

Dedication

This thesis is dedicated to the Lord Jehovah, my parents (Monyai Merriam and Monyai Andries), siblings and Minana MM.

Acknowledgements

I give thanks to God for giving me the strength to complete this study. I would like to extend my gratitude to my supervisor Prof. Addmore Shonhai for his patience, guidance, expertise and mentorship throughout the duration of the project. His support and encouragement imperatively made it possible for me to be part of this project.

I also wish to express my gratitude to my co-supervisor Dr. Tawanda Zininga for his support, mentorship, patience and guidance.

I also like to greatly thank Stanley Makumire for his guidance, encouragement and mentorship in the laboratory.

I would like also to appreciate Dr. Adelle Burger for her assistance and encouragement.

I wish to extend further acknowledgement to the following:

- National Research Foundation (NRF South Africa) for funding this research project
- University of Venda work study program for assisting with the tuition and accommodation expenses

Lastly, I would also like to express my gratitude to my lab mates, the ProBioM research team and the staff of the Biochemistry department (University of Venda) for their patience and moral support throughout this study.

Table of contents

List of Symbols and Abbreviations

Abbreviations of units	Symbol Interpretation
%	percent
µl	microliter
A_{600}	absorbance at 600 nanometres
bp	base pair
µM	micromolar
mM	milimolar
nm	nanometres
^oC	degree Celsius
ml	milliliter
L	liters
g/L	gram per liter
mg/ml	milligram per milliliter
µg/ml	microgram per liter
w/v	weight per volume
v/v	volume per volume
mg	miligram
µg	microgram
ng	nanogram
g	gram
β	beta
α	alpha
dH_20	deionized water
ER	endoplasmic reticulum
HPD	histidine-proline-asparatic acid
hHsp70	human heat shock protein 70
Hop	Hsp70-Hsp90 organizing protein
IPTG	isopropyl β-D-1 thiogalactopyranoside
kDa	kilo Daltons
NEF	nucleotide exchange factor
PMSF	Phenylmethylsulfonyl fluoride
PfEMP1	*Plasmodium falciparum* erythrocyte membrane protein 1
PEXEL	*Plasmodium* export element
PTEX	*Plasmodium* translocon of exported proteins
PV	parasitophorous vacuole
RESA	ring infected erythrocyte antigen
SBD	substrate binding domain
SDS-PAGE	sodium dodecyl sulphate polyacrylamide gel electrophoresis

List of Figures

List of Tables

Chapter 1

Introduction

1.1. Malaria

Malaria is a disease that is transmitted through bites from a female infected *Anopheles* mosquito. Human malaria is caused by parasitic protozoans of the *Plasmodium* genus (WHO, 2017). There are five species of *Plasmodium* that infect humans; namely, *P. falciparum, P. vivax, P. ovale, P. malariae* and *P. knowlesi* (WHO, 2017). *P. falciparum* is responsible for the most severe form of malaria, accounting for about 99 % of estimated cases globally and 80 % of deaths (WHO, 2017). In 2016, 216 million global cases were reported with 445 000 deaths of which most were children in sub-Saharan Africa (WHO, 2017). About 61 % of the infected population reported includes children aged less than 5 years (WHO, 2017). In 2015 alone, 303 000 (70.6%) deaths were estimated in children under 5 years of age worldwide (WHO, 2016). Children have an immune system that is not fully developed, hence, are the most vulnerable to be infected by malaria.

1.2. *P. falciparum* life cycle

The life cycle of *P. falciparum* involves two distinctive organisms, the human (host) and mosquito (vector) (Cox, 2010). During infection of humans, the female *Anopheles* mosquito acts as a transmission vector for a motile infective form of the parasite (sporozoites) to a vertebrate host (Figure 1.1). The life cycle begins when the infected mosquito feeds and injects the sporozoites from its salivary glands into the human bloodstream (Figure 1.1). The sporozoites circulate in the blood system and subsequently find their way to the liver. In the liver, the sporozoites invade and infect the liver cells (also known as hepatocytes). The sporozoites undergo the first cycle of the asexual replication producing merozoites which leads to the initiation of malarial pathogenicity (Nilsson *et al*., 2015).

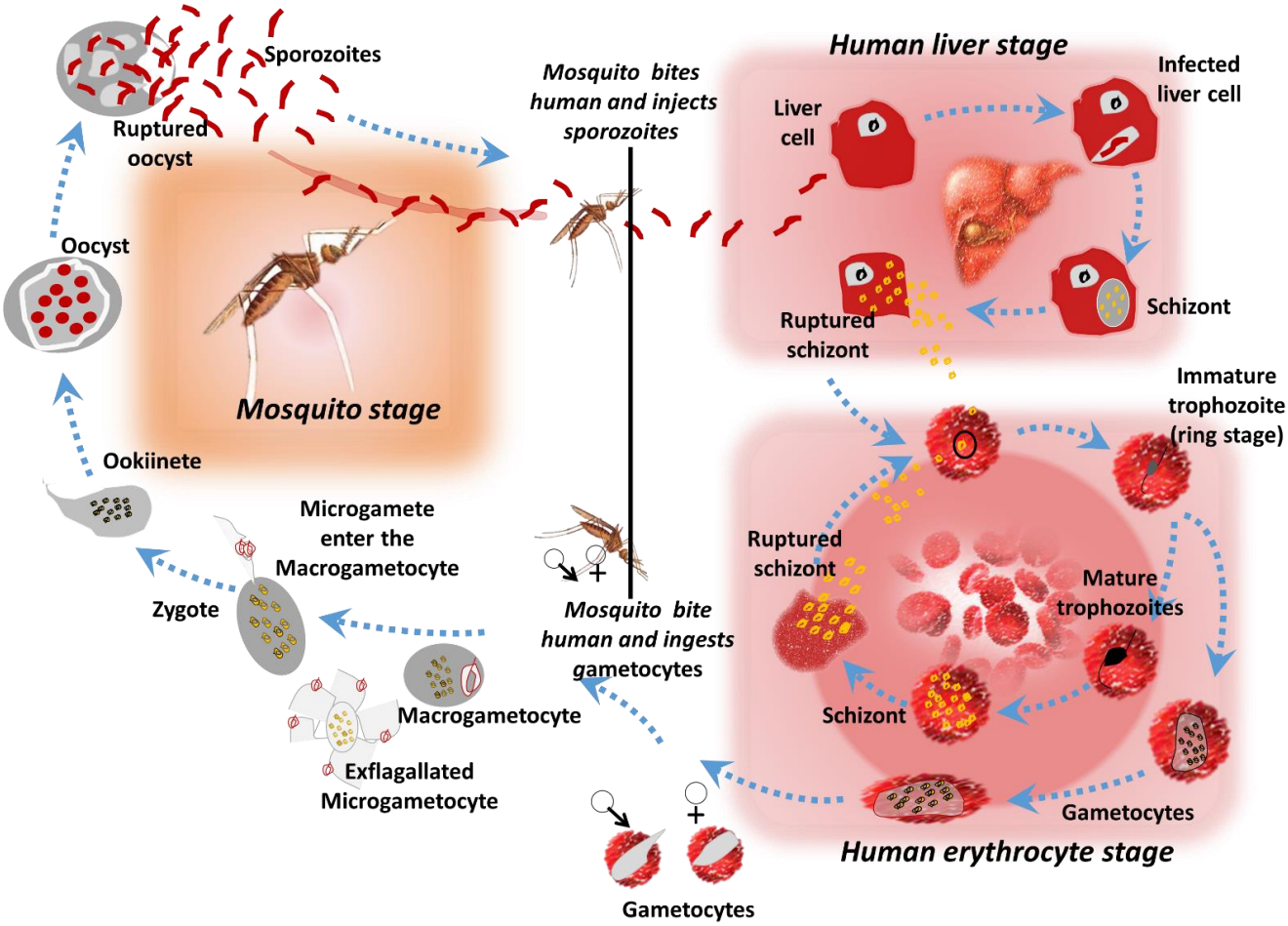

Figure 1.1: *P. falciparum* life cycle
The figure shows the female *Anopheles* mosquito injects infectious parasite *P. falciparum*. Sporozoites that enter the human host and subsequently infect the liver cells (human liver stage). The liver cells ruptures releasing schizonts into the blood stream initiating the human erythrocyte stage. Some of the schizonts commence the erythrocyte invasion cycle, while others differentiate into sexual forms, gametocytes. Gametocytes (macro- and microgametes) are ingested by the uninfected mosquito during blood meals and get fertilized in the midgut forming a zygote (mosquito stage). The zygote undergoes developmental stages leading to the production of sporozoites. The sporozoites are transmitted to an uninfected human host during the next blood meal. Figure adapted from Nilsson *et al. (*2015).

In the hepatocytes, the sprozoites mature into merozoites and multiply producing many uninucleated merozoites (schizonts). The schizonts rupture and release the merozoites into the blood stream (Figure 1.1; Eaton *et al.,* 2012). The merozoites attach to uninfected erythrocytes priming for invasion. Within the erythrocytes, the merozoites undergo three stages of development from ring, then trophozoite and finally the schizont (Figure 1.1; Bannister, 2001). The infected erythrocyte eventually ruptures, releasing more mature schizonts (merozoites) into the blood circulation and these invade uninfected erythrocytes

and commence another asexual replication cycle (erythrocytic stage, Figure 1.1). This is responsible for the periodic fever episodes (Bousema *et al.,* 2016).

During each erythrocytic cycle a subset of the merozoites (at the ring stage) replicates into sexual progeny that differentiates and develop into gametocytes, including microgametes (male) and macrogametes (female). The microgametes and macrogametes circulate in the peripheral blood. The gametocytes are ingested by the female *Anopheles* mosquito into the mosquito's midgut (mosquito stage) as it takes up a blood meal. In the midgut, the gametes mature and undergo sexual fertilization, and the microgamete enters the macrogamete forming a zygote (Figure 1.1). The zygote later develops into motile invasive ookinetes, which migrate and penetrates the gut wall. Ookinetes further develop into oocysts and subsequently into several sporozoites. The oocyst ruptures and release sporozoites that are motile. The sporozoites migrate through the mosquito haemocoele and are deposited into the salivary glands. The sporozoites are then transmitted into an uninfected human host during another blood meal, continuing the life cycle.

1.3. *P. falciparum* host erythrocyte invasion

The erythrocyte offers an environment suitable for parasite development. The parasite invades the erythrocyte eventually leading to host cell rupture. Upon leaving the ruptured infected erythrocytes, the extracellular egg-shaped merozoites initiate invasion (Cowman *et al.,* 2012). The merozoites recognize and adhere to the membrane surface of uninfected erythrocytes (Figure 1.2; Weiss *et al.,* 2015). The merozoites roll and glide on the erythrocyte membrane reorientating to bring the apical end of the merozoite in contact with the erythrocyte membrane ensuring closer access to the erythrocyte (Figure 1.2). The merozoites possess special organelles, called micronemes, rhoptries and dense granules which secrete adhesins and membrane altering agents. This secretion ensures attachment of merozoites to erythrocytes and reorganize the membrane cytoskeleton facilitating invasion (Figure 1.2; Zuccala & Baum, 2011).

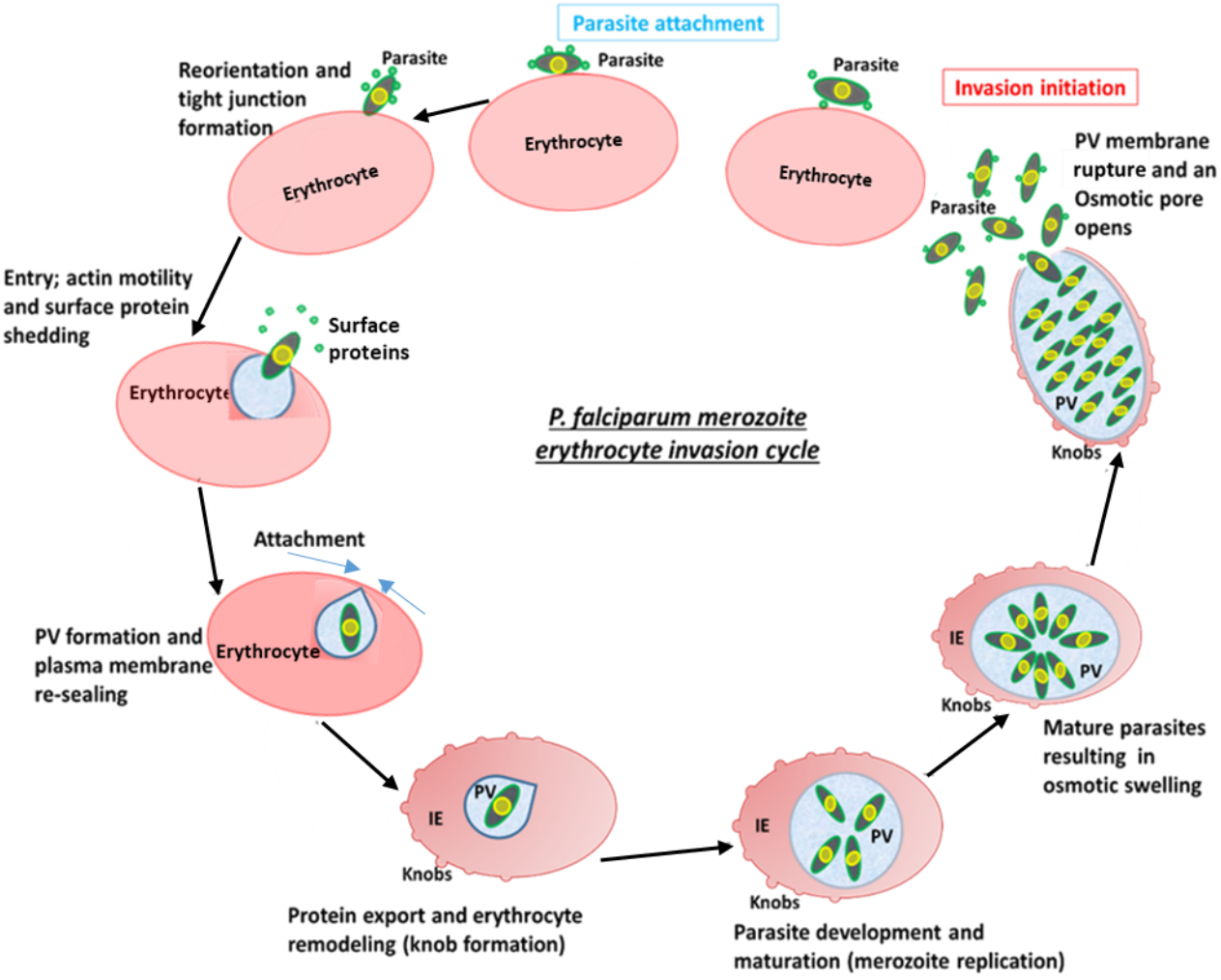

Figure 1.2: Merozoite erythrocyte invasion cycle
Merozoite attach to the erythrocyte membrane post-invasion. Parasite apically reorients and tightly attaches to the erythrocyte forming a tight junction (PfAMA-1-PfRON4 complex) and establishes entry point. During entry, the merozoite's surface proteins are shed through the activity of proteases (SUB1 and SUB2). At the same time, a parasitophorous vacuole is formed and include some erythrocyte membrane components. Once the tight junction reaches the posterior end of the parasite, the plasma membrane re-seals by an as-yet-unknown mechanism. The IE represent infected erythrocyte and PV; parasitophorous vacuole. Figure adapted from Cowman *et al.* (2012); Weiss *et al.* (2015).

Additionally, the merozoite apical organelles secrete two groups of proteins that form a complex which binds erythrocyte specific receptors and prompts invasion. For instance, the micronemes secrete the apical merozoite antigen 1 (AMA-1) protein and rhoptry secrete rhoptry neck protein 4 (RON4 protein) (Cowman *et al.,* 2012). These proteins associate and form a PfAMA-1-PfRON4 protein complex which forms a tight junction that create a bridge at the area of contact with the erythrocyte membrane (Riglar *et al.,* 2011). The tight junction occurs in association with the parasite's actin-myosin motor (also referred to as a gliding motor

machinery; Riglar *et al.,* 2011) which ensure erythrocyte capture. Furthermore, parasite utilize the tight junction (Zuccala and Baum, 2011; Weiss *et al.,* 2015) to enter into the erythrocyte with the assistance from the actin-myosin motor system. Merozoite parasite entry activates the actin-myosin causing the junction to move back from the apical membrane complex pulling the erythrocyte membrane as the parasite pushes into the erythrocyte until it is completely enclosed (Figure 1.2). More importantly, the merozoite microneme secretes serine proteases such as the subtilisin (SUB1 and SUB2). The proteases shed off the merozoite surface coating proteins during entry (Child *et al.,* 2010; Silmon de Monerri *et al.,* 2011). This leads to the parasite dragging the erythrocyte plasma membrane to cover its surface, forming a parasitophorous vacuole (PV; Figure 1.2). The PV eventually seals forming a PV membrane (PVM) that separates the parasite from the erythrocytic cytoplasm, creating a hospitable environment for parasite development. After entry and PV formation, the erythrocyte plasma membrane re-seals and returns to its original form. At this stage, the parasite is at the ring stage of development (Figure 1.2).

1.4*. P. falciparum* protein export

Following invasion, *P. falciparum* synthesizes proteins that are required for adaptation, growth and development within the infected erythrocytes. Most of the expressed proteins play a role in maintaining parasite proteostasis. Some of the *P. falciparum* proteins are exported into the erythrocyte's cytosol (Spielmann and Gilberger, 2010; 2015). Mature erythrocytes are anucleated and they lack protein export machinery (reviewed in Marti *et al.,* 2004, Proellocks *et al.,* 2016). Exported proteins play a major role in parasite survival and nutrients acquisition in the erythrocyte cytosol (Goldberg, 2012). The parasite lodged into the erythrocyte's cytosol establishes its own trafficking machinery to dispatch parasite derived proteins beyond its cell membrane into various destinations in the infected erythrocyte (Figure 1.3; Bullen *et al.,* 2012; Boddey *et al.,* 2016; Proellocks *et al.,* 2016).

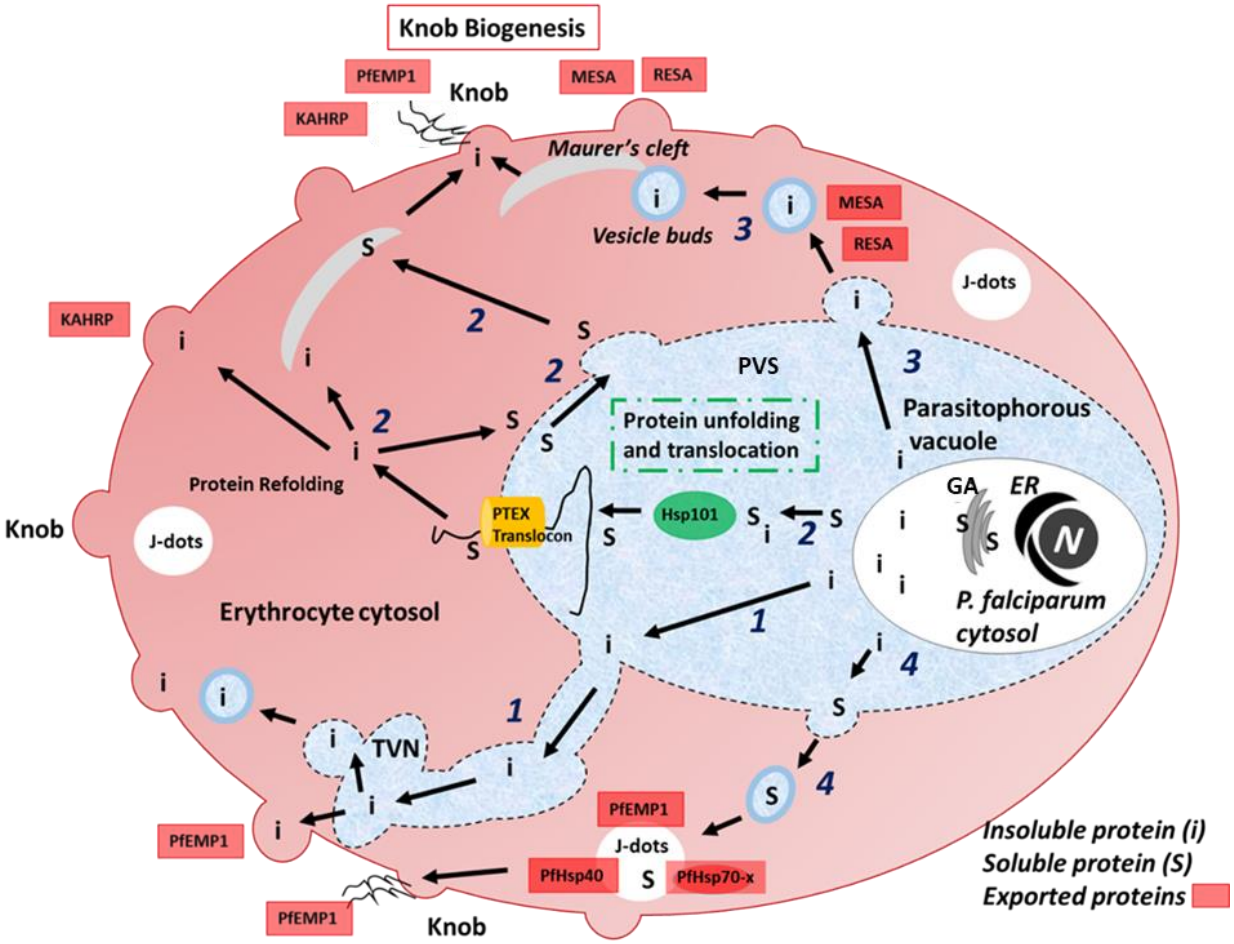

Figure 1.3: Export pathways of *Plasmodium*-encoded proteins to the infected erythrocyte
P. falciparum-encoded proteins are synthesized in the Nucleus (N) which are then exported into parasitophorous vacuolar space (PVS) through the Endoplasmic reticulum (ER) and Golgi apparatus (Ga). In the PVS proteins fuse with the parasitophorous vacuole (PV) membrane (PVM) generating different protein export channels. Four protein export pathways are known. (**1**) Membrane proteins fuse with PVM forming a tubular vascular network (TVN) trafficking pathway through lateral diffusion from vesicle budding from the TVN membrane. (**2**) *Plasmodium* translocon of exported proteins (PTEX) trafficking soluble proteins through the PVM to the Maurer's cleft and erythrocyte cytoskeleton. Soluble proteins that fail to refold in the cytosol are exported back to the PV through the PVM by diffusion where they get trafficked to the Maurer's clefts through membrane diffusion. (**3**) Insoluble proteins are trafficked by split cell diffusion that traffics post invasion; membrane; and knob-forming proteins through sub-cytosol compartments vesicle granules formed by PV membrane fusion. This channel traffics proteins to Maurer's cleft and erythrocyte surface where they form large aggregates (knobs). (**4**) Highly mobile small vesicles (J-dots) trafficking of soluble proteins through PVM fusion causeing membrane budding and deposit proteins to erythrocyte membrane. Figure adapted from Bullen *et al.* (2012).

Nearly 550 parasite proteins have been predicted to be exported to the infected erythrocyte's cytosol, cytoskeleton and plasma membrane (Maier *et al.,* 2008; Goldberg, 2012; Spielmann and Gilberger, 2015). Most of these proteins are exported from the endoplasmic reticulum (ER) through the PV beyond the PVM via four different pathways

(Figure 1.3; Boddey *et al.,* 2010; Sijwali and Rosenthal, 2010). Most but not all of these exported proteins are characterized by the presence of the ER export signal sequence located on the N-terminus (Boddey *et al.,* 2010). The ER export signal sequence is followed by an export motif termed the *Plasmodium* Export Element (PEXEL) also known as the host targeting signal (HT) or vascuolar transport signal (VT) (Hiller *et al.,* 2004; Marti *et al.,* 2004). This PEXEL motif facilitates transport of parasite-encoded proteins beyond the PVM (Hiller *et al.,* 2004; Marti *et al.,* 2004). Taken together this, it can be said that various signals are implicated in protein export into the erythrocytes cytosol.

PEXEL-containing proteins are characterized by a conserved five-residue pentameric consensus sequence RxLxE/Q/D (Bullen *et al.,* 2012). Exported PEXEL proteins primarily localize to the ER and possess a protease cleavage site (Boddey *et al.,* 2010) which is processed upon export. The PEXEL sequence is cleaved by the ER residing aspartic protease plasmepsin V after the L-x residues results in the establishment of a new N-terminus xE/Q/D which is then acetylated (Boddey *et al.,* 2010; Russo *et al.,* 2010; Boddey *et al.,* 2013). The acetylated sequence interacts with the PVM localized PEXEL-protein translocation machinery termed the PTEX (de Koning-Ward *et al.,* 2009). The role of the PTEX is to oversee protein export beyond the PVM into the erythrocyte cytosol (Figure 1.3; Boddey *et al.,* 2010, 2013). The PEXEL motif transports both soluble and surface-associated proteins (Grüring *et al.,* 2012). Protein export through the PTEX is ATP-dependent (Gehde *et al.,* 2009; Hasse and de Koning-Ward, 2010), and mainly export transmembrane proteins (Crabb *et al.,* 2010). The PEXEL-containing *P. falciparum* exported proteins, which have been documented, belong to five major families (Weng *et al.,* 2014; Proellocks *et al.,* 2016). Proteins from these families reside in the various compartments of the erythrocyte cytosol and surface membrane. For example, the *P. falciparum* erythrocyte membrane protein 1 (PfEMP1; Su *et al.,* 1995), a knob associated histidine-rich protein 1 (KAHRP; Pologe *et al.,* 1987), *P. falciparum* erythrocyte membrane protein 3 (PfEMP3; Pasloske *et al.,* 1993), a ring-infected erythrocyte surface antigen (RESA; Foley *et al.,* 1991) and the mature parasite-infected erythrocyte surface antigen (MESA; Coppel *et al.,* 2010).

Amongst the exported proteins, there is another group of exported parasite proteins that lack the PEXEL motif termed the PEXEL-negative exported proteins (PNEPs) (reviewed in Grüring *et al.,* 2012; Spielmann *et al.,* 2013). It is thought that PNEPs have a unique signaling motif, which suggests the utilization of an alternative export pathway (Marti and Spielmann, 2013). The PNEPs contain an N-terminal export signal peptide composed of 20 amino acids (Gruiring *et al.,* 2012; Heiber *et al.,* 2013). Export of this group of proteins is yet to be fully understood due to their structural complexity and the absence of valid sequence alignment data. However, only a few PNEPs have been reported. Amongst these PNEPs, are the skeleton-binding protein 1 (SBP1; Blisnick *et al.,* 2005), the membrane-associated histidine-rich protein (MAHRP1 and MAHRP2) (Spycher *et al.,* 2006; Pachlatko *et al.,* 2010), the ring exported proteins REX1 (Spielmann *et al.,* 2006; Dixon *et al.,* 2008) and REX2 (Haase *et al.,* 2009; Boodey *et al.,* 2013), the merozoites surface protein-7 (Msp-7) related proteins (Heiber *et al.,* 2013), and the *P. falciparum* erythrocyte membrane protein (PfEMP1; Boddey and Cowman, 2013). Most PNEPs localize to the membrane of infected erythrocyte where they facilitate “remodeling” of the cytoskeleton (Grüring *et al.,* 2012; Marti and Spielmann, 2013) promoting malaria pathogenicity.

1.5. *P. falciparum* infected host erythrocyte “remodeling”

Remodeling of the infected erythrocytes alters it’s biological, morphological and biochemical properties (Proellocks *et al.,* 2016). The alterations result in the rearrangements of the erythrocyte cytoskeleton, cytoplasm and plasma membrane leading to disruption of function (Haldar and Mohandas, 2007; Bullen *et al.,* 2012; Zuccala and Baum, 2011). These changes are brought about mainly by proteins that are exported from the parasite, and are crucial for nutrient acquisition, facilitating parasite survival (Tamez *et al.,* 2008; Zuccala and Baum, 2011). Erythrocyte remodeling involves the formation of membrane-bound organelles and the assembly of parasite exported proteins into unique membranous structures, for example the Maurer’s clefts (MCs). The MCs are the secretory organelles formed through membrane budding towards export of transmembrane proteins beyond the PVM (Mundwiiler-Pachlatko and Beck, 2013). The

MCs are displaced into the infected erythrocytes cytoplasm, and are located underneath the plasma membrane connected to the membrane skeleton by actin-filaments (Pachlatko *et al.,* 2010; Gruiring *et al.,* 2011).

The overall export pathways of *P. falciparum* infected erythrocytes are similar to trafficking pathways found in eukaryotes. However, in *P. falciparum,* protein export is implicated in virulence (Zhang *et al.,* 2015). Some of the parasite-exported proteins associate with proteins of host origin that are located on the erythrocyte's surface. Such an association forms protein complexes on the surface of the erythrocyte, termed "knobs" (Rug *et al.,* 2006; Shi *et al.,* 2013). The knobs are nanoscale electron-dense adherent protrusions on the surface of infected erythrocytes. Knobs occur generally a result of an association between KAHRP and the adhesion PfEMP1 (Figure 1.3; Rowe *et al.,* 2010). PfEMP1 is composed of cysteine-rich adhesion domain, the so-called Duffy Binding-Like (DBL) domain, and the cysteine-rich Inter-Domain Region (CIDR; Cyrklaff *et al.,* 2012). The DBL domain is essential for binding the KAHRP-PfEMP1 complex to host receptors (such as host immunoglobulin M; IgM) (Kraemer and Smith, 2006) and endothelial protein receptor (Smith *et al.,* 2013).

The KAHRP-PfEMP1 complex is formed through the association of PfEMP1 with the membrane section of the MCs which is then translocated to the membrane knobs (Su *et al.,* 1995). The C-terminus of PfEMP1 associates with KAHRP sub-membrane skeletal protein, which is found self-aggregated in the knobs (Fairhurst and Wellmes, 2006). Subsequently, interaction alters the membrane architecture of infected erythrocyte resulting in rigid and deformed erythrocytes (Rowe *et al.,* 2007; Maier *et al.,* 2008; Zhang *et al.,* 2015). As a result, the erythrocytes develop cytoadherent properties (Rug *et al.,* 2006). Therefore, the infected erythrocytes adhere and bind host endothelial cells (Maier *et al.,* 2008; Rowe *et al.,* 2010). Cytoadhesion of infected erythrocytes leads to rosetting of cytoadherent erythrocytes, where infected erythrocytes bind and cluster with uninfected erythrocytes (Rowe *et al.,* 2010; Proellocks *et al.,* 2016). Such a phenomenon enables clumping of erythrocytes (sequestration) and evasion from the surveillance mechanisms of the spleen (Zhang *et al.,* 2015).

Erythrocyte remodeling is an essential mechanism for parasite survival. The overall remodeling process of infected erythrocyte and protein export are regulated at a molecular level by a family of proteins called molecular chaperones. Most parasite proteins are exported in their unfolded conformations and are prone to aggregation and misfolding (Botha *et al.,* 2007). Therefore, molecular chaperones (proteins that facilitate folding of proteins) bind these proteins and stabilize them during export through membrane compartments to their designated locations (Rug *et al.,* 2006; Mbengue *et al.,* 2012), preventing aggregation and misfolding (Shonhai, 2014).

1.6. Molecular chaperones

Molecular chaperones are molecules found in all life forms known to maintain cellular proteostasis in biological systems (Shonhai, 2014), and serve as molecular folding machinery for other proteins (Saibil, 2013). Amongst these are so called heat shock cognate proteins (Hscs) (that are constitutively expressed) and heat shock proteins (Hsps) (stress inducible forms) (Ellis, 2006; Acharya *et al.,* 2007). Hsps are universally distributed amongst various organisms (from bacteria to humans) (Nonaka *et al.,* 2006). Under hostile environmental conditions, selected Hsps are upregulated to maintain proteostasis (Edkins and Boshoff, 2014). The malaria parasites undergo environmental changes and experience unfavorable physiological conditions in the human host. As a result, the parasite upregulates expression of some of its Hsps for protection (Shonhai, 2014). The Hsps have been classified into conserved classes based on their molecular weight (kDa), structures, localization and chaperone function (Shonhai *et al.,* 2011). In *P. falciparum* the following major Hsps members are represented; Hsp110, Hsp100, Hsp90, Hsp70, Hsp60, Hsp40 and small Hsps (Shonhai *et al.,* 2011; Zininga *et al.,* 2015a).

1.6.1. **Heat shock protein 90**

Heat shock protein 90 (Hsp90; 90 kDa), is a highly conserved molecular chaperone that occurs in all eukaryotic cells (Banumathy *et al*., 2003). Hsp90 is found to be mostly abundant in the cytosol under normal growth conditions, and is known to maintain cellular

viability (Acharya *et al.,* 2007). Hsp90 is a folding chaperone that reduces protein misfolding, and suppresses thermally induced aggregation of proteins (Krukenberg *et al.,* 2011). The chaperone activity of Hsp90 is ATP-dependent and thus governed by the capacity to bind and hydrolyze ATP (Edkins and Boshoff, 2014). Furthermore, the Hsp90 folding system is considered to be a late-stage folding system for proteins that are transferred from Hsp70 (Section 1.6.2). Hsp70 and Hsp90 cooperate via an adaptor Hsp70-Hsp90 organizing protein (Hop; Section 1.6.3) (Krukenberg *et al.,* 2011). Hsp90 plays a crucial role in late-stage folding of essential proteins such as kinases, steroid hormone receptors (reviewed in Krukenberg *et al.,* 2011), and proteins that mediate purine biosynthesis (French *et al.,* 2013). In developing cells, Hsp90 is essential for their development.

The structure of Hsp90 consists of three major domains (Figure 1.4); an N-terminal nucleotide binding domain (NBD), a substrate binding domain (SBD), and a C-terminal dimerization domain (reviewed in Edkins and Boshoff, 2014). The NBD is highly conserved in Hsp90s and is essential for the protein's ATPase activity (Meyer *et al.,* 2003). Hsp90 NBD binds ATP, and the signal is transmitted to the SBD to bind misfolded substrates, which mediates protein folding (Chiosis *et al.,* 2013). The dimerization domain facilitates self-association. The chaperone function of Hsp90 is activated by dimerization (Chiosis *et al.,* 2013). The C-terminal consists of an EEVD motif (Figure 1.4) that facilitates interaction of Hsp90 with tetratricopeptide repeats (TPR) containing co-chaperones, such as Hop (Section 1.6.3) (Onuoha *et al.,* 2008; Edkins and Boshoff, 2014). The negatively charged linker region (Pearl and Promodou, 2006) connecting the NBD and the SBD of Hsp90 is implicated in interdomain function and co-chaperone associations (Krukenberg *et al.,* 2011).

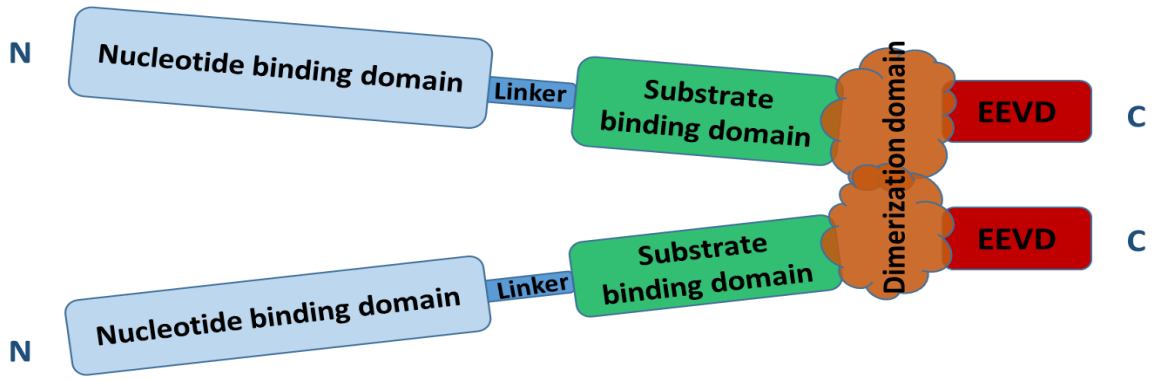

Figure 1.4: The structure of Hsp90 as a homodimer
Five domains of Hsp90; the N-terminus (nucleotide binding domain; light blue), the charged linker domain (dark blue), the middle domain (green), and the dimerization domain (orange) before the C-terminal EEVD motif (red) (Pearl and Promodou, 2006). The dimerization domain results in self-association of Hsp90 and activates chaperone function. Figure adapted from Krukenber *et al.* (2011); Edkins and Boshoff (2014).

In the human genome, there are four Hsp90 isoforms which facilitate normal cell growth and development. Amongst these isoforms, there are two distinct cytosolic isoforms; the induced Hsp90α (Hsp90AA1: NP_001017963.2) and the constitutively expressed Hsp90β (Hsp90AB1: NP_001258899.1) (Didelot *et al.,* 2008). Based on protein sequence analysis, these isoforms share 86 % identity (Acharya *et al.,* 2007). Furthermore, the isoforms exhibit a significant difference in their highly-charged linker regions; hence, alteration in length, amino acid composition and charge properties suggest a slight functional variation (Grammatikakis *et al.,* 2002).

In *P. falciparum*, four Hsp90 paralogs exist; full length cytosolic Hsp90 homologue (PfHsp90; PF3D7_0708400), endoplasmic reticulum (ER) Grp94 homologue (PF3D7_1222300), mitochondrial TRAP1 (PF3D7_1118200) and an Hsp90 lacking the cytosolic signal (PF3D7_1443900) (Acharya *et al.,* 2007). *P. falciparum* Hsp90 mediate processing of newly-synthesized proteins across various compartments of the parasite and is considered a target for drug discovery (Pallavi *et al.,* 2010; Zininga and Shonhai, 2014). The cytosolic PfHsp90 (Pf3D7_0708400) forms a dynamic multi-protein complex with PfHsp70-1 (Section 1.6.6.1) and PfHop (Zininga *et al.,* 2015b) that is implicated in folding of a specialized group of protein substrates (Pallavi *et al.,* 2010).

1.6.2. Hsp70-Hsp90 organizing protein

Hsp70-Hsp90 organizing protein (Hop) acts as an adapter protein that facilitates the association of Hsp70 (Section 1.6.4) and Hsp90 (Nicolet & Craig, 1989). Hop is a highly ubiquitous nuclear and cytosolic protein (Gitau *et al.,* 2012). Hop protein is expressed at moderate levels in most organisms under normal conditions and overexpressed under stressful conditions (Nicolet & Craig, 1989; Daniel *et al.,* 2008; Gitau *et al.,* 2012).

Structurally, Hop is composed of three major tetratricopeptide repeats (TPR: TPR1, TPR2A and TPR2B) and two dipeptide repeats (DP: DP1 and DP2) (Figure 1.5; Schmid *et al.,* 2012; Eckl & Richter 2013). The TPR1 domain binds the EEVD motif of Hsp70 (Gitau *et al.,* 2012; Zininga *et al.,* 2015b), while the TPR2A subdomain binds the EEVD motif of Hsp90 (Onuoha *et al.,* 2008; Röhl *et al.,* 2015). The TPR2B domain has been reported to exhibit affinity for Hsp70 binding in the absence of Hsp90 (Röhl *et al.,* 2015). As a result, TPR1 and TPR2B subdomains of Hop interact with Hsp70 while the TPR2A motif preferentially interacts with the C-terminus of Hsp90 (Gitau *et al.,* 2012; Röhl *et al.,* 2015; Zininga *et al.,* 2015b). Hop possesses a nuclear localization signal termed the nuclear localization signal 1 (NLS1) and a putative nuclear localization signal 2 (NLS2) downstream of the C-terminus (Figure 1.5). The DP repeats are composed of aspartate and proline repeats (Schmid *et al.,* 2012). The DP repeats serve a specific function within the protein. The DP1 is implicated in ATPase activity of Hop while DP2 facilitates and enhances the capability of Hop to bind Hsp70 (Schmid *et al.,* 2012; Yamamoto *et al.,* 2014). This suggests that the DP repeats enhance the function of Hop.

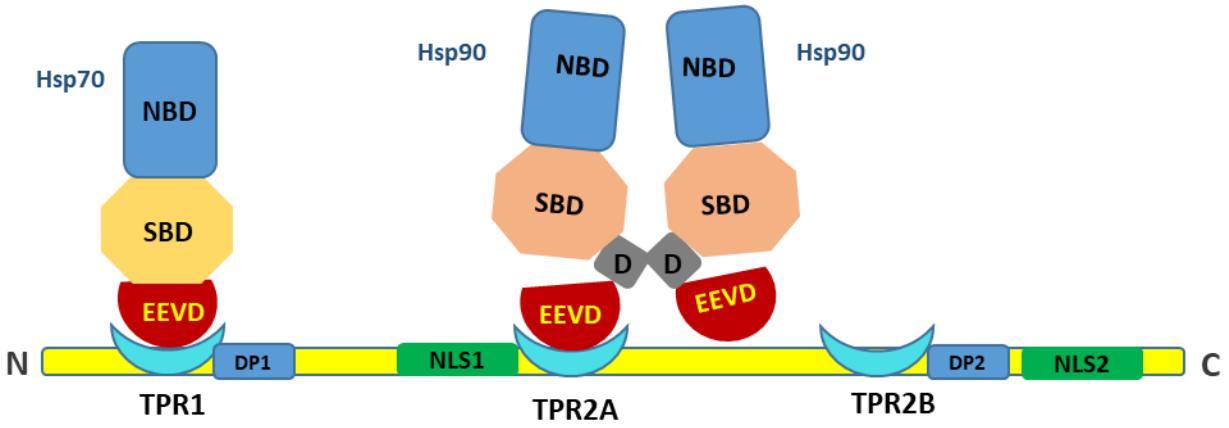

Figure 1.5: The structure of Hsp70-Hsp90 organizing protein (Hop)
The structure shows the three major tetratricopeptide repeats (TPR), two aspartate-proline dipeptide repeats (DP) domains and nucleus localization signal. The D in a gray box represent the dimerization domain. The Hsp70 EEVD motif binding the TPR1 domain and the dimerized Hsp90 EEVD motif binding TPR2A. Binding of Hsp90 increases Hsp70 binding affinity to TPR2B, and subsequently moves Hsp70 from TPR1 to TPR2B. Figure adapted from Zininga *et al.* (2015b).

Hop is highly conserved across *Plasmodium* genus and across species. However, *P. falciparum* Hop (PfHop: PF3D7_1434300) is slightly structurally divergent from that of the mammalian counterpart (Odunuga *et al.,* 2003; Gitau *et al.,* 2012). PfHop is expressed at the erythrocyte stage, and is implicated in proteostasis (Gitau *et al.,* 2012; Zininga *et al.,* 2015b). The surface of the TPR domains exhibit concave and convex regions which mediate hydrophobic interactions with Hsp70 and Hsp90 (Röhl *et al.,* 2015). Despite the presence of the NLS sequences, PfHop was reported to primarily localize in the cytosol of the parasite (Gitau *et al.,* 2012). Furthermore, PfHop has been shown to co-localize with PfHsp70-1 (Gitau *et al.,* 2012; Zininga *et al.,* 2015b) and PfHsp90 (Section 1.6.1) at the erythrocyte stage of the malaria parasites life cycle (Gitau *et al.,* 2012). As a result, the TPR domains of PfHop interacts with PfHsp70-1 and PfHsp90 to form a functional protein folding multi-chaperone complex (Gitau *et al.,* 2012; Zininga *et al.,* 2015b). The occurrence of PfHsp70-1 and PfHsp90 in a PfHop mediated complex has been reported (Gitau *et al.,* 2012). In addition, the formation of this complex has been reported to be nucleotide-dependent (Gitau *et al.,* 2012; Zininga *et al.,* 2015b).

1.6.3. Heat shock protein 40

Heat shock protein 40 (Hsp40) is a known co-chaperone for the Hsp70 chaperone. Hsp40 stimulates the ATPase activity of Hsp70 as well as serving as the substrates "carrier" (Hannessy *et al.,* 2005; Botha *et al.,* 2011). Hsp40 proteins are highly conserved molecules (Botha *et al.,* 2007). Hsp40s are characterized by a J-domain and are referred to as J-proteins (also DnaJ in *E. coli;* Botha *et al.,* 2007); and 'DNAJ' in humans (Kampinga *et al.,* 2009). Hsp40s are widely distributed across species. In humans there are at least 50 Hsp40s and 51 occur in *P. falciparum,* while *E. coli* expresses 6 Hsp40s (Kampinga *et al.,* 2009; Njunge *et al.,* 2013).

Hsp40s are classified into types based on the conservation of functional domains in relation to *E. coli* DnaJ (Figure 1.6; Botha *et al.,* 2007; Njunge *et al.,* 2013). Hsp40s possess four functional domains; a J domain, a Gly/Phe-rich region (GF), four cysteine-rich zinc-binding domains (CRR), and a less conserved C-terminal substrate-binding domain (SBD) (Figure 1.6; Botha *et al.,* 2007, 2011). Therefore, the J-domain of Hsp40s is highly conserved and made up of about 70 amino acid residues forming four highly conserved α-helices (helices I – IV) (Hennessy *et al.,* 2005).

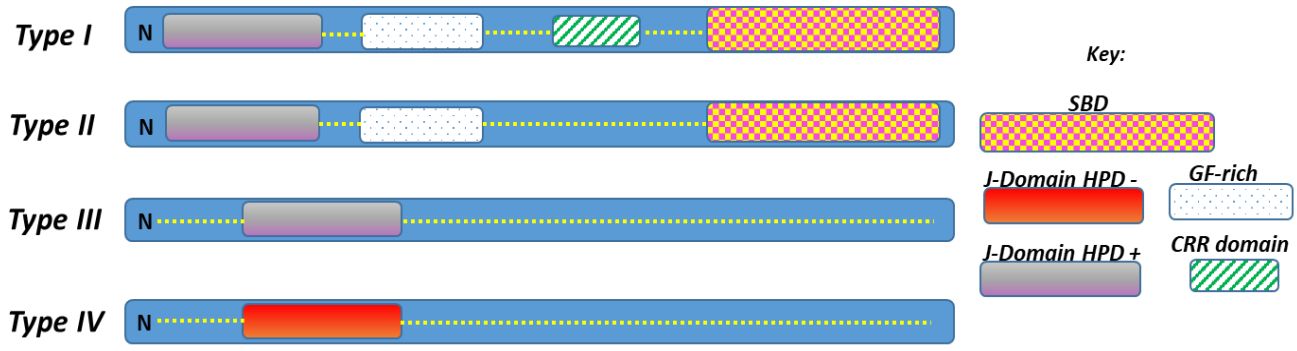

Figure 1.6: The classification of Hsp40s
Hsp40s are characterized into four types I – IV and have J-domain, the GF-rich region, the Zinc-finger region and the C-terminal region. Type I contains all domains, while type II lacks only the Zinc-finger domain. The types III and IV only have the J-domain, however, the J-domain of type IV does not have the HPD motif. Figure adapted from Rug & Maier (2011).

Furthermore, the J-domain consists of a tripeptide histidine-proline-aspartic acid (HPD) motif between helices II and III (Figure 1.6; Hennesy *et al.,* 2005). The HPD facilitates the formation of the Hsp40-Hsp70 complex (Botha *et al.,* 2011; Knox *et al.,* 2011; Bascos *et*

al., 2017). This interaction modulates and regulates the activity of Hsp70 as well as facilitates substrate binding by Hsp70 (Section 1.6.5; Acharya *et al.,* 2007). Type I Hsp40s have all the domains that are present in *E. coli* DnaJ. Type II are highly similar to type I, but lack the CRR region (Figure 1.6; Botha *et al.,* 2007; Kampinga & Craig, 2010). Examples of *P. falciparum* type II Hsp40s include Pfj4 (PF3D7_1211400) and Pfj2 (PF3D7_1108700) (Pesce *et al.,* 2008; Njunge *et al.,* 2013). Type III Hsp40s possess a J-domain with the HPD motif but lack all the other domains present in *E. coli* DnaJ (Figure 1.6; Botha *et al.,* 2007). The type IV group is similar to type III Hsp40s. However, type IV Hsp40s possess a J-domain that lacks the HPD motif (Figure 1.6; Kampinga & Craig, 2010).

The main functions of Hsp40s are to recruit and bind substrates within the aqueous environment of the cells (Bascos *et al.,* 2017). The CRR region and C-terminus of Hsp40s are implicated in substrates binding (Section 1.6.4; Botha *et al.* 2007, 2011). Types I and II Hsp40s have greater binding capability for substrates than types III and IV, hence they lack the SBD (Figure 1.6). Although type II Hsp40s lack the CRR region, the presence of the GF-C-terminal is enough to promote substrate binding by these Hsp40s making them capable of suppressing protein aggregation (Kampinga *et al.,* 2009; Zininga, 2015). Furthermore, types I and II Hsp40s are capable of passing their misfolded substrates to Hsp70 for refolding (Section 1.6.5) (Kampinga & Craig, 2010; Njunge *et al.,* 2013).

Some of the *P. falciparum* Hsp40 proteins contain the PEXEL export signal sequence that targets proteins to infected erythrocyte's cytosol (Section 1.4) (Miller *et al.,* 2004; Njunge *et al.,* 2013). Of these Hsp40s, 43 have been reported to be exported to the infected erythrocyte (2 type I's, 9 type II's, 20 type III's and 12 type IV's). *P. falciparum* Hsp40s that lack a substrate binding domain (the CRR region and C-terminal) are generally termed truncated Hsp40s (Figure 1.6). The study of Petersen and colleagues (2016), reported a novel export pathway mediated by a membrane vesicle diffusion phenomenon (Figure 1.3; Section 1.4), of which the truncated family of Hsp40s proteins are exported (Petersen *et al.,* 2016). Truncated Hsp40s, however, possess the N-terminal PEXEL which enables export into the erythrocytes cytosol (Petersen *et al.,* 2016). Furthermore,

they are translocated to their respective destination by highly mobile parasite induced structures termed the J-dots (Section 1.5; Külzer *et al.,* 2010; Petersen *et al.,* 2016).

1.6.4. Heat shock protein 70

Heat shock protein 70 (Hsp70) belongs to one of the major molecular chaperone families (Mayer & Bakau, 2005; Shonhai *et al.,* 2007). The Hsp70 family is widely distributed and is one of the most widely-studied molecular chaperones (Shonhai *et al.,* 2007). Hsp70 is present in all living cells and is conserved in all organisms (Kampinga *et al.,* 2009). The *E. coli* Hsp70 is known as 'DnaK' and the mammalian homologue is referred to as 'HSPA' (Kampinga *et al.,* 2009). Hsp70 proteins facilitate protein folding (Shonhai *et al.,* 2008). Thus, Hsp70s interact with unfolded polypeptide chains via their exposed hydrophobic surfaces. Hsp70 is capable of both protein folding as well as reversing and suppressing protein aggregation (Mayer, 2013; Edkins & Boshoff, 2014).

Hsp70 is composed of two major domains; the N-terminal ATPase domain (nucleotide binding domain, NBD) and a substrate-binding domain (SBD) (Shonhai, 2014). The SBD is further characterized by β-sheets and α-helical subdomains. The lid which turns the C-terminal of Hsp70 is α-helical and the extreme C-terminus is marked by EEVD residues (Figure 1.7). The β-sheets form the substrate binding domain (Shonhai, 2014). The lid encloses the bound substrate in the SBD. The EEVD motif is implicated in co-chaperone binding (Section 1.6.2). The NBD and SBD domains are connected by a highly conserved 7-residue linker region which facilitates interdomain allosteric functioning (Sharma & Masison, 2009).

Figure 1.7: The general structure of Hsp70
The structure of Hsp70 showing the N-terminal ATPase domain (NBD) (light blue), linker (dark blue), substrate binding domain (SBD); SBDβ (purple) and SBDα (gray), the lid (green) and an EEVD motif (red). Figure adapted from Zininga (2015).

1.6.5. Hsp70 functional cycle

The Hsp70 functional cycle facilitates protein folding function. Protein folding is driven by the Hsp70-Hsp40 chaperone system (Section 1.6.4). Hsp70 switches between the ATP- and ADP-bound states (Figure 1.8).

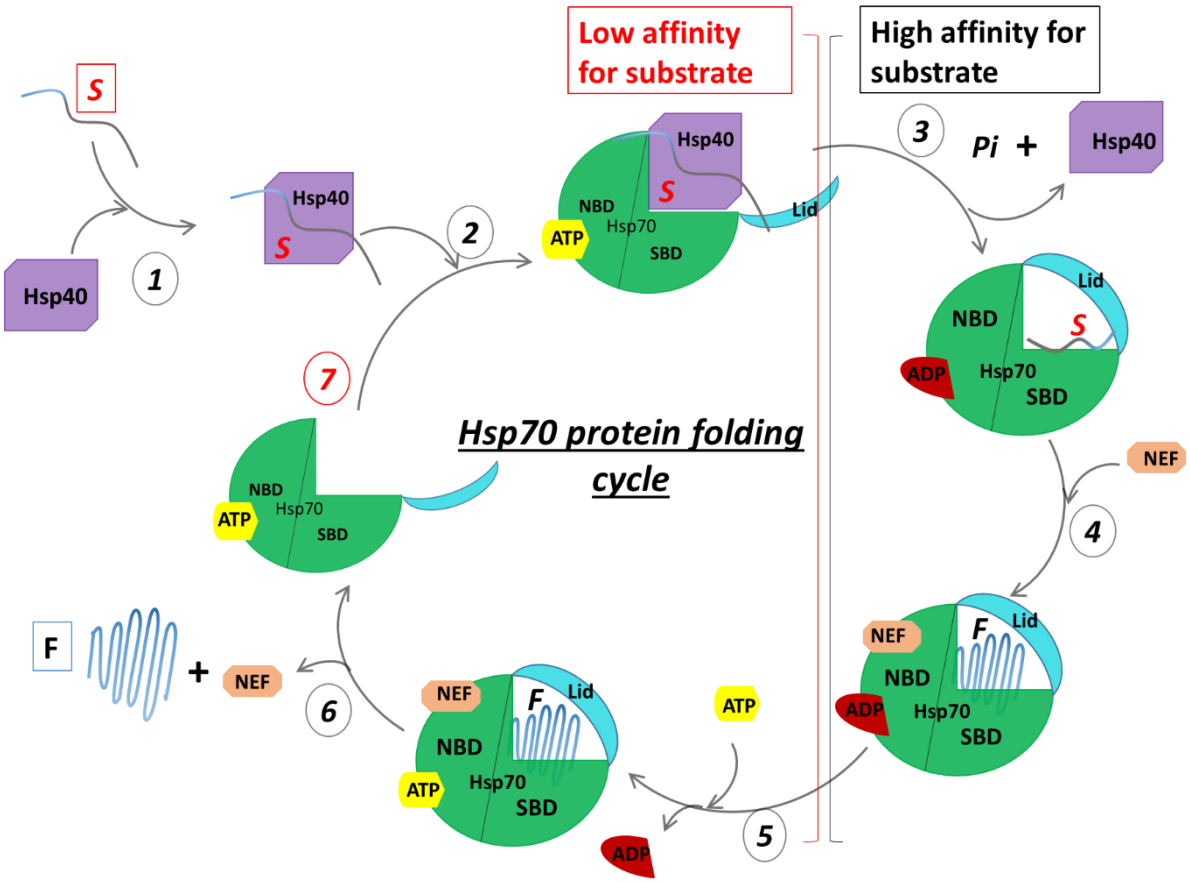

Figure 1.8: Hsp70 nucleotide dependent protein folding cycle
Hsp70 forms a complex with substrate bound Hsp40, and mediates folding of substrate. Hsp40 recruits unfolded substrate to Hsp70. The cycle is initiated when 1, Hsp40 captures nascent/misfolded substrate (S). 2, Hsp40-substrate complex is lodged on to the NBD of ATP-bound Hsp70 and delivers the substrate to the SBD Hsp70 eventually releasing Hsp40. Binding of the substrate stimulates hydrolysis of bound ATP resulting in the formation of an ADP-bound Hsp70-substrate-Hsp40 complex. 3, ATP is hydrolyzed, the conformation of the Hsp70 lid changes enclosing substrate and releasing Hsp40. At this point Hsp70 has high affinity for substrate and mediates substrate folding. 4, Once the substrate is fully folded, NEF binds the complex. 5, NEF facilitates ADP dissociation and subsequently binding of ATP. ATP lowers the substrate affinity of Hsp70. 6, ATP binding activates conformational changes causing the lid to open and release the fully folded substrate protein (F), and at the same time dissociates NEF. 7, Hsp70-ATP bound is ready for the next cycle when 1 (Hsp40-substrate complex) is formed. Figure adapted from Edkins & Boshoff *(*2014).

The NBD of Hsp70 proteins are known to confer ATPase activity which facilitates protein folding. The ATP bound to Hsp70 at the ATP-bound state undergo hydrolysis. As a result,

ATP gets hydrolyzed which then mediate substrate binding to the SBD (Figure 1.8; Kampinga *et al.,* 2009; Zininga *et al.,* 2016). In the ATP bound state, Hsp70 has rapid on-off rates, resulting in low affinity for substrate (Figure 1.8). In the ADP bound state, the on-off rates are reduced resulting in an overall high affinity for substrate (Figure 1.8; Kampinga & Craig, 2010). The Hsp70 chaperone cycle is regulated by a nucleotide exchange factor (NEF) (Zininga *et al.,* 2016). Once the substrate is folded, nucleotide ATP bind to the chaperone system generating a substrate free Hsp70 (Figure 1.8). The function of NEFs is to release ADP to make way for ATP binding to Hsp70.

1.6.6. *Plasmodium falciparum* heat shock protein 70 family

In *P. falciparum*, Hsp70s are widely expressed in different subcellular compartments of the parasite, however, some are up-regulated during stress (Shonhai, 2014). *P. falciparum* Hsp70s mediate parasite survival and development (Shonhai, 2014). Hsp70s of *P. falciparum* are thought to facilitate parasite thermotolerance through their role in proteostasis (Shonhai *et al.,* 2007; Zininga *et al.,* 2016). The genome of *P. falciparum* encodes six Hsp70s (Shonhai *et al.,* 2011; Shonhai, 2014). The Hsp70s are distributed in various cellular compartments (Table 1.2; Shonhai *et al.,* 2011; Shonhai, 2014; Przyborski *et al.,* 2015). The distribution of Hsp70s to various cellular compartments ensures specialized function (reviewed in Shonhai *et al.,* 2007).

Table 1.2: *Plasmodium falciparum* Hsp70 homologues

	Proteins	MW	Distribution	Functions	Signal sequences
1.	**PfHsp70-1 (PF3D7_0818900)**	74 kDa	parasite cytosol, nucleus [A, B, C]	protein folding and translocation [B, I]	NLS, GGMP, EEVD [B, C, H]
2.	**PfHsp70-2 (PF3D7_0917900)**	73 kDa	parasite ER [C, D]	protein import into ER and folding [C, D]	ER signal [D]
3.	**PfHsp70-3 (PF3D7_1134000)**	73 kDa	parasite mitochondrion [D, E]	protein import into the mitochondrion and refolding [D, E]	Mt signal [D]
4.	**PfHsp70-x (PF3D7_0811700)**	76 kDa	PV, erythrocyte cytosol [F, G]	protein translocation, folding, parasite virulence [F, G, I]	ER signal, export signal, EEVN [F, G]
5.	**PfHsp70-y (PF3D7_1344200)**	108 kDa	parasite ER [E]	chaperone function and NEF for PfHsp70-2 [D]	ER signal [D]
6.	**PfHsp70-z (PF3D7_0708800)**	110 kDa	parasite cytosol [B, D]	chaperone function; proposed NEF for PfHsp70-1 [B]	ND

***Plasmodium falciparum* Hsp70 proteins classification, MW-molecular weight (KDa), subcellular distribution and specialized function. The parenthesis represent PlasmoDB accession numbers. References: A-Shonhai *et al.,* 2008; B-Zininga *et al.,* 2016; C-Pesce *et al.,* 2008; D- Shonhai *et al.,* 2007; E-Sargent *et al.,* 2006; F-Külzer *et al.,* 2010; 2012; G-Daniyan *et at.,* 2016; H-Shonhai, 2014; I-Charnuad *et al.,* 2017; ER-endoplasmic reticulum; PV-parasitophorous vacuole; NEF-nucleotide exchange factor; ND-not determined. Table adapted from Przyborski *et al.* (2015).**

1.6.6.1. *P. falciparum* Hsp70-1

P. falciparum Hsp70-1 (PfHsp70-1, Table 1.2) is a cytosolic and nuclear localized protein (Table 1.2; Shonhai *et al.,* 2007; Zininga *et al.,* 2015a). PfHsp70-1 is a soluble protein that is highly expressed in the parasite and is upregulated at the blood stage of the parasitic life cycle (Joshi *et al.,* 1992; Sharma, 1992). PfHsp70-1 has a higher basal ATPase activity than *E. coli* DnaK. PfHsp70-1 exhibits ATP-dependent chaperone activity (Zininga *et al.,* 2015a). The ATPase chaperone activity of the PfHsp70-1 is stimulated by binding of substrate-bound PfHsp40 (Njunge *et al.,* 2013). PfHsp70-1 is thermostable and is thought to confer thermotolerance to the parasite to ensure its survival (Shonhai *et al.,* 2005; Bell *et al.,* 2011). In addition, PfHsp70-1 was reported to suppress heat-induced aggregation of a model substrate, malate dehydrogenase *in vitro* (Shonhai *et al.,* 2008).

Therefore, this highlights the role of PfHsp70-1 in maintaining cellular proteostasis (Stephens *et al.,* 2011; Makhoba *et al.,* 2016).

1.6.6.2. *P. falciparum* Hsp70-x

P. falciparum Hsp70-x (PfHsp70-x, Table 1.2) is expressed by the parasite and exported to the erythrocyte cytosol (Külzer *et al.,* 2012) where it is implicated in the modification of the host erythrocytes (Section 1.5). PfHsp70-x is closely related to PfHsp70-1 as they share a sequence identity of 73 %. The domain organization of PfHsp70-x is illustrated in Figure 1.9. The C-terminal EEVN residues of PfHsp70-x are thought to bind to co-chaperones (Figure 1.9; Mabate, 2017).

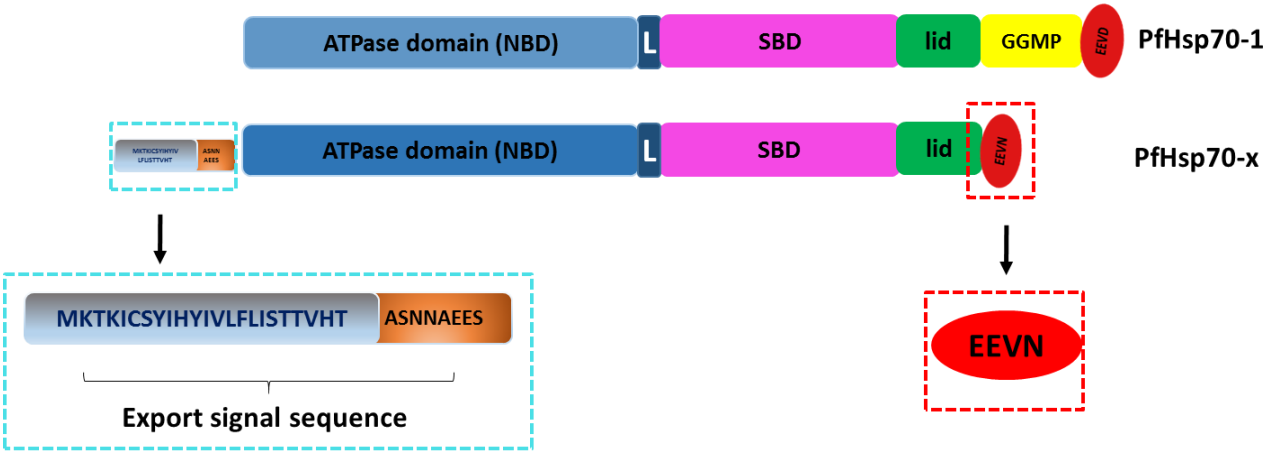

Figure 1.9: Structural depiction of PfHsp70-1 and PfHsp70-x domains
The structure of PfHsp70-1 and PfHsp70-x are composed of the N-terminal ATPase domain (NBD) (light blue), the linker region (dark blue), the substrate binding domain (SBD) (pink), a lid (green) and the C-terminal EEVD motif (red dashed box). The N-terminals of PfHsp70-x has a putative signal cleavage site (gray and orange, blue dashed box), whilst the C-terminals of PfHsp70-1 has additional sequences of GGMP repeats (yellow). Figure adapted from Külzer *et al.,* (2012).

PfHsp70-x lacks the PEXEL/VTS export motif and it falls within the exported PNEPs protein family (Section 1.4; Külzer *et al.,* 2012). PfHsp70-x possesses a unique N-terminal signal sequence for export into infected erythrocyte (Külzer *et al.,* 2012; Przyborski *et al.,* 2015). This signal is comprised of 25 amino acids. Essentially the residues represent an ER signal sequence (MKTKICSYIHYIVLFLIATTTVHT) which is followed by 8 residues that facilitate the protein's export (**ASNNAEES**) (Section 1.6.6.2). The **ASNNAEES** motif is located between amino acids 25-33, and is known as a novel octameric export signal

(termed NOES) (Külzer *et al.,* 2012). The N-terminal ER signal sequence consist of a signal peptide cleavage site (region between putative signal sequence cleavage site). In addition, the C-terminal of PfHsp70-x lacks the GGMP repeat that characterizes cytosolic PfHsp70-1 (Shonhai *et al.,* 2008; Zininga *et al.,* 2015). The C-terminus of PfHsp70-x differs from that of PfHsp70-1. Whereas PfHsp70-x contains a C-terminal EEVN motif, PfHsp70-1 possesses an EEVD motif (Figure 1.9; Külzer *et al.,* 2012; Shonhai *et al.,* 2007; Shonhai *et al.,* 2011). The EEVN motif may be essential to establish an association with the TPR1 domain of Hop (Section 1.6.2).

PfHsp70-x is trafficked through the PVM to the erythrocytes cytosol (Figure 1.10; Külzer *et al.,* 2012). In the erythrocyte, PfHsp70-x is reported to co-localize with parasite type II Hsp40s PFE0055c (PF3D7_0501100) and PFA00660w (PF3D7_0113700) (Külzer *et al.,* 2010). PfHsp70-x forms complexes with Hsp40s in distinct structures termed “J-dots” within the infected erythrocyte cytosol (Figure 1.10; Külzer *et al.,* 2010). Within the J-dots, PfHsp70-x interacts with a type II *P. falciparum* Hsp40s PFA0066w (Daniyan *et al.,* 2016) and PFA00660w (Zhang *et al.,* 2017). It is for this reason that PfHsp70-x is thought to be involved in refolding exported parasite proteins (Section 1.4). In addition, since PfHsp70-x also occurs in the PV, it is thought to play a role in facilitating trafficking of parasite proteins exported to the erythrocyte (Külzer *et al.,* 2012). However, the role of PfHsp70-x in the erythrocyte cytosol is yet to be fully understood.

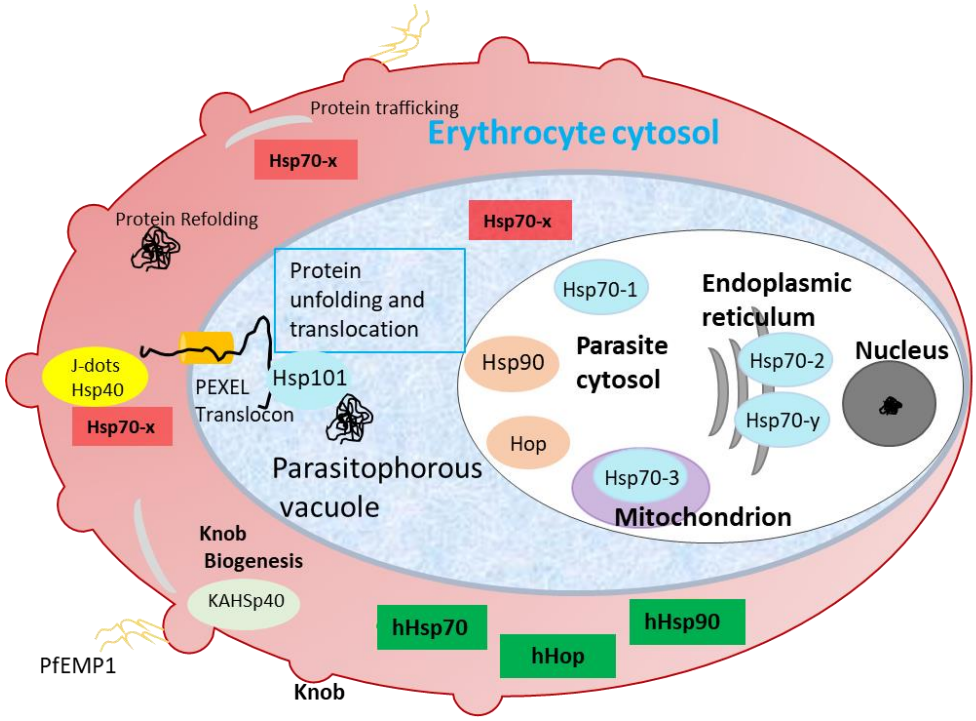

Figure 1.10: Localization of heat shock proteins in *Plasmodium* infected erythrocytes
Heat shock proteins are localized in different compartments within infected erythrocyte, and serve specialized functions. Heat shock proteins are distributed in the parasite cytosol and the PV. The *P. falciparum*–encoded proteins are exported into the erythrocyte cytosol with the involvement of the PTEX complex, J-dots and MCs and are distributed in various compartments of the infected erythrocytes. The proteins Hsp70-1, Hsp70-2, Hsp70-3, Hsp70-y, Hsp90 and Hop are restricted to *P. falciparum*. The *P. falciparum* encoded protein, Hsp70-x localizes to the PV and the erythrocytes cytosol along with human erythrocyte proteins hHsp90 and hHop. Host "remodeling" parasite-encoded proteins KAHSP40, Hsp40 localize in the erythrocyte's cytoplasm and membrane. Figure adapted from Grover *et al.* (2013).

1.7. Problem statement

P. falciparum is responsible for the deadliest form of malaria that accounts for millions of deaths worldwide (WHO, 2017). The erythrocytic stage of the parasites life cycle is responsible for periodic episodes of fever (Shonhai, 2014; Bousema *et al.,* 2016). As a result, the parasite is exposed to temperature fluctuations that prompt the parasite to develop various mechanisms of survival (Proellocks *et al.,* 2015). The parasite achieves this by expressing a subset of Hsps (Section 1.6) that maintain parasite proteostasis (Shonhai, 2014). Some of the Hsps are exported into the erythrocyte cytoplasm (Section 1.4) (Botha *et al.,* 2011; Külzer *et al.,* 2012). The exported proteins are linked with various mechanisms of survival which includes erythrocytes remodeling (Section 1.5; Proellocks *et al.,* 2015; Jha *et al.,* 2017). Amongst these parasite-encoded proteins is PfHsp70-x

(PF3D7_0831700), which is mostly expressed throughout the *P. falciparum* erythrocytic stages (Figure 1.1). In addition, PfHsp70-x localizes to the PV and the J-dots of the erythrocytes cytosol (Section 1.5; Külzer *et al.,* 2012; Grover *et al.,* 2013). Thus, it is implicated in parasite protein trafficking and refolding. Protein export results in the formation of direct parasite and host protein-protein interactions (Shi *et al.,* 2013), which are thought to facilitate protein folding, and erythrocyte remodeling (Külzer *et al.,* 2012; Jha *et al.,* 2017). Although, PfHsp70-x has been recently reported not to be essential for parasite survival (Cobbs *et al.,* 2017), it is shown to associate with virulent proteins (Charnuad *et al.,* 2017). As a result, PfHsp70-x is implicated in the developing parasite virulence in infected erythrocytes (Charnuad *et al.,* 2017).

The function of Hsp70s is regulated by Hsp40 co-chaperones (Section 1.6.5; Bascos *et al.,* 2017; Njunge *et al.,* 2013). It has also been demonstrated that the Hsp70-Hsp40 chaperone complex facilitates substrate transfer to Hsp90 via an adaptor protein, Hop (Banumathy *et al.,* 2002; Wegele *et al.,* 2006). In the cytosol of *P. falciparum*, PfHsp70-1 (Section 1.6.6.1) interacts with PfHsp90 (Section 1.6.1) via PfHop mediation (Gitau *et al.,* 2012; Zininga *et al.,* 2015b). Furthermore, PfHsp70-1 interacts with some *P. falciparum* Hsp40s (Section 1.6.4) to stimulate ATPase activity (Njunge *et al.,* 2013). The EEVD motifs of both PfHsp70-1 and PfHsp90 interact with PfHop TPR domains (Section 1.6.3; Gitau *et al.,* 2012; Zininga *et al.,* 2015a). PfHsp70-x, a homologue of PfHsp70-1, is exported to the erythrocyte cytosol and possesses an EEVN motif, which is distinct from the canonical EEVD motif (Section 1.4; Shonhai *et al.,* 2007 Külzer *et al.,* 2012; Mabate, 2017). Reports have shown the presence of human chaperones such as Hop (hHop), Hsp70 (HSPA) and Hsp90 within the infected erythrocytes cytosol (Banumathy *et al.,* 2002; 2003, Kampinga *et al.,* 2009; Wutchy *et al.,* 2011; Ramakrishnan *et al.,* 2015).

Some exported *P. falciparum* Hsp40s are thought to function as co-chaperones of PfHsp70-x (Külzer *et al.,* 2012) and human Hsp70 (HSPA) (Jha *et al.,* 2017). PfHsp70-x interacts with Hsp40 PFA0660w which stimulates the ATPase activity (Daniyan *et al.,* 2016). Additionally, Jha and colleagues (2017), also reported the interaction of human hHsp70 with the exported type II Hsp40 (PF3D7_0409400), forming a co-chaperone

complex which, however, lacks any chaperone activity (Jha *et al.,* 2017). Recently, PfHsp70-x has been shown to associate with human Hop *in vitro* (Mabate, 2017). Thus, PfHsp70-x exhibits the capability to interact with co-chaperones that mediate protein folding in the erythrocytes. However, the function of PfHsp70-x in infected erythrocytes is yet to be fully understood. Thus, the current study sought to characterize functional interactors of PfHsp70-x. The main aim of this study was to elucidate the interacting partners of PfHsp70-x that are resident in the infected erythrocyte cytosol. The establishment of the interactome of PfHsp70-x within infected erythrocytes could shed light on the function of this protein.

1.8. Hypothesis

PfHsp70-x associates with human chaperone and co-chaperone partners resident in the parasite infected erythrocyte.

1.9. General objective

To investigate interactome characteristics of PfHsp70-x in infected human erythrocytes.

1.10. Specific objectives of the study

1.10.1. Bioinformatics

To determine the structure and functional characteristics of PfHsp70-x and its interactors in infected human erythrocytes.

1.10.1.1. Approaches

a) The amino acid sequence of PfHsp70-x was retrieved from PlasmoDB (http://www.plasmodb.org/plasmo/) and BLAST searches were conducted to identify homologues using NCBI.

b) Homologous amino acid sequences retrieved were aligned to identify conserved functional domains using BioEdit.

c) The three-dimensional model of PfHsp70-x was generated and residues implicated in its function were mapped out.

d) The possible interactors of PfHsp70-x from *P*. *falciparum* exportome and the human erythrocytes proteome were predicted using STRING (https://string-db.org/cgi/network.pl) and were constructed using Cytoscape software (http://www.cytoscape.org/).

1.10.2. Biochemical and cell-based studies

To identify the interactors of PfHsp70-x from *P. falciparum* 3D7 infected erythrocyte lysates using the recombinant form of PfHsp70-x and antibodies specific to PfHsp70-x (α-PfHsp70-x).

1.10.2.1. Approaches

a) Recombinant protein forms of *P. falciparum* Hsp70-x, human Hop and human Hsp70 were expressed and purified using nickel affinity chromatography. The recombinant proteins were used to conduct co-affinity assays.

b) The interaction partners of PfHsp70-x were investigated through immuno-affinity assays using α-PfHsp70-x conducted on lysates obtained from *P. falciparum* 3D7 infected erythrocytes.

CHAPTER 2

MATERIALS AND METHODS

2.1. Bioinformatics

2.1.1. Multiple sequence analysis

Amino acid sequences of *P. falciparum* Hsp70-x (accession number: PF3D7_0831700); PfHsp70-1 (accession number: PF3D7_08118900) and PfHop (accession number: PFE3D7_1434300) were obtained from PlasmoDB (http://www.plasmodb.org/plasmo/; Aurrecoechea *et al.,* 2009). *Homo sapiens* amino acid sequences of Hsp70 (hHsp70) (accession number: NP_005336.3) and Hop (hHop) (accession number: NP_006810.1) were obtained from the National Centre for Biotechnology Information (NCBI) (http://www.ncbi.nlm.nih.gov). The sequence alignments were generated using MAFFT (http://www.ebi.ac.uk/Tools/msa/mafft/) and were shaded using Boxshade (http://embnet.vital-it.ch/software/BOX_form.html). The sequence identity values were calculated using BioEdit V7.2 software.

2.1.2. Three-dimensional structure analysis

Amino acids take up different structural orientations and are implicated in protein folding and function in their destined locations. The sequences of the Hsp70 homologues (section 2.1) were further analyzed for their folding pattern by homology modelling using Phyre^2 (www.sbg.bio.ic.ac.uk/phyre2; Kelley *et al.,* 2015) and viewed using University of California, San Francisco (UCSF) Chimera version 1.9 (www.cgl.ucsf.edu/chimera; Pettersen *et al.,* 2004) Chimera. Analysis to identify structural features of their functional domains was conducted. The models reveal the various conformational organization of the protein such as the α-helices, β-plated sheets or coils. The three-dimensional models of the NBD and SBD of PfHsp70-1 (PF3D7_08118900), PfHsp70-x (PF3D7_0831700) and hHsp70 (NP_005336.3) were generated using *Saccharomyces cerevisiae* (Sse1) crystal structures (c3d2fC.pdb; Polier *et al.,* 2008) as a template. The 3D models of PfHop (PFE3D7_1434300) and hHop (NP_006810) were generated using the crystal structure of a *Chlamydomonas* Hop homologue (c4uzyA.pdb; Taschner *et al.,* 2014) as template. The 3D models were developed

as PDB files using Phyre[2]. The PDB files used for structural analysis were visualized and compared using a match maker tool on Chimera. The predicted 3D-models generated in Chimera were analyzed for conformation and structural orientation of the protein sequences.

2.1.3. Prediction of PfHsp70-x interactors

In order to predict and construct the network of potential interactors of PfHsp70-x, various bioinformatics online tools, STRING 10.5 database (https://string-db.org/; Szklarczyk *et al.,* 2017) and Cytoscape software (http://www.cytoscape.org/; Shannon *et al*., 2003), as well as literature reports were used (Figure 2.1).

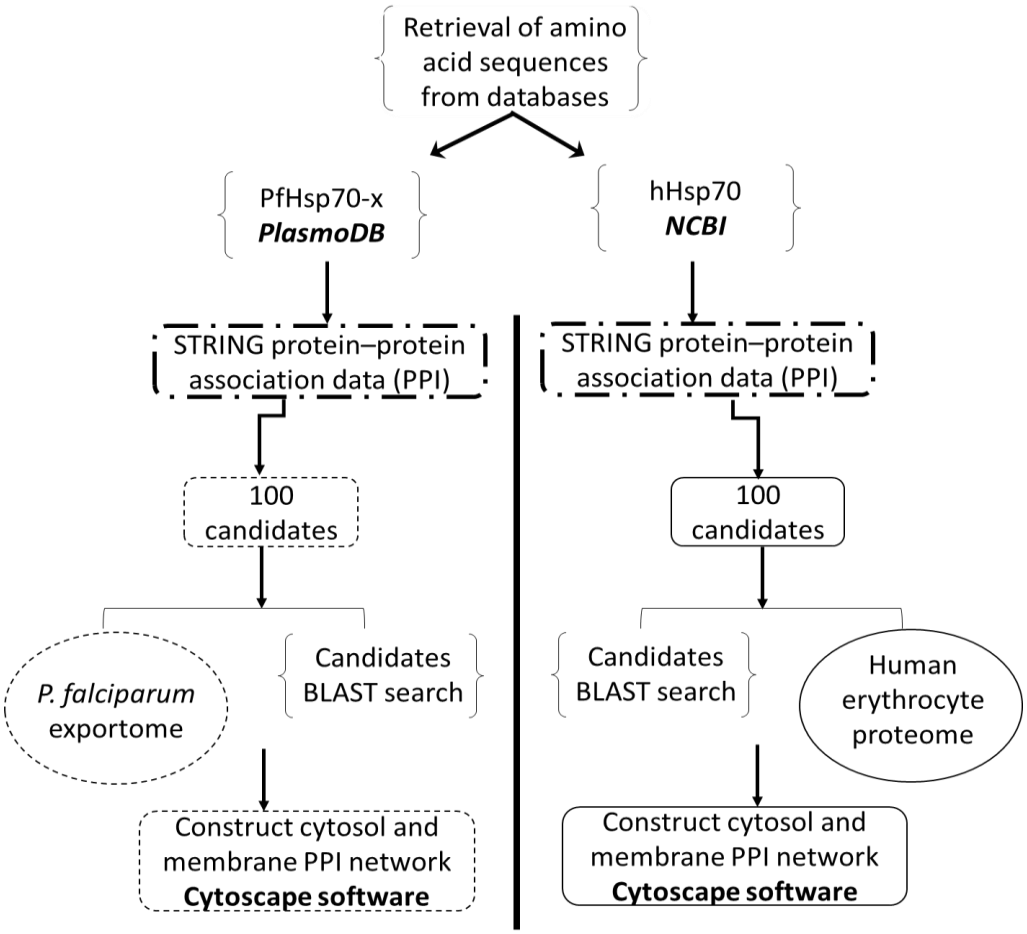

Figure 2.1: The schematic diagram of the construction of the PfHsp70-x
The predicted interactors of PfHsp70-x were retrieved from the *P. falciparum* exportome and the erythrocytes proteome. The candidates were analyzed by a BLAST search to retrieve homologous candidates in both species. The candidates were filtered according to localization. The candidates from the infected erythrocytes cytosol and membrane were used to conduct the interaction network using Cytoscape software. PPI represent protein-protein interaction and BLAST represent Basic Local Alignment Search Tool.

The interactome prediction was conducted using data retrieved from STRING database. The amino acid sequence of PfHsp70-x (Section 2.1) was used to establish a network of interactors from a STRING database (Figure 2.1). Furthermore, data on exported proteins was retrieved from the parasite exportome literatures (Botha *et al.,* 2007; Maier *et al.,* 2008; Spielmann *et al.,* 2010; de Koning-Ward *et al.,* 2016). Of the predicted PfHsp70-x interactors, some are not exported. This is because the STRING software used does not factor subcellular localization of selected proteins. Additionally, a network of human Hsp70 (Section 2.1) was also retrieved from STRING database to identify potential interactors localized in erythrocytes (Figure 2.1). A BLAST search was conducted in order to search for homologues in human erythrocytes which could potentially interact with PfHsp70-x within the infected erythrocytes (Wutchy *et al.*, 2011, Ramakrishnan *et al.,* 2015). The BLAST homology study resulted in the retrieval of potential interactors for the exported PfHsp70-x of human origin in the cytosol (Figure 2.1). Lately, some studies have experimentally validated and reported a set of interacting partners of PfHsp70-x (Külzer et *al.,* 2012; Charnuad *et al.,* 2017; Jha *et al.,* 2017; Mabate, 2017; Zhang *et al.,* 2017). This data was used to validate the findings from the bioinformatics study. To validate the potential interactors, proteome data of the erythrocyte that has been published in literature was further investigated (Kakhniashvili *et al.,* 2004; Pasini *et al.,* 2006; Goodman *et al.,* 2007). The predicted interactors from *P. falciparum* and human homologues were filtered according to sub-cellular localization, protein classes and molecular function. Furthermore, the human erythrocyte proteome was filtered from the predicted protein candidates (Kakhniashvili *et al.,* 2004; Pasini *et al.,* 2006; Goodman *et al.,* 2007; Zhang *et al.,* 2017).

The protein interaction network was constructed with a threshold set at a confidence level of 0.700 which suggests that the predicted interactions are probable at a confidence level 0.700 and above (Jensen *et al.* 2009). The proteins that were predicted to be functional partners of PfHsp70-x in the network are based on association scores representing interaction probability (the higher the association score, the better the chance of a biological protein-protein interaction to occur). The network edges (lines) represent chaperones class and the types (families) and were analyzed on Cytoscape (Shannon *et al.,* 2003). The size of edges reflects

the most likely interactions that may form known functional multi-chaperone complexes (Newman, 2003).

2.2. Biochemical assays

2.2.1. Materials

The following antibodies were used to validate the recombinant PfHsp70-x proteins; α-His antibody produced in rabbit from Thermo Scientific (USA), α-PfHsp70-x antibody produced in rabbit (a kind donation from Prof. J. Pryzbroski, Philipps Marburg University in Germany). Additionally, rabbit raised α-PfHsp70-1 (Shonhai *et al*., 2008), Secondary HRP conjugated goat raised anti-rabbit antibody (Zininga *et al*., 2015a; 2015b), α-His (Zininga *et al*., 2015a; 2015b) and mouse raised α-DnaK antibody from Enzo Life Science (UK) were used. The rest of the reagents used in the study are listed in the appendix section (Appendix C). The bacterial strains and plasmid constructs used for expression of the recombinant proteins are listed in Table 2.1 below.

Table 2.1: Description of *E. coli* strains and plasmid constructs used in this study

Strains and plasmids			
Competent strains for transformation	**Description**		**Supplier Reference**
E. coli JM109 DE3	e14– (McrA–) recA1 endA1 *gyr*A96 thi-1 hsdR17 (rK – mK+) supE44 *rel*A1 Δ(*lac*-proAB) (F´ traD36 proAB *lac*Iq ZΔM15)		Thermofisher Scientific, USA, Zininga, 2015
BL21 Star (DE3)	*F- ompT gal [dcm] [lon] hsdSB λDEs*		Studier *et al.,* 1990
Plasmids	**Description**	**Antibiotic(s) resistance of plasmid constructs**	
1. pQE30-*PfHsp70-x*$_F$	pQE30 encoding full length PfHsp70-x	ampicillin resistance (Amp^R)	Mabate, 2017
2. pQE30-*PfHsp70-x*$_T$	pQE30 encoding PfHsp70-x lacking EEVN residues at the C-terminus	Amp^R	Mabate, 2017
3. pQE30-*hHop*	pQE30 encoding human Hop	Amp^R	Genscript, USA
4. pQE30-*hHsp70*	pQE30 encoding human Hsp70	Amp^R	Genscript, USA

2.2.2. Confirmation of *PfHsp70-x*, *hHop* and *hHsp70* plasmid DNA constructs

Competent *E. coli* JM109 DE3 cells (Table 2.1, Appendix B1) were chemically prepared and transformed with the plasmid constructs, including pQE30-*PfHsp70-x*$_F$, pQE30-*PfHsp70-x*$_T$, pQE30-*hHop*, and pQE30-*hHsp70* (Appendix B2). The constructs expressing PfHsp70-x$_F$ or PfHsp70-x$_T$, hHop and hHsp70 were purified using the Zymo Research Plasmid Miniprep^{TM} (Epigenetics, USA) following the manufacturer's instructions (Appendix B3). Restriction analysis was conducted on each of the plasmid DNA constructs using restriction enzymes *Bam* HI and *Hind* III (Thermo Scientific, USA) to digest and confirm the integrity of the plasmid DNA. The digested products were analyzed using 0.8 % of agarose gel electrophoresis (Appendix B4).

2.2.3. Recombinant protein expression

Competent *E. coli* JM109 DE3 cells were transformed with plasmid constructs, pQE30-PfHsp70-x$_F$ or pQE30-*PfHsp70-x*$_T$, pQE30-*hHop* or pQE30-*hHsp70*, respectively (Table 2.1). Single colonies containing respective plasmids were grown overnight in 100 ml 2 X yeast/tryptone (2 X YT) (tryptone 16 g/L, yeast extract 10 g/L and NaCl 5 g/L, broth containing 100 µg/ml ampicillin) at 37 °C. The overnight culture was subsequently diluted using 900 ml 2 X YT and grown at 37 °C gently shaking at 250 rpm using the FMH 200 shaker (FMH Electronics, RSA). The cultures were incubated until they reached a mid-log phase at OD_{600} = 0.6. Recombinant protein expression was induced using 1 mM (final concentration) of isopropyl-β-D-1-thiogalactopyranoside (IPTG) and incubated at 37 °C. For *E. coli* BL21 Star (DE3) cells expressing pQE30-*PfHsp70-x*$_F$ or pQE30-*PfHsp70-x*$_T$, the cultures were incubated for 6 hrs in 1 L of 2 X YT broth at 30 °C. *E. coli* JM109 DE3 cells transformed with pQE30-*hHop* and pQE30-*hHsp70* were respectively expressed for 4 hrs and 5 hrs in 1 L of 2 X YT at 37 °C. Pre- and post-induction samples were collected at hourly intervals. The cells were harvested by centrifugation at 5000 xg for 20 min at 4 °C and the pellets were re-suspended in 50 ml lysis buffer (10 mM Tris-HCl, pH 7.5, 300 mM NaCl and 10 mM Imidazole containing 1 mM EDTA, 1 mM phenylmethylsulfonyl fluoride (PMSF) and 1 mg/ml lysozyme). The cell lysates were incubated at room temperature shaking for about 30 minutes and stored at -80 °C.

Protein expression samples were analyzed using 12 % sodium dodecyl sulfate-polyacrylamide gel electrophoresis (SDS-PAGE) and visualized using Coomassie Blue (Appendix B6). The production of the His-tagged recombinant protein was confirmed by Western blot analysis (Immunoblot; Appendix B10) using mouse monoclonal α-His-horseradish peroxidase antibodies [1:2000 dilution] (Sigma-Aldrich, USA). The production of recombinant proteins was further confirmed using rabbit-raised polyclonal α-PfHsp70-x antibody [1:2000 dilution] as primary antibody for PfHsp70-x. The secondary antibody used was goat raised α-rabbit horseradish peroxidase conjugated antibody [1:5000 dilution]. The production of human Hop and human Hsp70 was confirmed using α-His [1:2000 dilution] antibodies. Visualization of the Western blot was conducted using the enhanced chemiluminescent substrate (ECL) kit (Thermo Scientific, USA) as per manufacturer's instructions (Appendix B10). Images were captured using the ChemiDoc Imaging system (Bio-Rad, USA).

2.2.4. Recombinant protein purification

Recombinant proteins were successfully purified by sepharose nickel affinity chromatography under native conditions as previously described by Zininga *et al*., (2015a; 2015b), with minor modifications. Lysates were retrieved from the -80 °C freezer and thawed on ice for 1 hr. Polyethyleneimine (PEI) 0.1 % (v/v) was added to the thawed lysate (Shonhai *et al.,* 2008; Gitau *et al.,* 2012; Zininga *et al.,* 2015a;b). The lysates were sonicated and centrifuged at 5000 xg for 20 min at 4 °C to separate the insoluble and soluble protein fractions. The supernatant was loaded into a column with HisPur^{TM} Nickel nitrilotriacetic acid (Ni-NTA) (Thermo Scientific, USA) immobilized metal affinity chromatography column (IMAC) with 4 hrs incubation at 4 °C to enhance binding of recombinant proteins. The beads were washed off of the unbound proteins with 2 bed volumes of wash buffer I (10 ml Tris-HCl pH 7.5; 300 mM NaCl; 25 mM Imidazole; 1 mM PMSF) and wash buffer II (10 ml Tris-HCl pH 7.5; 300 mM NaCl; 80 mM Imidazole; 1 mM PMSF). Washes were performed in the presence of 5 mM ATP. The addition of ATP helps eliminate possible *E. coli* DnaK contamination of the target protein. Additionally, ATP further purifies the target heterologous protein by stripping off some misfolded *E. coli* proteins that may have bound to the target protein. The bound protein(s) were eluted with elution buffer I (10 mM Tris-HCl pH 7.5; 300 mM NaCl; 250 mM Imidazole

and 1 mM PMSF) and elution buffer II (10 mM Tris-HCl pH 7.5; 300 mM NaCl; 500 mM Imidazole and 1 mM PMSF). The eluents were collected and prepared for analysis with 12 % SDS-PAGE (Appendix B6) and Western blot (Appendix B10).

The proteins were extensively dialyzed using the Amicon® Ultra-15 10K centrifuge filter device (Merck Millipore, Germany) in dialysis buffer (300 mM NaCl, 10 mM Imidazole, 10 mM Tris-HCl, pH 7.5, 10 % (v/v) glycerol, containing 1 mM PMSF). The filter device was rinsed with dialysis buffer before use. Briefly, dialysis buffer was added up to 15 ml to the Amicon® Ultra-15 10K centrifuge filter device (Merck Millipore, Germany). The filter device was capped and placed in the centrifuge rotor. The filter device was centrifuged for 15 min at 4000 xg at 4 °C and collected dialysis buffer was discarded. The 4 ml of the protein was added into the filter device and centrifuged for 15 min at 4000 xg at 4 °C and flow through was discarded. The concentrated protein was resuspended in 4 ml of dialysis buffer and centrifuged for 15 min at 4000 xg at 4 °C. The concentrated protein solute was immediately recovered using a pipette in the bottom of the filter device. The solute was withdrawn using a side-to-side sweeping motion to ensure total recovery and stored in storage buffer (150 mM NaCl, 10 mM Tris-HCl, pH 7.5, 10 % (v/v) glycerol, containing 1 mM PMSF). The purity of the eluted proteins was assessed using 12 % SDS-PAGE (Appendix B6) and further confirmed by Western blotting (Appendix B10). To validate that the purified proteins were not contaminated with traces of *E. coli* Hsp70 (DnaK), the purified proteins were analyzed by Western blot using α-DnaK antibody (Enzo Life Science, UK). The concentrations of the respective proteins were estimated by Bradford's assay (Sigma-Aldrich, USA) following manufacturer's instructions using Bovine Serum Albumin as protein standard (Appendix B7). The concentrations of the proteins were further computed using the Christoph-Leidig logarithm (http://christophleidig.de/tprot.html; Appendix B8, Zininga, 2015).

2.3. Analysis of the interaction of PfHsp70-x with hHop in parasites maintained at the erythrocytic stage

Parasite culture: Investigation of the direct association of PfHsp70-x with hHop using a co-affinity and immuno-affinity chromatography

P. falciparum 3D7 infected erythrocytes were cultured as previously described (Trager & Jensen, 1976; Gitau *et al.,* 2012; Zininga *et al.,* 2015a). The parasites were synchronized using sorbitol and harvested at the trophozoite stage. Infected erythrocytes were lysed with 0.1 % (w/v) saponin containing lysis buffer (Zininga *et al.,* 2015a) and incubated for 10 minutes at 25 °C. The saponin lysed erythrocyte and the PVM leaving the *P. falciparum* 3D7 parasite membrane intact (Figure 2.2).

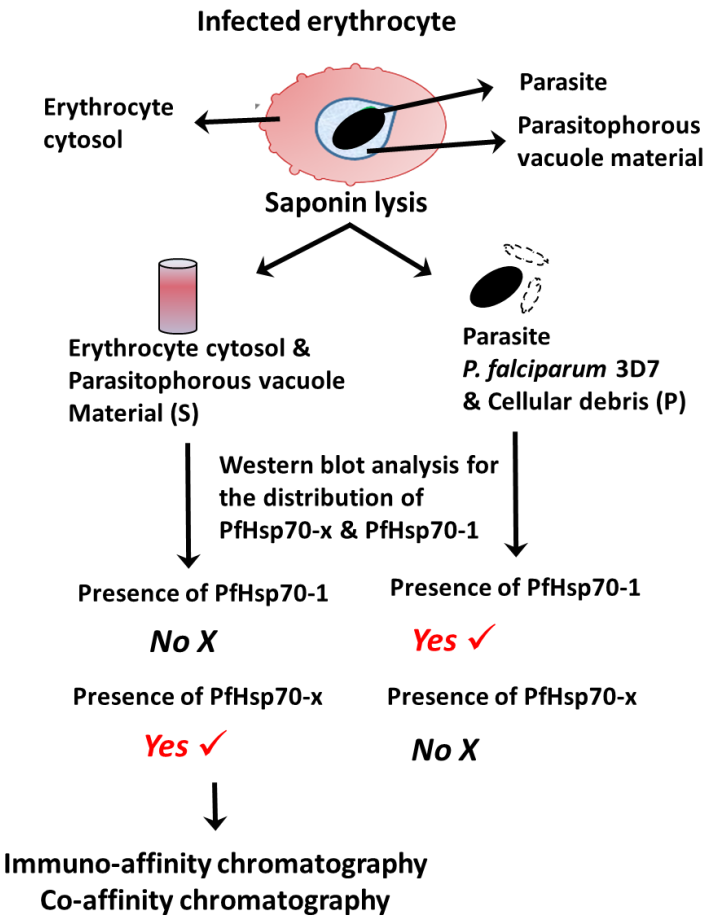

Figure 2.2: Schematic flow diagram of the preparation of parasite *P. falciparum* 3D7 infected erythrocyte
The *P. falciparum* 3D7 parasite infected erythrocytes were prepared by saponin surfactant producing two fractions, the supernatant (erythrocyte and the PV material) and the pellet (whole *P. falciparum* 3D7 parasite). The S represent the supernatant and P the parasite fraction. A mixed culture at the trophozoite stage was obtained and lysed using saponin. The cytosolic material and the parasite material and debris were analyzed using Western blot in order to evaluate the subcellular distribution of PfHsp70-x and pfHsp70-1.

After lysing the erythrocyte, cytosol and parasite fractions were respectively collected by centrifugation at 5000 xg for 10 minutes. The pellet (of the parasites obtained from lysis) was extensively washed using Phosphate-Buffered Saline (PBS) pH 7.4 (NaCl 137 mM, KCl 2.7 mM, $Na_2HPO_4$8 mM, and $KH_2PO_4$1.46 mM; Zininga *et al.,* 2015a). The pellet and supernatant fractions were obtained from the lysis (Figure 2.2). The fractions obtained were investigated in order to elucidate the distribution pattern of PfHsp70-x using antibodies specific for PfHsp70-x (Figure 2.2).

The erythrocyte cytosolic fraction (prey: input) was used to investigate the direct association of PfHsp70-x and hHop *in vitro*. Co-affinity chromatography as illustrated in Figure 2.3 below was conducted using a Pierce Protein Interaction kit (Thermo Scientific, USA), with modifications. Briefly, the erythrocyte cytosol fraction obtained (input) from saponin lysed erythrocytes in Figure 2.2 was re-suspended in Pierce lysis buffer (Thermo Scientific, USA). This was followed by incubation of recombinant PfHsp70-x_F/PfHsp70-x_T proteins (bait) with HisPur^{TM} cobalt affinity beads for 2 hrs at 4 °C to allow binding. Beads without immobilized recombinant PfHsp70-$x_{T/F}$ protein were used as a control. The samples were extensively washed using a solution of Tris-Buffered Saline (TBS; 25 mM Tris, 0.15M NaCl, pH 7.5): Pierce lysis buffer to remove unbound proteins and some non-specific bound proteins. Following washes, the bait-prey complex was subsequently pulled down as elutes in 250 µL of elution buffer (TBS: Pierce lysis buffer: Imidazole 290 mM). The co-affinity chromatography eluates were analyzed with silver stain (Appendix B11).

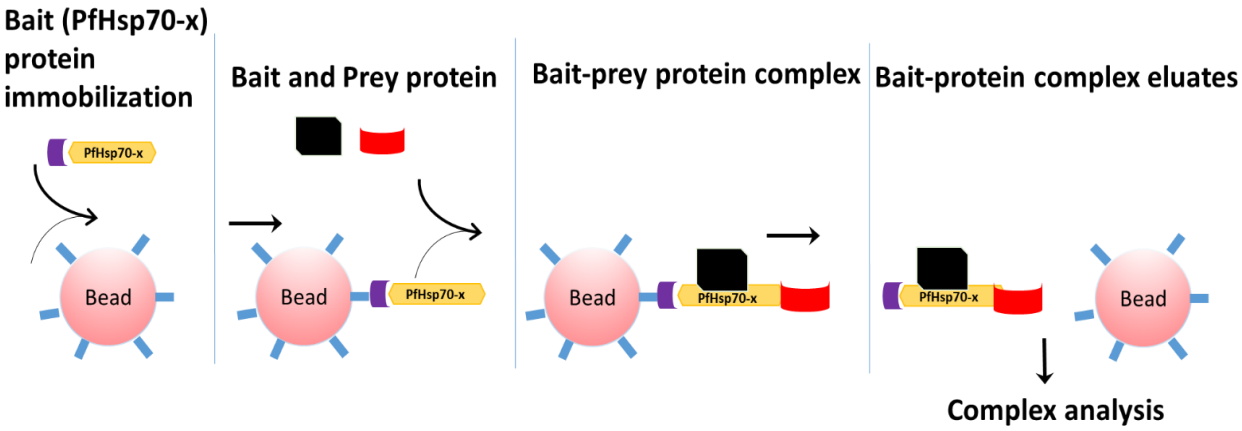

Figure 2.3: Co-affinity chromatography schematic diagram using recombinant proteins
Recombinant proteins (bait) immobilized on beads followed by incubation with the erythrocyte cytosol fraction (input: prey). The bait and prey associates and form a complex. The complex is analyzed using silver stain and Western blot analysis.

Additionally, the association of PfHsp70-x and hHop was conducted using immuno-affinity chromatography. The input fraction was resuspended in a volume of 500 µl immunoprecipitation lysis buffer (25 mM Tris-HCl pH 7.5, 150 mM NaCl, 1 mM EDTA, and 1 % (v/v) Tween-20) containing 1 mM PMSF. The chromatography was carried out using Pierce® Protein A/G Magnetic Beads according to the manufacturer's instructions with slight modifications (Thermo scientific, USA). Briefly, the input fraction was reconstituted to a volume of 500 µl. The constituents were added to the α-PfHsp70-x antibodies coupled to Pierce® Protein A/G Magnetic Beads. The mixture was incubated to allow binding to occur for 2 hrs at 4 °C with gentle shaking. The flow through was collected and the column was extensively washed. A 150 µl volume of elution buffer (50 mM glycine, pH 2.8) was used to elute the immunoprecipitate, which were concentrated using trichloroacetic acid at 10 % (v/v). The immunoprecipitate was analyzed using silver stain (Appendix B11). Erythrocyte cytosol fraction (input) was included as a control to show the presence of PfHsp70-x in the lysate prior to immino-affinity chromatography. As a negative control, the Pierce® Protein A/G Magnetic Beads incubated with input to validate non-specific binding of PfHsp70-x to the resin was also included. The assay was conducted as illustrated in Figure 2.4.

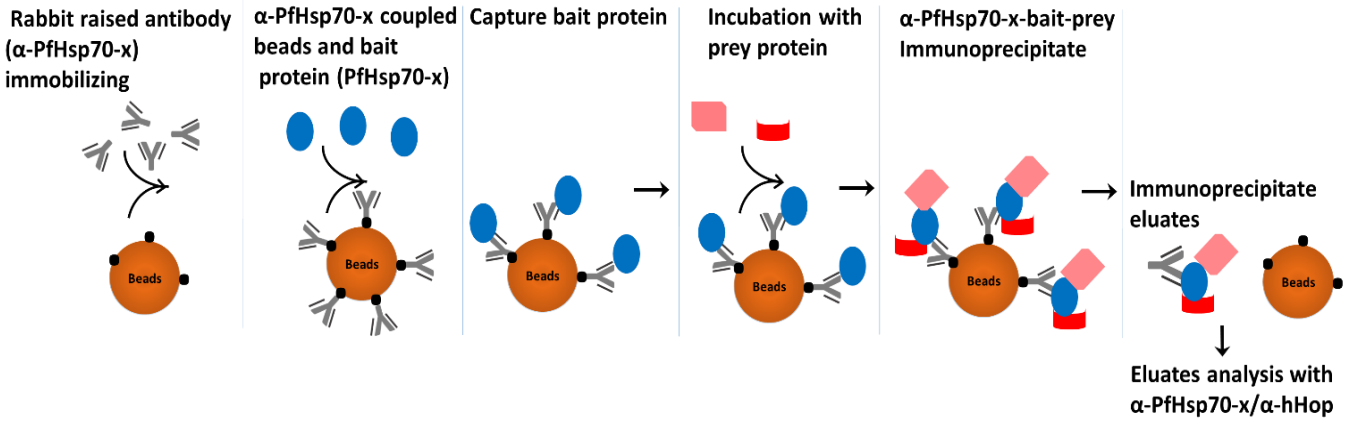

Figure 2.4: Schematic for immuno-affinity chromatography using specific antibody
Antibody specific for a target protein is immobilized on the beads. The antibody coupled beads are then incubated with recombinant protein (bait) followed by incubation with the input (prey). The bait protein immunoprecipitates with prey protein complex. The Immunoprecipitate eluates were analyzed by silver stain and Western blot analysis.

Chapter 3

Results

3.1. Bioinformatics based studies

3.1.1. The 3D models of the carboxyl ends of PfHsp70-x/PfHsp70-1/hHsp70

The protein sequences of the Hsp70 homologues are highly conserved as well as the structural orientation of their functional domains (Appendix A1; Appendix A2). Generally, Hsp70s are composed of three main domains the NBD, SBD and the C-terminal domain. The C-terminal domain of the Hsp70s are predominantly coiled, and are joined to the α-helical lid (Figure 3.1). The carboxyl-ends of PfHsp70-x and hHsp70 are composed only of coils (Figure 3.1). PfHsp70-1 possesses the tetrapeptide sequence Glycine-Glycine-Methionine-Proline (GGMP) motif that is generally known for immunomodulation, which is absent in both PfHsp70-x and hHsp70 (Figure 3.1, Appendix A3). The GGMP motif defines the orientation (fold) of the carboxyl end of PfHsp70-1 which is an elongated coil (Figure 3.1). Furthermore, in the absence of the GGMP motif the ends are compact and are in close proximity with the lid (Figure 3.1). This suggests that PfHsp70-1 is structurally distinct compared to PfHsp70-x and hHsp70.

The carboxyl-terminal end of PfHsp70-x possesses an asparagine (N) residue at position $N_{679,}$ which is different from the aspartic acid (D) residue in PfHsp70-1 and hHsp70 (Figure A3, Appendix A2). However, the N_{679} residue showed structural conservation with the D_{641} of hHsp70 (Figure 3.1). The overall folding pattern of the EEVN motif of PfHsp70-x is in reverse orientation but is structurally conserved with that of hHsp70 (Figure 3.1). However, the EEVD motif of PfHsp70-1 completely folds differently from that of PfHsp70-x and hHsp70 (Figure 3.1). The EEVD motif of PfHsp70-1 forms a short α-helix, showing structurally divergence from PfHsp70-x and hHsp70 (Figure 3.1). This suggests the role that the GGMPs may have in the structural conformation of the PfHsp70-1 EEVD motif.

The overall structural orientation of regions of Hsp70 homologues that are important for ATPase activity and substrate folding are conserved (Figure A1, A2; Appendix A1). Therefore,

PfHsp70-x and human hHsp70 may be functional substitutes (redundancy). Thus, PfHsp70-x may potentially form functional complexes with human co-chaperones. The EEVN motif of PfHsp70-x could facilitate its interaction with human TPR containing co-chaperones such as hHop, subsequently forming a complex with Hsp90.

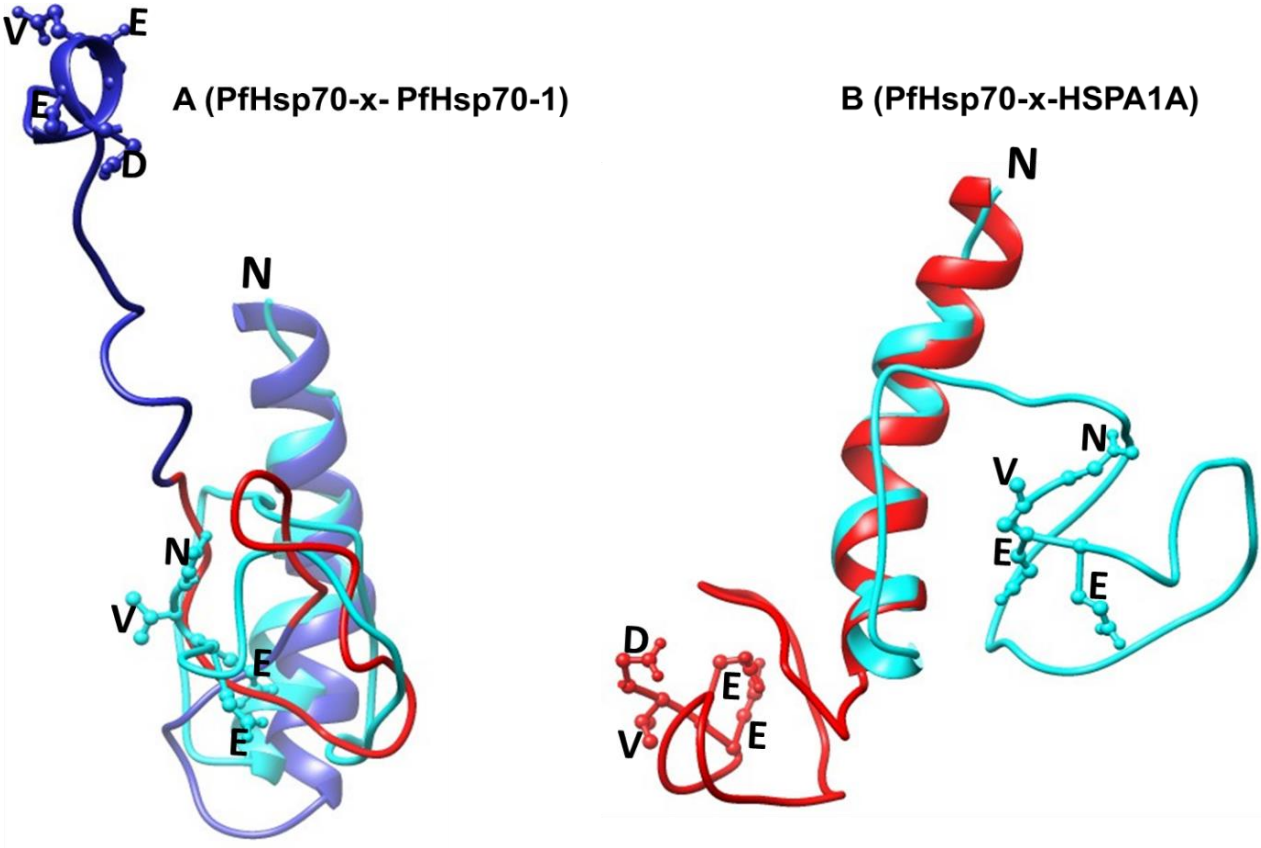

Figure 3.1. Comparison of 3D models of the carboxyl-terminal end of Hsp70 homologues.
The 3D models of the carboxyl-terminal structural orientation of PfHsp70-x (cyan) compared with PfHsp70-1 (medium blue) and hHsp70 (red). (**A**) PfHsp70-x-PfHsp70-1 carboxyl terminus, with the GGMP motif of PfHsp70-1 represented with a red segment. (**B**) PfHsp70-x-hHsp70 carboxyl terminus. The orientation of the carboxyl-terminal motifs showing residues involved in co-chaperone association (EEVD/EEVN represented by ball and stick). The models were generated by Phyre2 (www.sbg.bio.ic.ac.uk/phyre2) and visualized using Chimera (www.cgl.ucsf.edu/chimera; Pettersen *et al.,* 2004).

The Hsp70 C-terminal domain contains a conserved motif, EEVD, but PfHsp70-x has EEVN. The asparagine (N) residue is non-polar and hydrophilic. The aspartate (D) is a hydrophilic residue. Therefore, the D residue in the EEVD motif is negatively charged and is found exposed on the external surface of the folded proteins (Betts and Russell, 2003; 2007). At physiological cellular pH aspartate interacts with amino acids of opposite charge forming strong ionic bonds which is observed in the EEVD motifs of PfHsp70-1 and hHsp70 (Figure

3.1). Additionally, D is known to interact with the positively charged and hydrophilic lysine (K) residue that is also surface exposed in the co-chaperone Hop (Appendix A3). The uncharged N residue obtains a negative charge at physiological condition and is also surface exposed. Thus, the carboxyl-terminal EEVN motif of PfHsp70-x may interact with oppositely charged residues forming weak hydrogen bonds (Betts & Russell, 2003; 2007). The proposed interaction with the TPR domain of co-chaperone Hop is important for the formation of multi-chaperone complexes with other chaperones such as Hsp90. It is thus possible that the C-terminal N residue of PfHsp70-x may equally facilitate co-chaperone binding.

3.1.2. Prediction of PfHsp70-x's interaction partners

The data generated predicts the interaction of PfHsp70-x with chaperones such as human Hop, and human Hsp90 (Figure 3.2). Interestingly, PfHsp70-x is predicted to interact with host erythrocyte cytosol co-chaperones, hHop (STIP1: NP_6202661) and hHsp90 (alpha: NP_001017963.2 and beta: NP_001258899.1) (Figure 3.2; Table 3.1). Human NEF hBag2 (NP_004273.1) was also predicted to be a potential interactor (Figure 3.2; Table 3.1). NEFs regulate substrate binding and release (Shonhai, 2014). PfHsp70-1 nucleotide exchange is thought to be regulated by PfHsp70-z which acts as a NEF (Zininga *et al.,* 2016). Therefore, hBag2 may serve as a potential NEF for PfHsp70-x (Figure 3.2).

Hsp40s are known to recruit substrates and bind to Hsp70 handing over the substrate to the Hsp70 SBD (Botha *et al.,* 2011; Shonhai, 2014). Recent studies have shown interaction of Hsp70s with type II PfHsp40 (PF3D7_0113700) (Daniyan *et al.,* 2016; Jha *et al.,* 2017). The ATPase activity of PfHsp70-1 has been shown to be stimulated by its interaction with Hsp40. Furthermore, the function of the association of hHsp70 with *P. falciparum* Hsp40 has not been understood (Jha *et al.,* 2017). However, the function of such associations has not been fully characterized. Therefore, PfHsp70-x may possibly interact with the Hsp90 human chaperone through human Hop in a similar manner to that of PfHsp70-1/PfHop and PfHsp90. Thus, the interaction of PfHsp70-x with the human chaperone system may facilitate exported parasite proteins being transfered from PfHsp70-x to hHsp90 through hHop in infected erythrocytes (Figure 3.2).

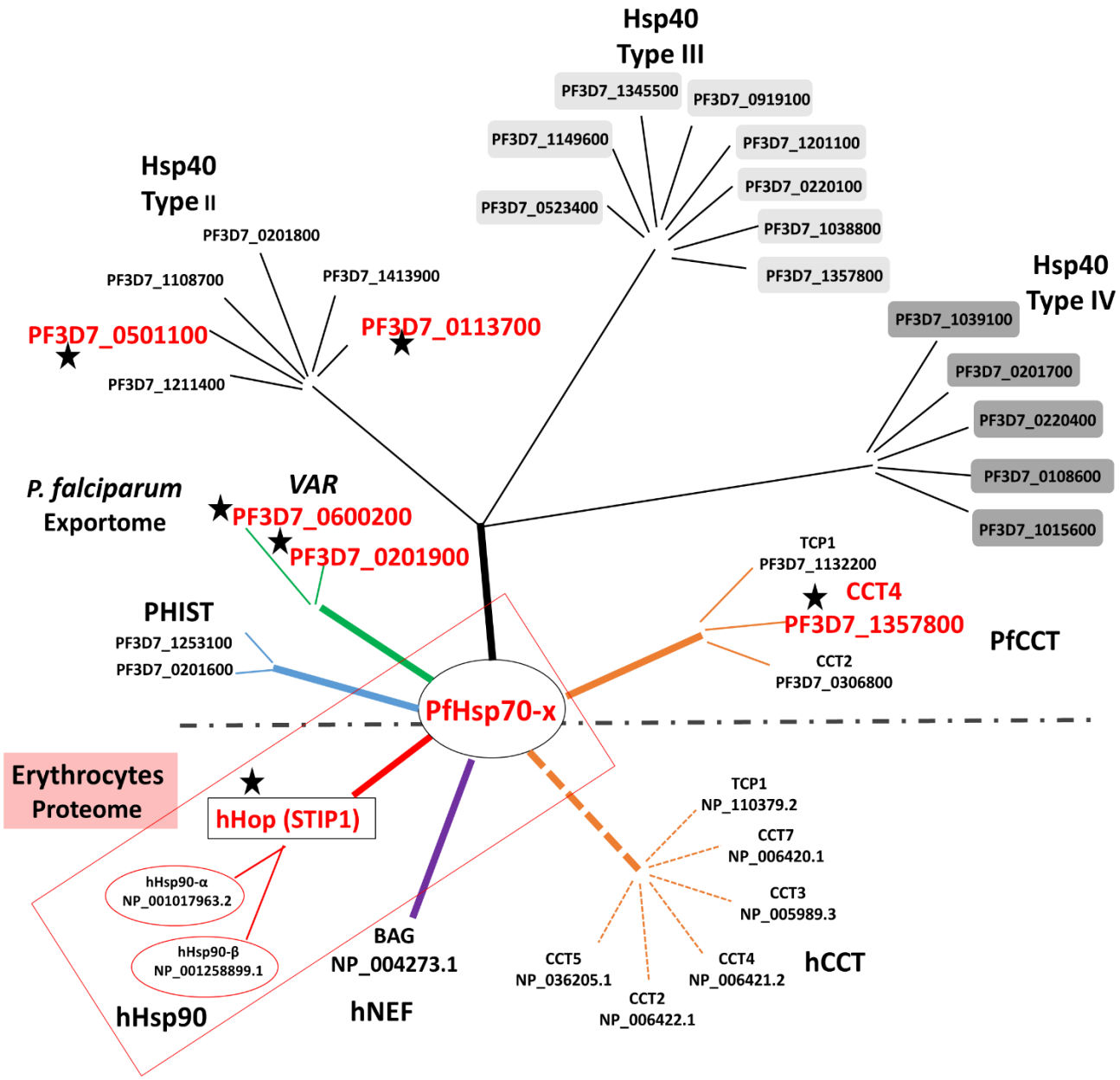

Figure 3.2. Network for the predicted potential partners of PfHsp70-x
The predicted network of potential interactions PfHsp70-x within the *P. falciparum* infected erythrocyte. The lines (edges) sizes and colors represent distinct chaperones that interact with PfHsp70-x. The thick edges connected to PfHsp70-x represent distinct chaperones families, i.e., the Hsp70 co-chaperones Hsp40s (black), PHIST (blue), VAR membrane proteins (green), chaperonins (solid orange - *P. falciparum* and broken orange – human chaperonins) and NEF (purple). The red edges and box represent the co-chaperone system of PfHsp70-x with Hop (NP_620266.1), and hHsp90s (hHsp90-α; NP_001017963.2, hHsp90-β; NP_001258899.1). The thin (orange) edges represents group II chaperonin folding system while the black represent the PfHsp40 types. The stars (black) indicates the experimentally validated interactions. The interaction network was predicted using STRING (www.string-db.org; Szklarczyk *et al.,* 2017) and analyzed using Cytoscape (Shannon *et al.,* 2003).

Furthermore, PfHsp70-x was also predicted to interact with the exported group of *Plasmodium* proteins such as the *Plasmodium* helical interspersed subtelomeric (PHIST) family (Figure 3.2). PHIST proteins are erythrocyte membrane destined, and thus are implicated in erythrocyte remodeling facilitating knob formation and PfEMP1 distribution onto the erythrocyte's surface (Proellocks *et al.,* 2015). Therefore, interaction of PfHsp70-x with PHIST family of proteins suggests its involvement in protein translocation within the infected erythrocyte and enhancing remodeling. Human chaperones and some *P. falciparum* exportome mainly the Hsp40 (DnaJ) family, predicted to interact with PfHsp70-x (Figure 3.2) are listed together with their probability scores of interactions (the most likely chance of interactions) (Table 3.1).

Table 3.1: The predicted chaperone functional interactors of PfHsp70-x

PfHsp70-x Interactors of parasite *P. falciparum* origin

Protein PlasmoDB accession #	MW (KDa)	Protein description	Characterized localization	Scores/ Reference
1. PF3D7_1434300	66.06	STI1-like protein, Hsp70/Hsp90 organizing protein	cytosol	0.940
2. PF3D7_0201800	48.28	Knob associated heat shock protein 40 (KAHsp40), Type II	membrane	*0.988*
3. PF3D7_1108700	62.37	Heat shock protein DnaJ homologue Pfj2, Type II	cytosol	*0.938*
4. PF3D7_0501100	46.36	Heat shock protein putative (DnaJ), Type II	membrane	*0.924* Jha *et al.,* 2017 Zhang *et al.,* 2017
5. PF3D7_1211400	28.06	Heat shock protein DnaJ homologue Pfj4, Type II	cytosol	*0.913*
6. PF3D7_1413900	45.23	DnaJ protein, putative, Type II	membrane	*0.899*
7. PF3D7_0113700	46.98	Heat shock protein 40, Type II	cytosol	*0.840* Daniyan *et al.,* 2016
8. PF3D7_1201100	107.62	RESA-like protein with PHIST and DnaJ domains, Type III	membrane	*0.862*
9. PF3D7_0220100	117.28	DnaJ protein, putative, Type III	membrane	*0.862*
10. PF3D7_1038800	107.58	RESA-like protein with PHIST and DnaJ domains, Type III	membrane	*0.860*
11. PF3D7_0523400	61.90	DnaJ protein, putative, Type III	membrane	*0.849*
12. PF3D7_0201700	105.90	DnaJ protein, putative, Type IV	membrane	*0.979*
13. PF3D7_0220400	61.90	DnaJ protein, putative, Type IV	membrane	*0.849*
14. PF3D7_0114000	17.09	exported protein family 1 (EPF1)/ PFGEXP06, Type IV	membrane	*0.849*
15. PF3D7_0108600	37.63	Conserved *Plasmodium* protein, unknown function	membrane	*0.899*
16. PF3D7_1253100	34.78	*Plasmodium* exported protein (PHISTa) , unknown function	membrane	*0.870*
17. PF3D7_0831200	11.41	DNAJ protein, putative	membrane	*0.862*
18. PF3D7_0201600	58.58	*Plasmodium* exported protein (PHISTb) RLP1	membrane	*0.862*
19. PF3D7_1333000	29.06	20 kDa chaperonin (CPN20), chaperonin	cytosol	*0.856*
20. PF3D7_1357800	57.97	T-complex protein 1 subunit delta CCT4, chaperonin	cytosol	*0.757* Zhang *et al.,* 2017
21. PF3D7_0113200	70.11	T-complex protein 1, alpha subunit TCP1, chaperonin	cytosol	*0.937*
22. PF3D7_0306800	59.19	T-complex protein 1 subunit beta CCT2, chaperonin	cytosol	*0.847*
23. PF3D7_1240300	30.03	erythrocyte membrane protein 1 (PfEMP1), VAR	membrane	*0.605*

24. PF3D7_0600200	33.34	erythrocyte membrane protein 1 (PfEMP1), VAR	membrane	*0.595* Külzer *et al.,* 2012
25. PF3D7_0201900	27.36	erythrocyte membrane protein 3 (EMP3)	membrane	Cobb *et al.,* 2017
PfHsp70-x Interactors of human origin				
Protein accession #	**MW (KDa)**	**Protein description**	**Characterized localization**	**Scores/ Reference**
26. NP_001017963.2	98.16	Heat shock protein Hsp 90-alpha (hHsp90-α)	cytosol	*0.984*
27. NP_001258899.1	83.26	Heat shock protein Hsp 90-beta (hHsp90-β)	cytosol	*0.980*
28. NP_006810.01	62.63	Stress-induced-phosphoprotein 1 (STIP1)	cytosol	*0.957* Mabate, 2017
29. NP_004273.1	23.77	BAG family molecular chaperone regulator 2 (BAG2), NEF	cytosol	*0.763*
30. NP_110379.2	60.34	T-complex , chaperonin protein 1 subunit alpha isoform a (CCT1/TCP1), chaperonin	cytosol	*0.807*
31. NP_006420.1	59.36	T-complex protein 1 subunit eta isoform a (CCT7), chaperonin	cytosol	*0.760*
32. NP_005989.3	60.53	T-complex protein 1 subunit gamma isoform a (CCT3), chaperonin	cytosol	*0.759*
33. NP_006421.2	57.92	T-complex protein 1 subunit delta isoform a (CCT4), chaperonin	cytosol	*0.757*
34. NP_006422.1	57.48	T-complex protein 1 subunit beta isoform 1 (CCT2), chaperonin	cytosol	*0.757*
35. NP_036205.1	59.67	T-complex protein 1 subunit epsilon isoform a (CCT5), chaperonin	cytosol	*0.757*

Parenthesis represent molecular weights (MW; kDa) and the references are of interactions that have been experimentally validated. The following represent chaperone families; NEF-nucleotide exchange factor, PfHsp40 type II, III and IV, CCT- chaperonin containing TCP-1 also known as TCP-1 Ring Complex (TRiC).

3.2. Biochemical assays

3.2.1. Confirmation of pQE30-*PfHsp70-x$_F$/PfHsp70-x$_T$* plasmids

The integrity of pQE30-*PfHsp70-x$_F$/PfHsp70-x$_T$* plasmid constructs (Section 2.2.1; Figure 3.3A;B) were verified using restriction digestion analysis (Figure 3.3C). A single restriction digest was conducted with either *Bam* HI or *Hind* III resulting in a linearized plasmid of 5462 bp for pQE30-*PfHsp70-x$_F$* and 5450 bp for pQE30-*PfHsp70-x$_T$*. Double digestion was conducted using both *Bam* HI and *Hind* III which resulted in two linearized fragments of 3424 bp corresponding to the pQE30 expression vector, as well as 2040 bp for *PfHsp70-x$_F$* and 2028 bp for *PfHsp70-x$_T$* (Figure 3.3C).

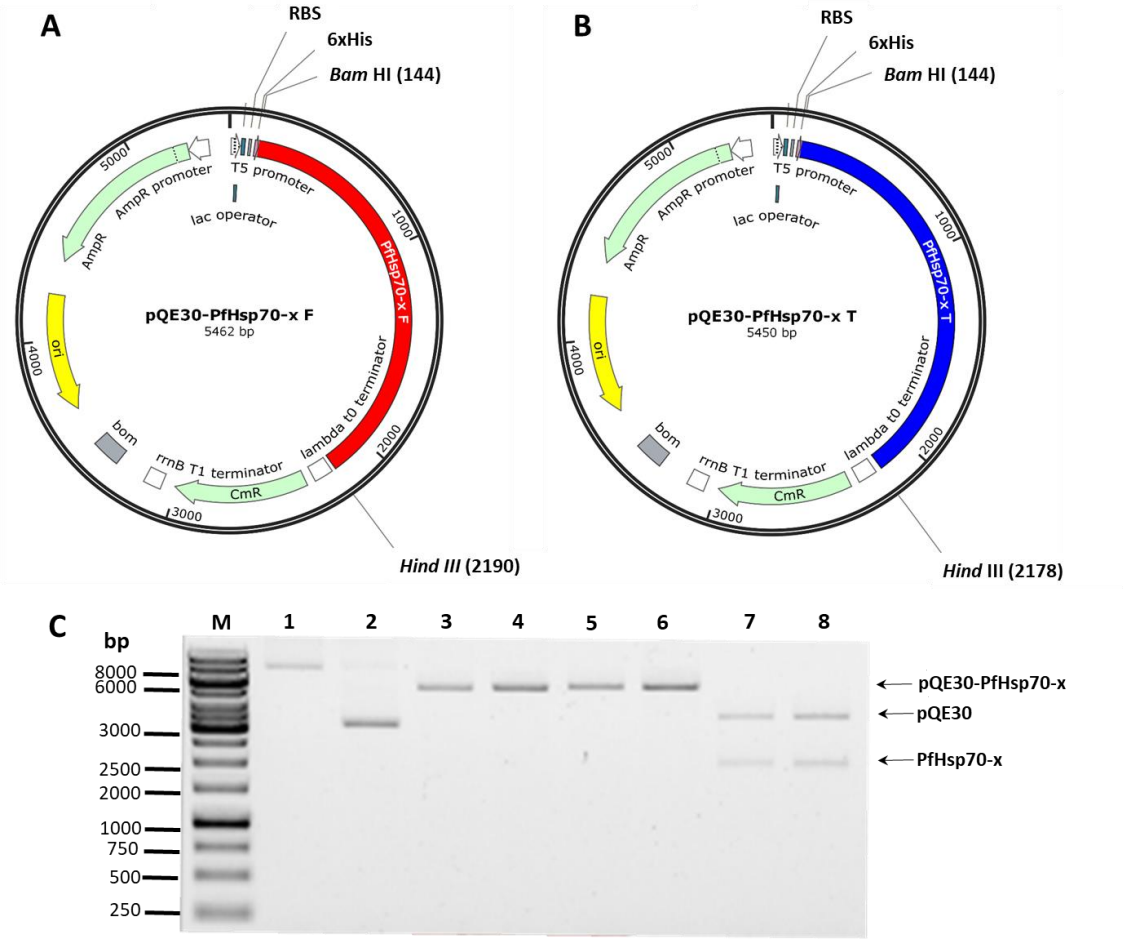

Figure 3.3: pQE30-*PfHsp70-X$_F$/ PfHsp70-x$_T$* plasmid maps and restriction agarose gels
Restriction analysis of DNA plasmids. (**A**) Plasmid map of pQE30-*PfHsp70-x$_F$* and (**B**) pQE30-*PfHsp70-x$_T$* constructs showing the *Bam* HI and *Hind* III restriction sites. (**C**) Agarose gel electrophoresis of pQE30-*PfHsp70-x$_F$/PfHsp70-x$_T$*: lane M, DNA molecular weight ladder in bp; lane 1, undigested pQE30-*PfHsp70-x$_F$*, lane 2, undigested pQE30- *PfHsp70-x$_T$*; lane 3, pQE30-*PfHsp70-x$_F$* and lane 4, pQE30-*PfHsp70-x$_T$* digested with *Hind* III; lane 5, pQE30-*PfHsp70-x$_F$* and lane 6, pQE30-*PfHsp70-x$_T$* digested with *Bam* HI; lane 7, pQE30-*PfHsp70-x$_F$* and lane 8, pQE30- *PfHsp70-x$_T$* digested with both *Bam* HI and *Hind* III.

3.2.2. Confirmation of pQE30-*hHop* plasmid

Single restriction digest of pQE30-*hHop* plasmid construct with either *Bam* HI or *Hind* III (Figure 3.4A) resulted in a linearized plasmid that resolved at 4979 bp (Figure 3.4B). Double digestion with both *Bam* HI and *Hind* III resulted in two linearized fragments of 3424 bp corresponding to the pQE30 vector and 1644 bp for the *hHop* insert size (Figure 3.4B).

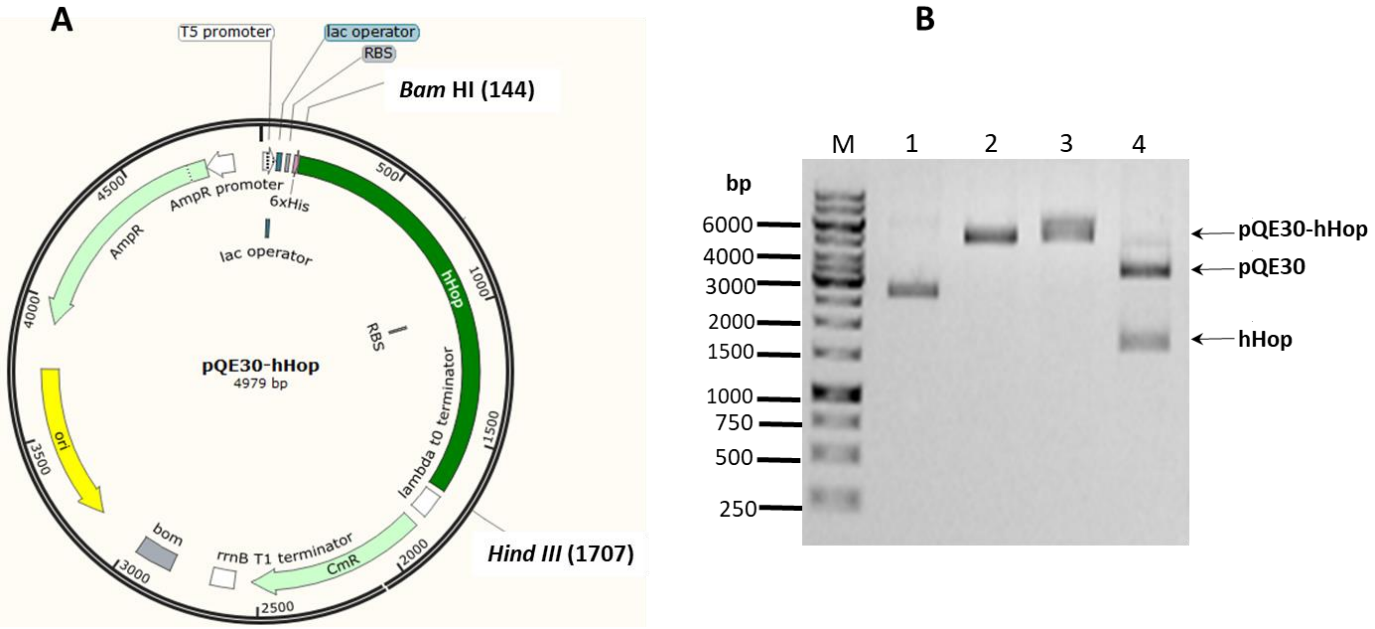

Figure 3.4: pQE30-*hHop* plasmid map and restriction agarose gel
Restriction analysis of pQE30-*hHop* DNA plasmids (**A**) Plasmid map of pQE30-*hHop* showing the *Bam* HI and *Hind* III restriction sites. (**B**) Agarose gel electrophoresis of pQE30-*hHop*: lane M, DNA molecular weight ladder in bp; lane 1, undigested pQE30-*hHop* plasmid; lane 2, pQE30-*hHop* digested with *Bam* HI; lane 3, pQE30-*hHop* digested with *Hind* III; lane 4, pQE30-*hHop* digested with both *Bam* HI and *Hind* III.

3.2.3. Confirmation of pQE30-*hHsp70* plasmid

The pQE30-*hHsp70* plasmid construct's integrity (Section 2.2.1) was verified using restriction analysis (Figure 3.5A). The construct was digested using either *Bam* HI or *Hind* III which resulted in a linearized plasmid of 5363 bp (Figure 3.5B). A double digestion using both restriction enzymes *Bam* HI and *Hind* III resulted in two linearized fragments of 3424 bp corresponding to the pQE30 vector and 1953 bp of the *hHsp70* insert (Figure 3.5B). In lane 2 and 3, single digested plasmid constructs were observed to take up linear conformations. In lane 2 the plasmid DNA migrated slowly at approximately 6000 bp. This suggests that the plasmid DNA was supercoiled.

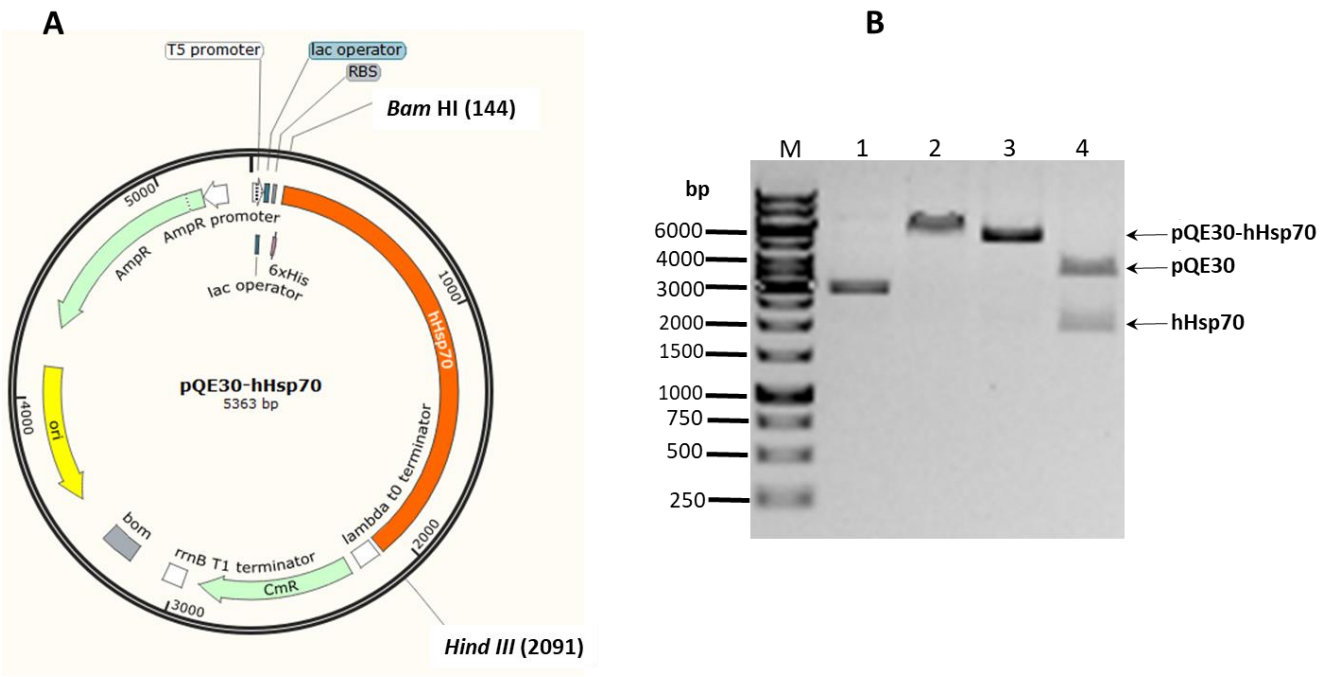

Figure 3.5: pQE30-*hHsp70* plasmid map and restriction agarose gel
Restriction analysis of pQE30-*hHsp70* DNA plasmids. (**A**) Plasmid map of pQE30-*hHsp70* showing the *Bam* HI and *Hind* III restriction sites. (**B**) The agarose gel electrophoresis lane M, DNA molecular weight ladder in bp; lane 1, undigested pQE30-*hHsp70* plasmid; lane 2, pQE30-*hHsp70* digested with *Bam* HI; lane 3, pQE30-*hHsp70* digested with *Hind* III; lane 4, pQE30-*hHsp70* digested with both *Bam* HI and *Hind* III.

3.2.4. Recombinant PfHsp70-x_F/PfHsp70-x_T protein expression and purification

Recombinant PfHsp70-x_F/PfHsp70-x_T proteins were successfully expressed in *E. coli* BL21 Star (DE3) cells (Figure 3.6). Protein products were analyzed by SDS-PAGE and confirmed using Western blot analysis using peptide specific antibodies raised against PfHsp70-x (α-PfHsp70-x; Külzer *et al.,* 2012) and α-His specific antibodies. SDS-PAGE analysis showed a band whose intensity increased over time as a band of approximately 76 kDa in size (Figure 3.6). *E. coli* BL21 Star (DE3) cells transformed with pQE30 were used as a negative control. The pQE30 transformed *E. coli* BL21 Star (DE3) cells showed absence of the 76 kDa band. The expected proteins were only detected in cells transformed with the constructs. This suggests that the 76 kDa band represented recombinant PfHsp70-x_F and PfHsp70-x_T respectively, as confirmed by Western blot analysis (Figure 3.6, lower panels). Both PfHsp70-$x_{F/T}$ were expressed prior to induction due to leaky expression. Unregulated promoters such as the T5 promoter cause leaky expression (Rosano & Ceccarelli, 2014). However, the

expression of PfHsp70-x_F/PfHsp70-x_T was further induced by IPTG, with the greatest expression at 6 hr (Figure 3.6A, lower panel).

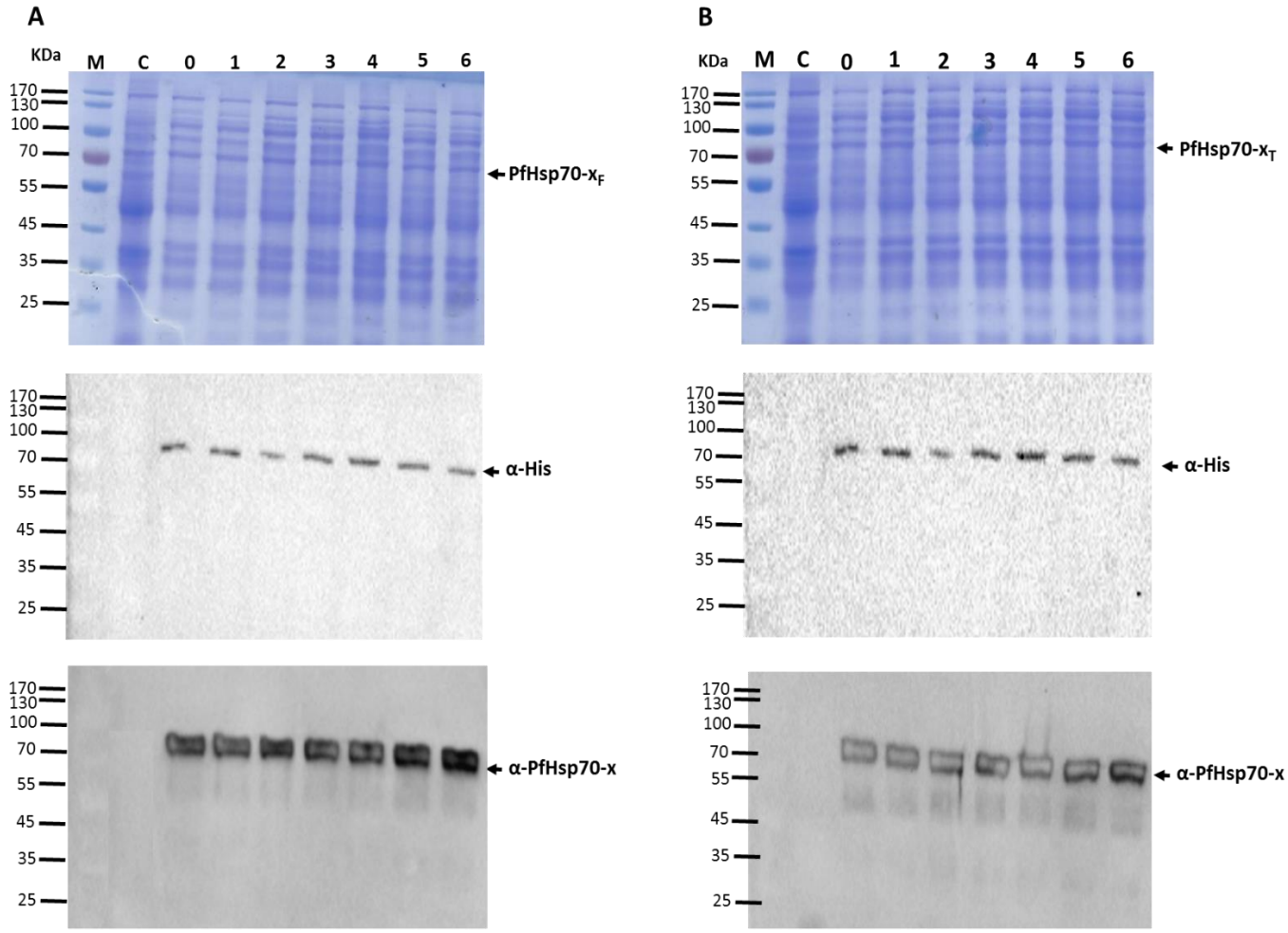

Figure 3.6: Expression of recombinant PfHsp70-x_F/PfHsp70-x_T proteins
SDS-PAGE (12%) analysis of the protein expression of (**A**) PfHsp70-x_F, (**B**) PfHsp70-x_T in *E. coli* BL21 Star (DE3) cells. Samples collected of *E. coli* BL21 Star (DE3) cells transformed with pQE30-*PfHsp70-*x_F/pQE30-*PfHsp70-*x_T plasmids at different time intervals were assessed by SDS-PAGE and Western blot analysis. Lane M-Page ruler in kDa; lane C-total extract from the IPTG induced cells transformed with a neat pQE30 plasmid; lane 0-total extract of cells transformed with pQE30/*PfHsp70-*x_F/*PfHsp70-*x_T prior to IPTG induction; lanes 1 - 6 – total extracts from cells transformed with pQE30/*PfHsp70-*x_F/*PfHsp70-*x_T obtained 1 - 6 hr post IPTG induction. Lower panels: Western blot analysis was conducted using α-His and α-PfHsp70-x antibodies, confirming expression of PfHsp70-x_F and PfHsp70-x_T proteins.

The PfHsp70-$x_{F/T}$ proteins were expressed in a partially soluble form and were hence purified from the soluble fraction. The purification was analyzed by 12 % SDS-PAGE and Western blot analysis. The SDS-PAGE showed PfHsp70-x proteins in both pellet and soluble fractions (Figure 3.7). Western blot analysis using α-His and α-PfHsp70-x antibodies confirmed the presence of the protein in the pellet and supernatant fractions (Figure 3.7; lower panel). The

expressed PfHsp70-x_F and PfHsp70-x_T recombinant proteins were purified natively using nickel affinity chromatography (Figure 3.7).

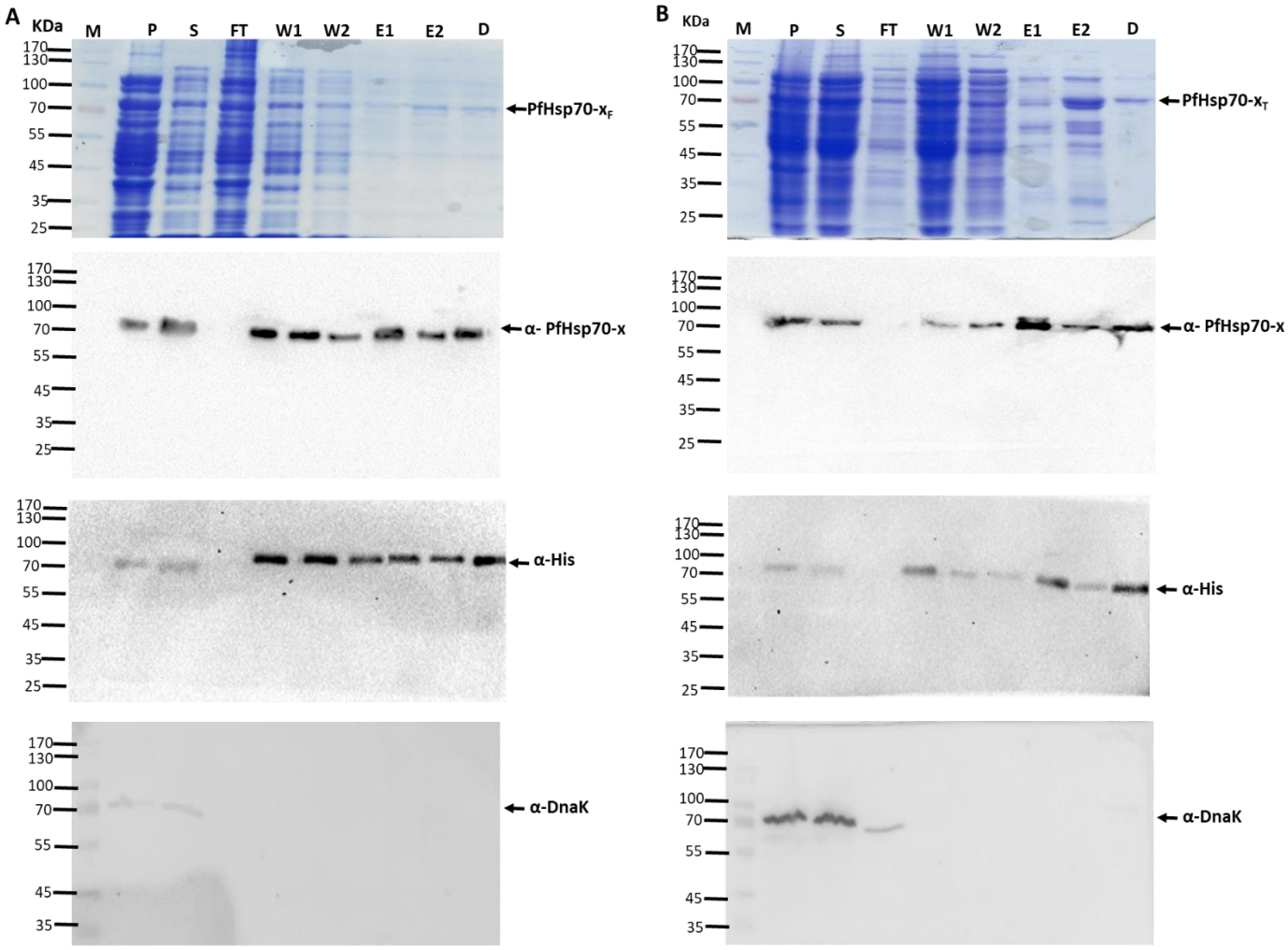

Figure 3.7: Purification of recombinant PfHsp70-x_F/PfHsp70-x proteins
Recombinant PfHsp70-x_F and PfHsp70-x_T expressed in *E. coli* BL21 Star (DE3) cells transformed with (**A**) pQE30-*PfHsp70-x_F*, (**B**) *pQE30-PfHsp70-x_T* were successfully purified. SDS-PAGE (12%) and Western blot analysis for the purification; lane M-Page ruler in kDa; lane P, S- pellet and soluble fractions obtained from the total lysate of cells transformed with pQE30-*PfHsp70-x_F/PfHsp70-x_T*, respectively. Lane FT- flow through; lane W- wash samples, lane E- eluted samples using 500 mM Imidazole and lane D- dialyzed protein. Lower panels: Western blot analysis based on use of α-His and α-PfHsp70-x antibodies confirming purification of the proteins. Western blot analysis was conducted using α-DnaK antibodies to confirm the proteins' purity.

Some of the protein was lost in washes (Figure 3.7; lane W). However, the recombinant PfHsp70-x protein(s) were successfully purified as a band of approximately 76 kDa (Figure 3.7; lanes E1; E2) and dialyzed (Figure 3.7; Lane D). The final yield of the purified proteins resulted in 19.2 mg obtained from 1 L of culture for PfHsp70-x_F and 16.0 mg for PfHsp70-x_T obtained from 1 L of culture. Purified proteins were further validated using α-DnaK antibody.

Western blot analysis confirmed that the eluted and dialyzed products were DnaK-free and also free from any other protein contaminants' (Figure 3.7, lower panels).

3.2.5. Recombinant hHop protein expression and purification

The recombinant hHop protein was expressed successfully at 37 ˚C in *E. coli* JM109 (DE3) cells and purified as previously described (Figure 3.8; Zininga *et al.,* 2015a;b).

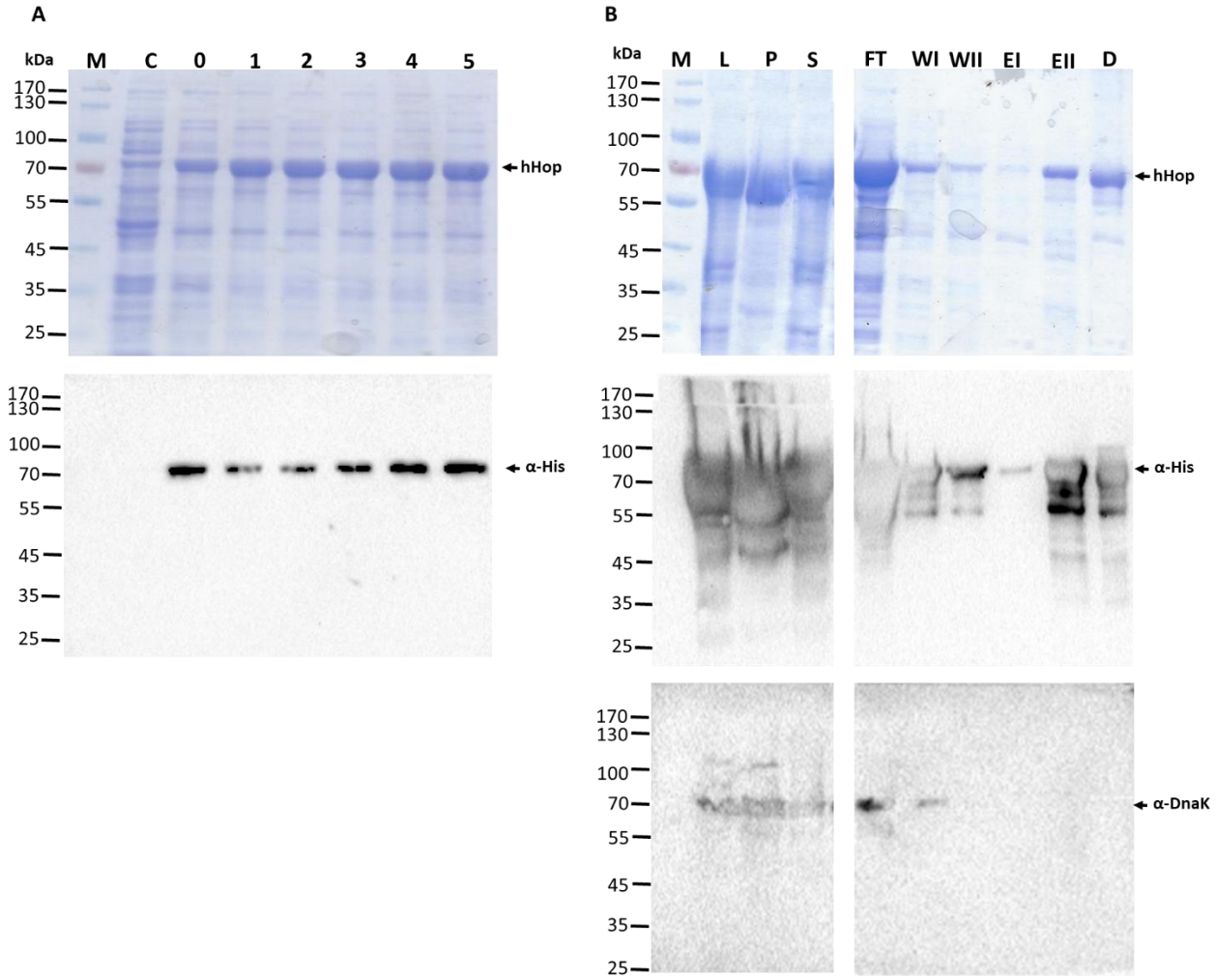

Figure 3.8: Expression of recombinant hHop protein and purification
The hHop was successfully expressed in *E. coli* JM109 DE3 cells transformed with pQE30-*hHop*. SDS-PAGE (12%) and Western blot analyses. (**A**) Expression and (**B**) purification of hHop protein. Lane M-Page ruler in kDa; lane C -Total extract for cells transformed with a neat pQE30 plasmid; lane 0 - total cell extract transformed with pQE30-*hHop* prior to IPTG induction; lanes 1 - 5 hrs post induction, respectively. Lane L, total cell extract; lane P, pellet and S, soluble fractions obtained from the total lysate for cells transformed with pQE30-*hHop*, respectively; lane FT; flow through; lanes W; wash samples, lanes E; hHop protein eluted using 500 mM Imidazole and lane D, dialyzed protein. Lower panel: Western blot analysis of hHop was conducted using of α-His and α-Dnak antibodies confirming purification of hHop protein.

Cells transformed with pQE30 were used as control and SDS-PAGE showed absence of a 66 kDa band in these cells (Figure 3.8A). The protein was expressed upon induction with 1 mM IPTG (Figure 3.8A). Western blot analysis confirmed the expression of hHop protein at 66 kDa using α-His antibody. Recombinant hHop protein was expressed as a partially soluble protein (Figure 3.8B, lane S). The hHop was purified successfully by affinity chromatography under native conditions (Figure 3.8B). Most of the protein was lost in the flow through (FT). This suggesting that some of the protein was not bound to the beads (Figure 3.8B, lane FT). Some of the protein was lost in washes (Figure 3.8, lane W). The recombinant hHop protein was purified successfully and represented in elution 2 as a band of approximately 62 kDa (Figure 3.8B, lanes E2). Western blot analysis using α-His antibodies confirmed the presence of the protein (Figure 3.8B; lower panel). Furthermore, the purified product was dialyzed and quantified. The yield of the final protein was 39.2 mg obtained from 1 L of culture.

3.2.6. Expression of recombinant hHsp70 protein and purification

The human Hsp70 protein (hHsp70) was expressed in *E. coli* JM109 (DE3). The expressed hHsp70 protein was assessed by SDS-PAGE and confirmed by Western blot analysis using α-His antibody (Figure 3.9A). The pQE30 transformed *E. coli* JM109 (DE3) cells were used as a negative control for the expression study. The control and pre-induction samples did not exhibit heterologous expression of the 74 kDa band (Figure 3.9A). The post-induction samples showed an increase in the level of expression of a band of approximately 74 kDa with optimum expression at 4 hr (Figure 3.9A). Western blot analysis successfully confirmed induction and expression of the 74 kDa band hHsp70 (Figure 3.9A, lower panel).

Recombinant hHsp70 protein was successfully purified by affinity chromatography (Figure 3.9B). The recombinant protein was detected in the total cell lysate and was expressed in soluble form as a band of 74 kDa (Figure 3.9B, lower panel). Some protein was detected in the FT sample, hence suggesting that some protein did not bind to the column beads (Figure 3.9B, lane FT). The protein was successfully eluted (Figure 3.9B, lane E1 and E2). Additionally, some of the protein was lost during washing, suggesting that not all of the hHsp70 bound onto the column (Figure 3.9B, lane W). Western blot analysis of the purified hHsp70

was conducted (Figure 3.9B, lower panel). The final yield of the purified hHsp70 protein resulted in 30.5 mg obtained from 1 L of culture.

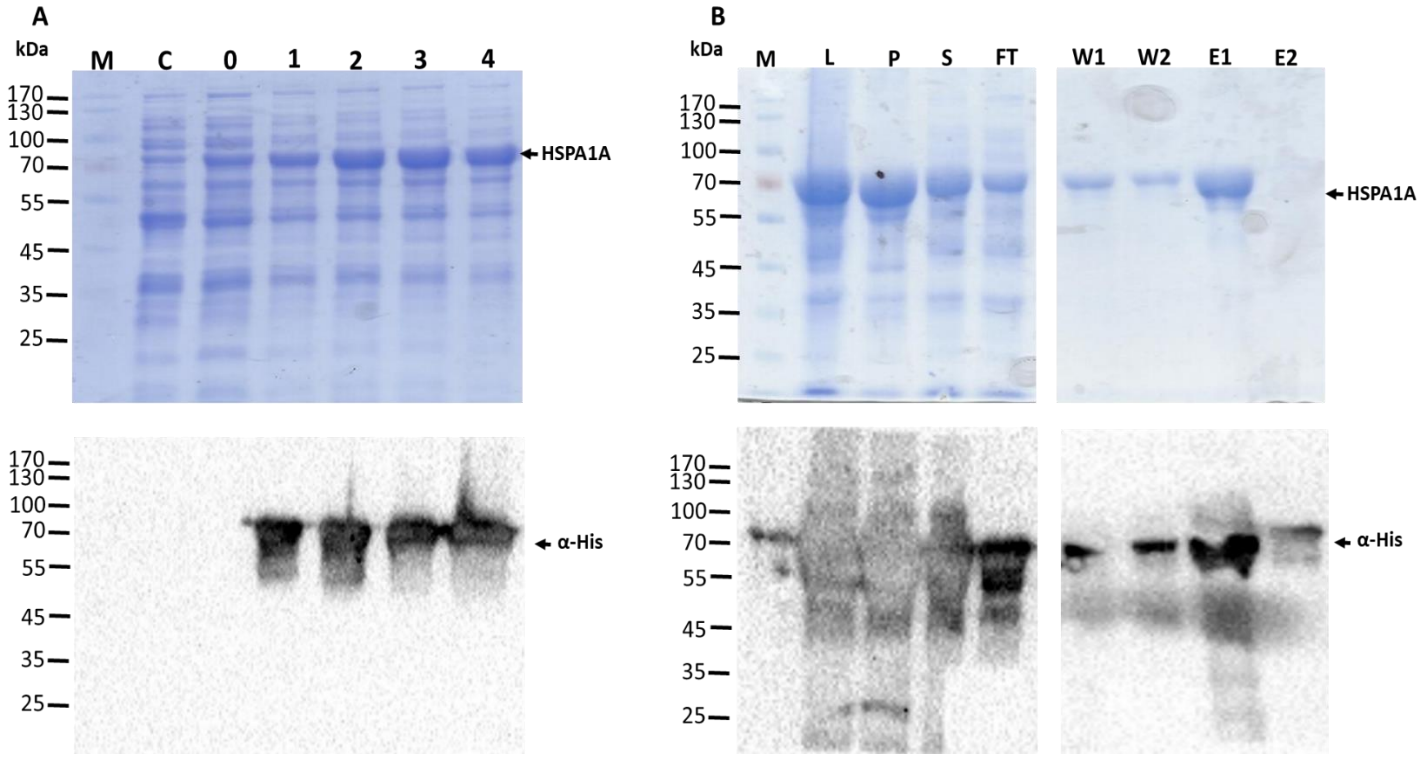

Figure 3.9: Expression of recombinant hHsp70 protein and purification
The hHsp70 was successfully expressed in *E. coli* JM109 DE3 cells transformed with pQE30-*hHsp70*. SDS-PAGE (12%) and Western blot analyses of the (**A**) expression and (**B**) purification of hHsp70 protein. Lane M-Page ruler (Thermo Scientific, USA) in kDa; lane C -Total extract for cells transformed with neat pQE30 plasmid; lane 0 - total cell extract transformed with pQE30-*hHsp70* prior to IPTG induction; lanes 1 - 4 hr post induction, respectively. Lane L, total lysate, P, pellet and S, soluble fractions obtained from the total lysate for cells transformed with pQE30-*hHsp70*, lane FT; flow through; lanes W; washes, and lanes E; hHsp70 eluted using 500 mM Imidazole. Lower panel: Western blot analysis of hHsp70 using of α-His antibodies.

3.2.7. Validation of the distribution of PfHsp70-x in *P. falciparum* 3D7 cellular fractions

PfHsp70-x is exported by the parasite into the PV as well as the cytosol of infected erythrocytes (Section 1.6.6.2; Külzer *et al.,* 2012). The bioinformatics results in this study predicted PfHsp70-x protein to share high sequence identity with homologue PfHsp70-1 (Appendix A1, A2; Zininga, 2015). *P. falciparum* 3D7 parasite fractions used for analysis were obtained from infected erythrocytes lysed using saponin, as previously described (Zininga *et al.,* 2015b) and illustrated in Figure 2.2. In this study, the fractions were investigated using silver stain and Western blot analysis in order to elucidate the presence and distribution of PfHsp70-x using antibodies specific for PfHsp70-x. PfHsp70-1 was used as a control which

was identified using antibodies specific for PfHsp70-1. Recombinant PfHsp70-x and PfHsp70-1 were included as positive controls (Figure 3.10). PfHsp70-1 was detected in the pellet fraction (Figure 3.10). On the other hand, PfHsp70-x was not detected in pellet fraction, signifying that it was exported and not associated with the parasite fraction (Figure 3.10). The rabbit raised PfHsp70-x antibody (α-PfHsp70-x) confirmed the presence of PfHsp70-x in the erythrocyte cytosolic material as reported by Külzer and colleagues (2012) (Figure 3.10, lane S). However, the PfHsp70-x band formed a smear and resulted in some strong signals which could suggest that some of the protein was degrading.

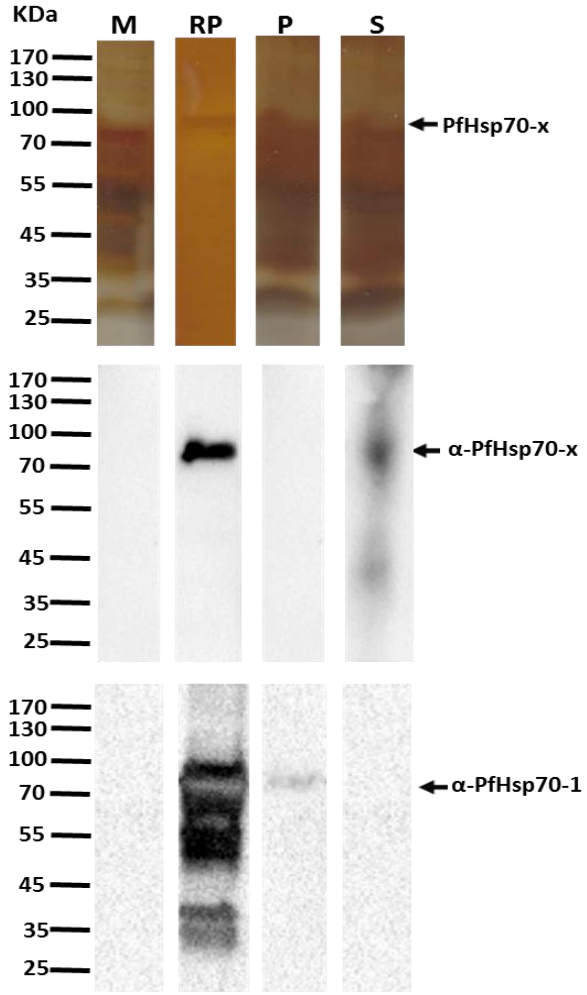

Figure 3.10: Validation of presence of PfHsp70-x and PfHsp70-1 in saponin lysed erythrocyte fractions
Silver stain and Western blot analysis of saponin lysed erythrocyte fractions to validate the presence of PfHsp70-x and PfHsp70-1. Lane M; marker, positive controls, lane RP; recombinant PfHsp70-x and PfHsp70-1, P; whole 3D7 parasite (pellet), S; lysed erythrocyte-parasitophorous vacuole material (supernatant).

The erythrocytes have high concentration of hemoglobin which may contaminate the lysate. Hence, the background could be a result of cross reactivity of the antibody with hemoglobin (Figure 3.10, lane S). These data validated the cell lysate which was used for affinity chromatography studies in this study.

3.2.8. Investigation of the direct association of PfHsp70-x with hHop

The bioinformatics study conducted here predicted interaction of PfHsp70-x with hHop (Section 3.1.5; Figure 3.2). Mabate, (2017), using the recombinant form of the proteins, experimentally validated that PfHsp70-x interacts with hHop *in vitro*. The current study investigated the possible association of PfHsp70-x with hHop under physiological conditions, as illustrated (Figure 2.3, Appendix A6). The recombinant PfHsp70-$x_{F/T}$ proteins (in Section 3.2.4) were used as bait and the erythrocyte cytosolic material served as a source of prey protein (hHop). The eluate complex was analyzed using silver stain (Appendix B11) (Figure 3.11). As control, the input was run through the cobalt beads without recombinant PfHsp70-$x_{F/T}$. Another control of beads immobilized with recombinant PfHsp70-$x_{F/T}$ without input was used. The input eluate fraction showed the presence of bands with molecular weights 35 kDa and 100 kDa (Figure 3.11, lane EI and EII), including the ones above 170 kDa (Figure 3.11, lane EII).

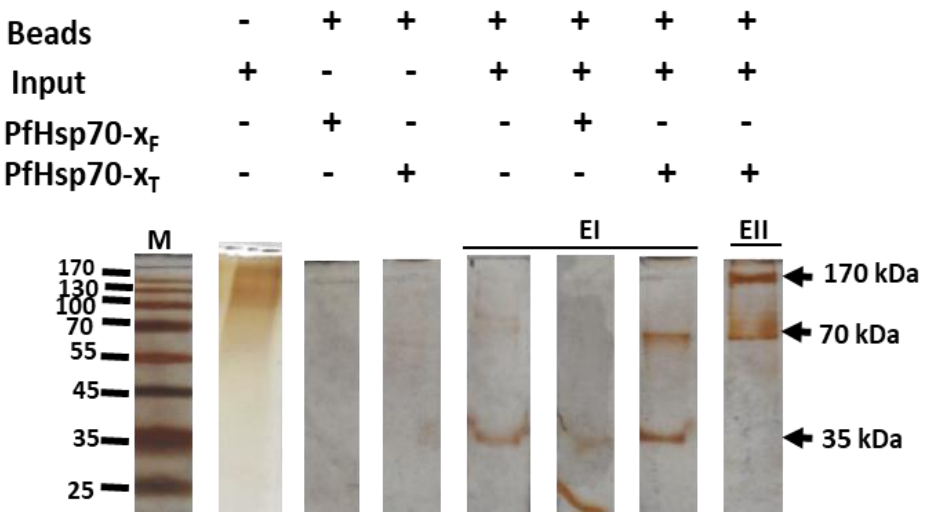

Figure 3.11: Direct interaction of PfHsp70-x and hHop using co-affinity chromatography
Co-affinity chromatography using recombinant PfHsp70-x_F and PfHsp70-x_T. The eluates were analyzed by silver staining. Lane M; marker. The input is the erythrocyte cytosolic material, EI and EII are elutions of the complexes (eluates).

The results from this study did not establish the predicted interaction of PfHsp70-x with hHop (Table 3.1). In the biological system some interactions are not stable, therefore, more sensitive techniques such as surface plasmo resonance (SPR) and isothermal titration calorimetry (ITC) are required to detect such interaction. PfHsp70-x could be transiently interacting with hHop, which may be the reason why the interaction could not be confirmed by co-affinity chromatography.

3.2.9. Direct association of PfHsp70-x with hHop using immuno-affinity chromatography

The interaction between PfHsp70-x with hHop was further investigated using immuno-affinity chromatography (Appendix A7). The assay was performed using input fraction (Section 3.2.7), protein A/G magnetic beads and specific rabbit raised antibodies against the exported PfHsp70-x (α-PfHsp70-x). To validate the assay, beads immobilized with α-PfHsp70-x antibody only were used as a negative control in order to demonstrate the migration pattern of the reduced antibodies (Figure 3.12).

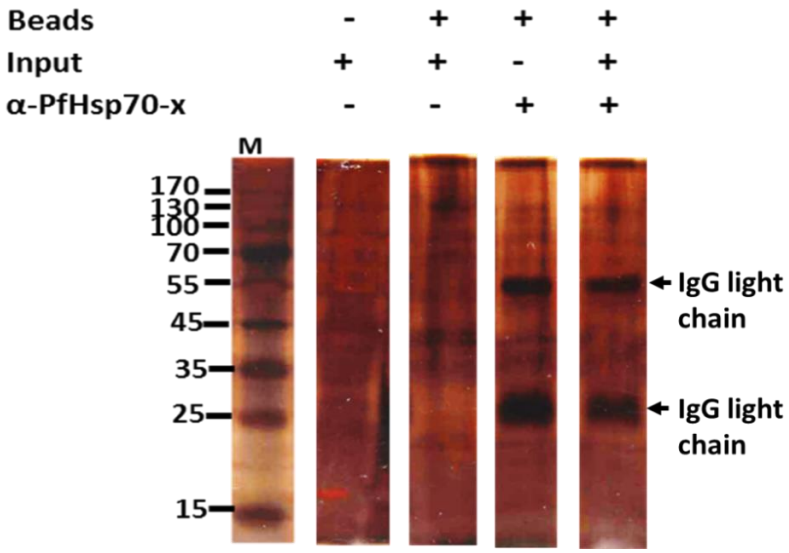

Figure 3.12: Direct interaction of PfHsp70-x and hHop using immuno-affinity chromatography
Co-affinity chromatography was conducted using antibodies against PfHsp70-x and erythrocyte cytosolic fraction (input) obtained from *P. falciparum* 3D7 cell cultures grown under temperature condition of 37 °C. The eluate and controls were analyzed using silver staining. Lane M; marker.

The input was included as a control to show the presence of the bait protein, as well as beads immobilized with input to show that there was non-specific binding (Figure 3.12). The input

together with the immunoprecipitate eluates were analyzed using silver stain. The endogenous PfHsp70-x may have been degraded as it was not detected by the antibody during immuno-affinity chromatography (Figure 3.12). The assay was conducted under reducing conditions, hence, the α-PfHsp70-x antibody was reduced to heavy chain (55 kDa) and light chain (25 kDa) which were detected using silver stain (Figure 3.12). In this study, the co-affinity chromatographic assay failed to confirm interaction between PfHsp70-x and human Hop as predicted by bioinformatics analysis (Figure 3.2) and the study by Mabate, (2017).

Chapter 4

Discussion and concluding remarks

P. falciparum expresses six Hsp70s throughout the blood stage of the parasite's development (Shonhai *et al.,* 2007). Of these proteins, PfHsp70-x is exported to the cytosol of infected erythrocytes (Külzer *et al.,* 2012). In addition, PfHsp70-x has been reported to directly interact with co-chaperones resident in the infected erythrocytes, such as hHop (Mabate, 2017) and the parasite Hsp40 that is exported to the erythrocyte (Daniyan *et al.,* 2016). The function of PfHsp70-x is still not known, however, it is thought to be important for virulence (Charnuad *et al.,* 2017). Therefore, this study investigated the structural features and potential interactors of PfHsp70-x within the infected erythrocytes using bioinformatics analysis as well as biochemical assays. Of particular interest, was to explore the interaction of PfHsp70-x with hHop under physiological conditions.

P. falciparum and human Hsp70s have been shown to be highly conserved (Shonhai *et al.,* 2007; Hatherley *et al.,* 2014; Shonhai, 2014). Furthermore, the functional TPR domains of *P. falciparum* and human Hop are conserved (Gitau *et al.,* 2012). Bioinformatics analysis showed high sequence conservation amongst *P. falciparum* and human Hsp70s as well as Hop protein (Appendix A). Important functional features of PfHsp70-x were also identified (Figure A1; A2; Appendix A1). For examples, residues implicated in direct contact between PfHsp70-x and Hsp40 co-chaperone and the substrate are conserved (Appendix A1; A2). Furthermore, residues of the TPR domains of Hop known to bind to Hsp70 and Hsp90 are conserved (Appendix A3; Figure A5).

The structural prediction analysis of Hsp70s from *P. falciparum* and human origin revealed similar folding pattern (Appendix A1; A2). This suggests that these Hsp70 proteins may have similar conformations. Also the Hop of *P. falciparum* and human origin showed similar folding patterns (Appendix A3). Both hHop and hHsp70 are reportedly available in the erythrocyte cytosol and may thus co-localize with PfHsp70-x (Grover *et al.,* 2013; Jha *et al.,* 2017). The occurrence of proteins in the same subcellular compartments enhance their capability to

interact (Jah *et al.,* 2017). Furthermore, hHsp70 and PfHsp70-x could have functional redundancy with respect to their protein folding roles in infected erythrocytes.

The carboxyl end of PfHsp70-x is represented by the residues, EEVN (Figure 3.1; Külzer *et al.,* 2012; Shonhai & Blatch, 2014). In contrast, canonical Hsp70s possess EEVD residues at the C-termini that interact with the TPR1 and TPR2A domains (Figure A6) of Hop (Röhl *et al.,* 2015; Zininga *et al.,* 2015b). The C-terminal aspartate (D) is negatively charged while the asparagine (N) is polar (neutral). Polar residues are surface exposed and are more soluble in aqueous environments than negatively charged residues (Betts & Russell, 2003; 2007). The lysine (K) residues are highly charged and form strong ionic bonds with the D residue. Although, N has no net charge, it is known to gain a negative charge under physiological conditions within the cytosol of cells (Betts & Russell, 2003; 2007). Therefore, it is likely that the N residue associates with the K residue resulting in unstable transient interactions within the aqueous cytosolic environment. Taken together, this suggests that the EEVN of PfHsp70-x may form transient hydrogen interaction with the K residue of hHop TPR1 domain (Figure 3.1). Hence, direct interaction between hHop and PfHsp70-x has been reported *in vitro* (Mabate, 2017). It is possible that the interaction between PfHsp70-x and human Hop would possibly be enhanced *in vivo* through post translational modification of the two proteins (Khoury *et al.,* 2011).

There is paucity on PfHsp70-x biochemical interaction data in infected erythrocytes. So far PfHsp70-x has been shown to co-localize with type II exported *Plasmodium* Hsp40s PFE0055C (PF3D7_0501100) and PFA0660w (PF3D7_0113700) in structures called J-dots (Külzer *et al.,* 2010). Recent studies have shown interaction of PfHsp70-x with both Hsp40s (Daniyan *et al.,* 2016; Jha *et al.,* 2017; Zhang *et al.,* 2017), which were also predicted by bioinformatics analysis (Table 3.1). Bioinformatics predicted several possible functional associations. Of interest was prediction of the interaction between PfHsp70-x and hHop (NP_006810.1), as was proposed in agreement with the study of Mabate, (2017) (Figure 3.2, Table 3.1). Furthermore, PfHsp70-x was also predicted to interact with erythrocyte cytosolic human Hsp90s, hHsp90-α (NP_001017963.2) and hHsp90-β (NP_001258899.1) (Figure 3.2; Table 3.1). In infected erythrocytes, hHop and hHsp90 co-localize to the erythrocyte's cytosol.

It is thus possible that hHop may directly bind PfHsp70-x in the erythrocyte. In addition to *Plasmodium* Hsp40s type II PFE0055C and PFA0660w (Daniyan *et al.,* 2016; Jha *et al.,* 2017), a group of other exported type II, III and IV protein and Hsp40-like proteins were predicted as possible interactors of PfHsp70-x (Figure 3.2; Table 3.1; Table A5). The possible interaction of PfHsp70-x with PFA0660w could facilitate stimulation of PfHsp70-x activity (Daniyan *et al.,* 2016). The ATPase activity of Hsp70s has been shown to be regulated by NEFs (Shonhai, 2014). The interactome data predicted association of PfHsp70-x with hBAG2 (NP_004273.1) (Figure 3.2). This suggests that Bag2 may act as a NEF of Hsp70s resident in the erythrocytes.

In addition, the interactome data predicted direct association of PfHsp70-x with a group of chaperones from other families with various functions (Table 3.1; Appendix A4). Amongst them, are the membrane proteins (PHIST, RESA and RESA-like proteins, PfEMP1/3) (Table 3.1) that are implicated in cellular modification, and facilitate knob formation (Maier *et al.,* 2008; Kilili *et al.,* 2011). Furthermore, several parasite and human chaperones from the Hsp60 and TCP-1 Ring Complex (TRiC) are also known as chaperonin containing TCP-1 (CCT/TCP-1) chaperoning complexes (Table 3.1) were also predicted. Apart from these families of proteins, PfHsp70-x is predicted to interact with a group of proteins of human origin that reside in the erythrocyte, which were also reported in the study by Zhang and colleagues (2017) (Table 3.1). Proteins that form the PTEX *Plasmodium* translocon were also predicted as interactors of PfHsp70-x (Table A5; Zhang *et al.,* 2017). Based on these observation, this study proposes that PfHsp70-x may bind parasite proteins destined for export and aid in trafficking as cargo across the PVM PTEX into the erythrocyte.

Taken together, the bioinformatics protein-protein interaction results established in this study, suggest that PfHsp70-x interacts with parasite and human chaperones in the cytosol of infected erythrocytes (Figure 3.2). Moreover, PfHsp70-x may form prominent protein folding pathways which could represent an important role of PfHsp70-x in maintaining the proteostasis in the parasite-infected erythrocyte (Shonhai, 2014). The functional role of PfHsp70-x in the predicted complexes is yet to be fully understood, but could possibly be important for folding of substrate proteins in infected erythrocyte (Shonhai, 2014). However

some studies have suggested that PfHsp70-x is involved in translocation of proteins to the membrane of the erythrocytes that mediate membrane modification (Zhang *et al.,* 2017). This observation implicates PfHsp70-x in host cell remodeling processes and malaria pathogenicity. However, PfHsp70-x knockout studies suggested that the protein is not essential for parasite survival (Charnuad *et al.,* 2017; Cobb *et al.,* 2017).

Furthermore, the recombinant proteins; PfHsp70-x_F, PfHsp70-x_T, hHop and hHsp70 were successfully expressed and purified under native conditions. However, leaky expression was observed in the *E. coli* BL21 Star (DE3) cells for recombinant PfHsp70-x proteins and JM109 (DE3) cells for hHop prior induction with IPTG. Leaky expression is caused by unregulated T5 promoters of pQE30 which may lead to cytotoxicity and low protein yields (Saida *et al.,* 2006). Therefore, leaky expression can be avoided by using an inducible T7 RNA polymerase system which produce high yield of soluble nontoxic recombinant proteins (Briand *et al.,* 2016).

Analysis of the erythrocyte cytosolic material that was used in the current study showed that PfHsp70-x was highly unstable (Figure 3.11). Using the recombinant forms of PfHsp70-x the SPR and slot blot analyses showed direct protein-protein interaction between human Hop and PfHsp70-x *in vitro* (Mabate, 2017). Therefore, co-affinity chromatography and immuno-affinity chromatography studies failed to confirm the interaction of PfHsp70-x with human Hop. This could be as a result of transient interactions between the two proteins which were not stable enough to be confirmed by affinity chromatography. However, co-affinity chromatography established interaction of PfHsp70-x with unidentified bands of molecular weights 35 kDa, 100 kDa and 170 kDa (Figure 3.13). On the other hand, immuno-affinity chromatography did not identify the PfHsp70-x complex. This could be as a result of the lack of adequate level of full PfHsp70-x in the cell lysate. Nonetheless, it would be important to identify co-precipitates observed in this study (Figure 3.13).

In conclusion, bioinformatics analysis predicted the formation of the PfHsp701-PfHop-PfHsp90 complex in the erythrocyte infected by the parasite. Further work is required to validate interaction of PfHsp70-x with hHop using more sensitive assays such as isothermal titration calorimetry (ITC).

References

Acharya, P., Kumar, R., & Tatu, U. (2007). Chaperoning a cellular upheaval in malaria: Heat shock proteins in *Plasmodium falciparum*. *Mol. Biochem. Parasitol.*, **153**: 85-94.

Aurrecoechea, C., Brestelli, J., Brunk, B.P., Dommer, J., Fischer, S., Gajria, B., Gao, X., Gingle, A., Grant, G., Harb, O.S., Heiges, M., Innamorato, F., Iodice, J., Kissinger, J.C., Kraemer, E., Li, W., Miller, J.A., Nayak, V., Pennington, C., Pinney, D.F., Roos, D.S., Ross, C., Stoeckert, C.J. Jr., Treatman, C., & Wang, H. (2009). PlasmoDB: a functional genomic database for malaria parasites. *Nucleic Acids Res,* **37**: D539-43.

Bannister, L.H. (2001). Looking for the exit: How do malaria parasites escape from red blood cells? *Proc. Natl. Acad. Sci. USA.*, **98**: 383-4.

Banumathy, G., Singh, V., & Tatu, U. (2002). Host chaperones are recruited in membrane-bound complexes by *Plasmodium falciparum*. *J. Biol. Chem.*, **277**: 3902-3912.

Banumathy, G., Singh, V., Pavithra, S.R., & Tatu, U. (2003). Heat shock protein 90 function is essential for *Plasmodium falciparum* growth in human erythrocytes. *J. Biol. Chem.*, **278**: 18336-45.

Bascos, N.A.D., Mayer, M.P., Bukau, B. & Landry, S.J. (2017). "The Hsp40 J-domain modulates Hsp70 conformation and ATPase activity with a semi-elliptical spring." *Protein. Sci.*, **26**: 1838-1851.

Beck, J.R., Muralidharan, V., Oksman, A., & Goldberg, D.E. (2014). PTEX component Hsp101 mediates export of diverse malaria effectors into host erythrocytes. *Nature*, **51:** 592-595.

Bell, S.L., Chiang, A.N., & Brodsky, J.L. (2011). Expression of a malarial Hsp70 improves defects in chaperone-dependent activities in ssa1 mutant yeast. *PLoS One*, **6**: 1-10.

Betts, M.J. & Russell, R.B. (2003). Amino acid properties and consequences of substitutions. Bioinformatics for geneticists*,* Geneticists (eds M. R. Barnes and I. C. Gray), *John Wiley & Sons, Ltd, Chichester,* UK. **317:** 289.

Betts, M.J. and Russell, R.B. (2007). Amino-acid properties and consequences of substitutions. Bioinformatics for geneticists, Geneticists (eds M. R. Barnes and I. C. Gray), *John Wiley & Sons, Ltd, Chichester,* UK. **2:** 311-339.

Blisnick, T., Betoulle, M.E.M., Barale, J., Uzureau, P., Berry, L., Desroses, S., Fujioka, H., Mattei, D., & Breton, C.B. (2005). Pfsbp1, a Maurer's cleft *Plasmodium falciparum* protein, is associated with the erythrocyte skeleton. *Mol. Biochem. Parasitol.,* **111**: 107-121

Boddey, J.A., Moritz, R.L., Simpson, R.J., & Cowman, A.F. (2010). Role of the *Plasmodium* export element in trafficking parasite proteins to the infected erythrocyte. *Traffic*, **10**: 285-299.

Boddey, J.A., O'Neill, M.T., Lopaticki, S., Carvalho, T.G., Hodder, A.N., Nebl, T., Wawra, S., van West, P., Ebrahimzadeh, Z., Richard, D., Flemming, S., Spielmann, T., Przyborski, J., Babon, J.J., & Cowman, A.F. (2016). Export of malaria proteins requires co-translational processing of the PEXEL motif independent of phosphatidylinositol-3-phosphate binding. *Nat. Commun.*, **7**: 10470.

Boddey, J.A., Carvalho, T.G., Hodder, A.N., Sargeant, T.J., Sleebs, B.E., Marapana, D., Lopaticki, S., Nebl, T., & Cowman, A.F. (2013). Role of plasmepsin V in export of diverse protein families from the *Plasmodium falciparum* exportome. *Traffic,* **14**: 532-550.

Bonnefoy, S., & Ménard, R. (2008). Deconstructing export of malaria proteins. *Cell*, **134**: 20-22.

Botha, M., Chiang, A.N., Needham, P.B., Stephens, L.L., Hoppe, H.C., Külzer, S., Przyborski, J.M., Lingelbach, K., Wipf, P., Brodsky, J.L., Shonhai, A., & Blatch, G.L. (2011). *Plasmodium falciparum* encodes a single cytosolic type I Hsp40 that functionally interacts with Hsp70 and is upregulated by heat shock. *Cell Stress Chaperone.*, **16**: 389-401.

Botha, M., Pesce, E.R., & Blatch, G.L. (2007). The Hsp40 proteins of *Plasmodium falciparum* and other apicomplexa: Regulating chaperone power in the parasite and the host. *Int. J. Biochem. Cell Biol.*, **39**: 1781-803.

Bousema, T., Stresman, G., Baidjoe, A.Y., Bradley, J., Knight, P., Stone, W., Osoti, V., Makori, E., Owaga, C., Odongo, W., & China, P. (2016). The impact of hotspot-targeted interventions

on malaria transmission in Rachuonyo South District in the Western Kenyan Highlands: a cluster-randomized controlled trial. *PLoS Med.*, **13**: e1001993.

Briand, L., Marcion, G., Kriznik, A., Heydel, J.M., Artur, Y., Garrido, C., Seigneuric, R. and Neiers, F. (2016). A self-inducible heterologous protein expression system in *Escherichia coli*. *Sci. Rep.,* **6:** 33037.

Buchberger, A., Theyssen, H., Schröder, H., McCarty, J. S., Virgallita, G., Milkereit, P., Reinstein, J., & Bukau, B. (1995). Nucleotide-induced conformational changes in the ATPase and substrate binding domains of the DnaK chaperone provide evidence for interdomain communication. *J. Biol. Chem.*, **270**: 16903-16910.

Bullen, H.E., Crabb, B.S., & Gilson, PR. (2012). Recent insights into the export of PEXEL/HTS-motif containing proteins in *Plasmodium* parasites. *Curr. Opin. Microbiol.*, **15**: 699-704.

Charnaud, S.C., Dixon, M.W., Nie, C.Q., Chappell, L., Sanders, P.R., Nebl, T., Hanssen, E., Berriman, M., Chan, J.A., Blanch, A.J. & Beeson, J.G. (2017). The exported chaperone Hsp70-x supports virulence functions for *Plasmodium falciparum* blood stage parasites. *PLoS One*, **12**: e0181656

Child, M.A., Epp, C., Bujard, H., & Blackman. M.J. (2010). Regulated maturation of malaria merozoite surface protein-1 is essential for parasite growth. *Mol. Microbiol.,* **78**:187-202.

Chiosis, G., Dickey, C.A. & Johnson, J.L. (2013). A global view of Hsp90 functions.

Cobb, D.W., Florentin, A., Fierro, M.A., Krakowiak, M., Moore, J.M., & Muralidharan, V. (2017). The exported chaperone PfHsp70x is dispensable for the *Plasmodium falciparum* intraerythrocytic life cycle. *mSphere,* **2**: e00363- 17.

Coppel, R.L., Lustigman, S., Murray, L., & Anders, R.F. (2010). MESA is a *Plasmodium falciparum* phosphoprotein associated with the erythrocyte membrane skeleton. *Mol. Biochem. Parasit.,* **31**: 223-31.

Cowman, A.F., Berry, D., & Baum, J. (2012). The cellular and molecular basis for malaria parasite invasion of the human red blood cell. *J. Cell Biol.,* **198**: 961-71.

Cox, F.E. (2010). History of the discovery of the malaria parasites and their vectors. *Parasit. Vectors*, **3**: 5.

Crabb, B., de Koning-Ward, T.F., & Gilson, P.R. (2010). Protein export in *Plasmodium* parasites: from the endoplasmic reticulum to the vacuolar export machine. *Int. J. Parasitol.,* **40**: 50913.

Cyrklaff, M., Sanchez, C.P., Frischknecht, F., & Lanzer, M. (2012). Host actin “remodeling” and protection from malaria by hemoglobinopathies. *Trends Parasitol.,* **28**: 479-485.

Daniel, S., Bradley, G., Longshaw, V.M., Söti, C, Csermely, P., & Blatch, G.L. (2008). Nuclear translocation of the phosphoprotein Hop (Hsp70/Hsp90 organizing protein) occurs under heat shock, and its proposed nuclear localization signal is involved in Hsp90 binding. *BBA Mol. Cell Res.*, **1783**: 1003-1014.

Daniyan, M.O., Boshoff, A., Prinsloo, E., Pesce, E.R., & Blatch, G.L. (2016). The malarial exported PFA0660w Is an Hsp40 co-chaperone of PfHsp70-x. *PLoS One*, **11**: e0148517.

de Konig-Ward, T.F., Gilson, P.R., Boddey, J.A., Rug, M., Smith, B.J., Papenfuss, A.T., Sanders, P.R., Lundie, R.J., Maier, A.G., Cowman, A.F., & Crabb, B.S. (2009). A newly discovered protein export machine in malaria parasites. *Nature*, **459**: 945-949.

Didelot, C., Lanneau, D., Brunet, M., Bouchot, A., Cartier, J., Jacquel, A., Ducoroy, P., Cathelin, S., Decologne, N., Chiosis, G., Dubrez-Daloz, L., Solary, E., & Garrido, C. (2008). Interaction of heat-shock protein 90 beta isoform (HSP90 beta) with cellular inhibitor of apoptosis 1 (c-IAP1) is required for cell differentiation. *Cell Death Differ.*, **15**: 859-866.

Dixon, M.W.A., Hawthorne, P.L., Spielmann, T., Anderson, K.L., Trenholme, K.R., & Gardine, D.L. (2008). Targeting of the ring exported protein 1 to the Maurer’s clefts is mediated by a two-phase process. *Traffic,* **9**: 1316-1326.

Eaton, P., Zuzarte-Luis, V., Mota, M.M., Santos, N.C., & Prudêncio, M. (2012). Infection by *Plasmodium* changes shape and stiffness of hepatic cells. *Nanomedicine,* **8**: 17-9.

Eckl, J.M., & Richter, K. (2013). Functions of the Hsp90 chaperone system: Lifting client proteins to new heights. *Int. J. Biochem. Mol. Biol.*, **4**: 157-165.

Edkins, A.L., & Boshoff, A. (2014). Gereneral structural and functional features of molecular chaperones: In Shonhai, A., Blatch, G., Editors. *Heat Shock Proteins of Malaria*, Springer New York; **p**.5-45.

Ellis, R.J. (2006). Molecular chaperones: assisting assembly in addition to folding. *Trends Biochem. Sci.*, **31**: 395-401.

Fairhurst, R.M., & Wellems, T.E. (2006). Modulation of malaria virulence by determinants of *Plasmodium falciparum* erythrocyte membrane protein-1 display. *Curr. Opin. Hematol.,* **13**: 124-130.

Foley, M., Tilley, L., Sawye, W.H., & Anders, R.F. (1991). The ring-infected erythrocyte surface antigen of *Plasmodium falciparum* associates with spectrin in the erythrocyte membrane. *Mol. Biochem. Parasitol.*, **46**: 137-147.

French, J.B., Zhao, H., An, S., Niessen, S., Deng, Y., Cravatt, B.F., & Benkovic, S.J. (2013). Hsp70/Hsp90 chaperone machinery is involved in the assembly of the purinosome. *Proc. Natl. Acad. Sci. U.S.A.*, **110**: 2528-2533.

Gehde, N., Hinrichs, C., Montilla, I., Charpian, S., Lingelbach, K., & Przyborski, J.M. (2009). Protein unfolding is an essential requirement for transport across the parasitophorous vacuolar membrane of *Plasmodium falciparum*. *Mol. Microbiol.,* **71**: 613-628.

Gitau, G.W., Mandal, P., Blatch, G.L., Przyborski, J.M., & Shonhai, A. (2012). Characterisation of the *Plasmodium falciparum* Hsp70-Hsp90 organising protein (PfHop). *Cell Stress Chaperone.*, **17**: 191-202.

Goldberg, D.E. (2012). *Plasmodium* protein export at higher PEXEL resolution. *Cell Host Microbe,* **12:** 717-729.

Goodman, S.R., Kurdia, A., Ammann, L., Kakhniashville, D., & Daescu, O. (2007). The human red blood cell proteome and interactome. *Exp. Biol. Med.,* **232**: 1391-1408.

Grammatikakis, N., Vultur, A., Ramana, C.V., Siganou, A., Schweinfest, C.W., Watson, D.K., & Raptis, L. (2002). The role of Hsp90N, a new member of the Hsp90 family, in signal transduction and neoplastic transformation. *J. Biol. Chem.,* **277**: 8312-20.

Grover, M., Chaubey, S., Ranade, S., & Tatu, U. (2013). Identification of an exported heat shock protein 70 in *Plasmodium falciparum*. *Parasite,* **20**: 2.

Grüring, C., Heiber, A., Kruse, F., Flemming, S., Franci, G., Colombo, S.F., Fasana, E., Schoeler, H., Borgese, N., Stunnenberg, H.G., Przyborski, J.M., Gilberger, T.W., & Spielmann, T. (2012). Uncovering common principles in protein export of malaria parasites. *Cell Host Microbe,* **12**: 717-29.

Grüring, C., Heiber, A., Kruse, F., Ungefehr, J., Gilberger, T.W., & Spielmann, T. (2011). Development and host cell modifications of *Plasmodium falciparum* blood stages in four dimensions. *Nat. Commun.,* **2**: 165.

Haase, S., Herrmann, S., Grüring, C., Heiber, A., Jansen, P. W., Langer, C., Treeck, M., Cabrera, A., Bruns, C., Struck, N.S., Kono, M., Engelberg, K., Ruch, U., Stunnenberg, H.G., Gilberger, T., & Spielmann, T. (2009). Sequence requirements for the export of the *Plasmodium falciparum* Maurer's clefts protein REX2. *Mol. Microbiol.,* **71**: 1003-1017.

Haldar, K., & Mohandas, N. (2007). Erythrocyte "remodeling" by malaria parasites. *Curr. Opin. Hematol.,* **14**: 203-9.

Hanssen, E., Hawthorne, P., Dixon, M.W., Trenholme, K.R., McMillan, P.J., Spielmann, T., Gardiner, D.L., & Tilley, L. (2008). Targeted mutagenesis of the ring-exported protein-1 of *Plasmodium falciparum* disrupts the architecture of Maurer's cleft organelles. *Mol. microbiol*, **69:** 938-953.

Hasse, S., & de Koning-Ward, T.F. (2010). New insights into protein export in malaria parasites*. Cell. Microbiol.*, **12**: 580-587.

Hatherley, R., Blatch, G.L., & Bishop, Ö.T. (2014). *Plasmodium falciparum* Hsp70-x: A heat shock protein at the host-parasite interface. *J. Biomol. Struct. Dyn.*, **32**: 1766-1779.

Heiber, A., Kruse, F., Pick, C., Grüring, C., Flemming, S., Oberli, A., Schoeler, H, Retzlaff, S., MesénRamírez, P., Hiss, J.A., Kadekoppala, M., Hecht, L., Holder, A.A., Gilberger, T.W., & Spielmann, T. (2013). Identification of new PNEPs indicates a substantial non-PEXEL exportome and underpins common features in *Plasmodium falciparum* protein export. *PLoS Pathog.*, **9**: e1003546.

Hennessy, F., Nicoll, W.S., Zimmermann, R., Cheetham, M.E., & Blatch, G.L. (2005). Not all J domains are created equal: implications for the specificity of Hsp40–Hsp70 interactions. *Protein Sci.*, **14:** 1697-1709.

Hiller, N.L., Bhattacharjee, S., van Ooij, C., Liolios, K., Harrison, T., Lopez-Estrano, C., & Haldar, K. (2004). A host targeting signal in virulence proteins reveals a secretome in malarial infection. *Science*. **306**: 1934-1937.

Jensen, L.J., Kuhn, M., Stark, M., Chaffron, S., Creevey, C., Muller, J., Doerks, T., Julien, P., Roth, A., Simonovic, M., Bork, P., & von Mering, C. (2009). STRING 8 - A global view on proteins and their functional interactions in 630 organisms. *Nucleic Acids Res.*, **37**: 412-416.

Jha, P., Laskarb, S., Dubeyb, S., Bhattacharyyaa, M. K., & Bhattacharyyab, S. (2017). *Plasmodium* Hsp40 and human Hsp70: A potential cochaperone-chaperone complex. *Mol. Biochem. Parasitol.,* **214**: 10-13.

Joshi, B., Biswas, S., & Sharma, Y.D. (1992). Effect of heat-shock on *Plasmodium falciparum* viability, growth and expression of the heat-shock protein “PFHSP70-I” gene. *FEBS Lett*, **312**: 91-94.

Kakhniashvili, D.G., Bulla, L.A., & Goodman, S.R. (2004). The human erythrocyte proteome analysis by ion trap mass spectrometry. *Mol.Cell. Prot.*, **3**: 501-509.

Kampinga, H.H., & Craig, E.A. (2010). The HSP70 chaperone machinery: J proteins as drivers of functional specificity. *Nat. Rev. Mol. Cell Biol.*, **11**: 579-92.

Kampinga, H.H., Hageman, J., Vos, M.J., Kubota, H., Tanguay, R.M., Bruford, E., Cheetham, M.E., Chen, B., & Hightower, L.E. (2009). Guidelines for the nomenclature of the human heat shock proteins. *Cell Stress Chaperone.*, **14**: 105–111.

Keeley, A., & Soldati, D. (2004). The glideosome: a molecular machine powering motility and host-cell invasion by Apicomplexa. *Trends Cell Biol.,* **14**: 528-32.

Kelley, L.A., Mezulis, S., Yates, C.M., Wass, M.N. & Sternberg, M.J. (2015). The Phyre^2 web portal for protein modeling, prediction and analysis. *Nat. Protoc.*, **10**: 845-58.

Khoury, G.A., Baliban, R.C. & Floudas, C.A. (2011). Proteome-wide post-translational modification statistics: frequency analysis and curation of the swiss-prot database. *Scientific Rep.*, **1**: 90.

Kilili, G.K. & La Count, D.J. (2011). An erythrocyte cytoskeleton-binding motif in exported *Plasmodium falciparum* proteins. *Eukaryot. Cell*, **10**: 1439-1447.

Knox, C., Luke, G.A., Blatch, G.L., & Pesce, E.R. (2011). Heat shock protein 40 (Hsp40) plays a key role in the virus life cycle. *Virus Res.,* **160**: 15-24.

Kraemer, S.M., & Smith, J.D. (2006). A family affair: *var* genes, PfEMP1 binding, and malaria disease. *Curr. Opin. Microbiol.,* **9**: 374-80.

Krukenberg, K.A., Street, T.O., Lavery, L.A., & Agard, D.A. (2011). Conformational dynamics of the molecular chaperone Hsp90. *Q. Rev. Biophys.* **44**: 229-255.

Külzer, S., Charnaud, S., Dagan, T., Riedel, J., Mandal, P., Pesce, E.R., Blatch, G.L., Crabb, B.S., Gilson, P.R., & Przyborski, J.M. (2012). *Plasmodium falciparum*-encoded exported hsp70/hsp40 chaperone/cochaperone complexes within the host erythrocyte. *Cellular Microbiol.*, **14**: 1784-1795.

Külzer, S., Petersen, W., Baser, A., Mandel, K., & Przyborski, J.M. (2013). Use of self-assembling GFP to determine protein topology and compartmentalisation in the *Plasmodium falciparum*-infected erythrocyte. *Mol. Biochem. Parasitol.*, **187**: 87-90.

Külzer, S., Rug, M., Brinkmann, K., Cannon, P., Cowman, A., Lingelbach, K., Blatch, G.L., Maier, A.G., & Przyborski, J.M. (2010). Parasite-encoded Hsp40 proteins define novel mobile structures in the cytosol of the *P. falciparum*-infected erythrocyte. *Cellular Microbiol.*, **12**: 1398-1420.

Mabate, B. (2017). Exploration of interaction between *Plasmodium falciparum* Hsp70-x (PfHsp70-x) and human Hsp70-Hsp90 organizing protein (human Hop) (Masters dissertation). Available at http://univendspace.univen.ac.za/handle/11602/934. Accessed June 2017.

Maier, A.G., Rug, M., O'Neill, M.T., Brown, M., Chakravorty, S., Szestak, T., Chesson, J., Wu, Y., Hughes, K., Coppel, R.L., Newbold, C., Beeson, J.G., Craig, A., Crabb, B.B., & Cowman, A.F. (2008). Exported proteins required for virulence and rigidity of *Plasmodium falciparum*-infected human erythrocytes. *Cell*, **134**: 46-61.

Makhoba, X.H., Burger, A., Coertzen, D., Zininga, T., Birkholtz, L.M. & Shonhai, A. (2016). Use of a chimeric Hsp70 to enhance the quality of recombinant *Plasmodium falciparum* S-adenosylmethionine decarboxylase protein produced in *Escherichia coli*. *PloS one*, **11**: e0152626.

Marti, M., & Spielmann, T. (2013). Protein export in malaria parasites: many membranes to cross. *Curr. Opin. Microbiol.,* **1:** 7.

Marti, M., Good, R.T., Rug, M., Knuepfer, E., & Cowman, A.F. (2004). Targeting malaria virulence and remodeling proteins to the host erythrocyte. *Science*, **306**: 1930-1933.

Mayer, M.P. (2013). Hsp70 chaperone dynamics and molecular mechanism. *Trends Biochem. Sci.*, **38**: 507-514.

Mayer, M.P., & Bukau, B. (2005). Hsp70 chaperones: cellular functions and molecular mechanism. *Cell Mol. Life Sci.*, **62**: 670-84.

Mbengue, A., Yam, X.Y., & Braun-Breton, C. (2012). Human erythrocyte "remodeling" during *Plasmodium falciparum* malaria parasite growth and egress. *Br. J. Haematol.*, **157**: 171-179.

Meyer, P., Prodromou, C., Hu, B., Vaughan, C., Roe, S.M., Panaretou, B., Piper. P.W., & Pearl, L.H. (2003). Structural and functional analysis of the middle segment of Hsp90: Implications for ATP hydrolysis and client protein and cochaperone interactions. *Mol. Cell*, **11**: 647-658.

Mundwiler-Pachlatko, E., & Beck, H.P. (2013). Maurer's clefts, the enigma of *Plasmodium falciparum*. *Proc. Natl. Acad. Sci. U.S.A*, **110**: 19987-19994.

Newman, M.E.J. (2003). A measure of betweenness based on random walks. *Soc. Networks*, **27**: 39-54.

Nicolet, C.M., & Craig, E.A. (1989). Isolation and characterization of STI1, a stress-inducible gene from *Saccharomyces cerevisiae*. *Mol. Cell. Biol.*, **9**: 3638-3646.

Nilsson, S.K., Childs, L.M., Buckee, C., & Marti, M. (2015). Targeting human transmission biology for malaria elimination. *PLoS Pathog*, **11**: e1004871.

Njunge, J.M., Mandal, P., Przyborski, J.M., Boshoff, A., Pesce, E.R., & Blatch, G.L. (2013). PFB0595w is a *Plasmodium falciparum* J protein that co-localizes with PfHsp70-1 and can stimulate its in vitro ATP hydrolysis activity. *Int. J. Biochem. Cell Biol.*, **62**: 47-53.

Nonaka, G., Blankschien, M., Herman, C., Gross, C.A., & Rhodius, V.A., (2006). Regulon and promoter analysis of the *E. coli* heat-shock factor, sigma32, reveals a multifaceted cellular response to heat stress. *Genes Dev.,* **20**: 1776-1789.

Odunuga, O.O., Hornby, J.A., Bies, C., Zimmermann, R., David J., & Pugh, D.J. (2003). Tetratricopeptide repeat motif-mediated Hsc70-mSTI1 interaction. Molecular characterization of the critical contacts for successful binding and specificity. *J. Biol. Chem.,* **278**: 6896-6904.

Onuoha, S.C., Coulstock, E.T., Grossmann, J.G., & Jackson, S.E. (2008). Structural studies on the co-chaperone Hop and its complexes with Hsp90. *J. Mol. Biol.*, **379**: 732-744.

Pachlatko, E., Rusch, S., Müller, A., Hemphill, A., Tilley, L., Hanssen, E., & Beck, H.P. (2010). MAHRP2, an exported protein of *Plasmodium falciparum*, is an essential component of Maurer's cleft tethers. *Mol. Microbiol.,* **77**: 1136-1152.

Pallavi, R., Roy, N., Nageshan, R.K., TalukDar, P., Pavithra, S.R., Reddy, R., Venketesh, S. Kumar, R., Gupta, A.K., Singh, R.K., Yadav, S.C., & Tatu, U. (2010). Heat shock protein 90 as a drug target against protozoan infections: Biochemical characterization of HSP90 from *Plasmodium falciparum* and *Trypanosoma evansi* and evaluation of its inhibitor as a candidate drug. *J. Biol. Chem.*, **285**: 37964-37975.

Papakrivos, J., Newbold, C.I., & Lingelbach, K. (2005). A potential novel mechanism for the insertion of a membrane protein revealed by a biochemical analysis of the *Plasmodium falciparum* cytoadherence molecule PfEMP-1. *Mol. Microbiol.,* **55:** 1272-1284.

Pasini, E.M., Kirkegaard, M., Mortensen, P., Lutz, H.U., Thomas, A.W., & Mann, M. (2006). In-depth analysis of the membrane and cytosolic proteome of red blood cells. *The American Society Hematol.,* **108**: 791-801.

Pasloske, B.L., Baruch, D.I., van Schravendijk, M.R., Handunnetti, S.M., Aikawa, M., Fujioka, H., Taraschi, T.F., Gormley, J.A., & Howard, R.J. (1993). Cloning and characterization of a *Plasmodium falciparum* gene encoding a novel high molecular weight host membrane-associated protein, PfEMP3. *Mol. Biochem. Parasitol.*, **59**: 59-72

Pearl, L.H., & Prodromou, C. (2006). Structure and mechanism of the Hsp90 molecular chaperone machinery. *Annu. Rev. Biochem.*, **75**: 271-294.

Pesce, E.R., & Blatch G. L. (2014). *Plasmodial* Hsp40 and Hsp70 chaperones: current and future perspectives. *Parasitol.*, **141**: 1167-1176.

Pesce, E.R., Acharya, P., Tatu, U., Nicoll, W. S., Shonhai, A., Hoppe, H.C., & Blatch, G.L. (2008). The *Plasmodium falciparum* heat shock protein 40, Pfj4, associates with heat shock protein 70 and shows similar heat induction and localisation patterns. *Int. J. Biochem. Cell Biol.*, **40**: 2914-2926.

Pesce, E.R., Maier, A.G., & Blatch, G.L. (2014). Role of the Hsp40 family of proteins in the survival and pathogenesis of the malaria parasite. In Shonhai, A., Blatch, G., Editors. *Heat Shock Proteins of Malaria*, Springer New York; **p**.71-85.

Petersen, E.F., Goddard, T.D., Huang, C.C., Couch, G.S., Greenblatt, D.M., Meng, E.C. & Ferrin, T.E. (2004). UCSF Chimera-a visualization system for exploratory research and analysis. *J. Comput. Chem.,* **25**: 1605-1612.

Polier, S., Dragovic, Z. and Hartl, F.U., & Bracher, A. (2008). Structural basis for the cooperation of Hsp70 and Hsp110 chaperones in protein folding. *Cell*, **133**: 1068-1079.

Pologe, L.G., Pavlovec, A., Shio, H., & Ravetch, J.V. (1987). Primary structure and subcellular localization of the knob-associated histidine-rich protein of *Plasmodium falciparum*. *Proc. Natl. Acad. Sci. USA.*, **84:** 7139-7143.

Proellocks, N.I., Coppel, R.L., Mohandas, N., & Cooke, B.M. (2016). Malaria parasite proteins and their role in alteration of the structure and function of red blood cells. *Adv. Parasitol*, **91**: 1-86.

Pryzborski, J.M. (2014). The importance of molecular chaperones in survival and pathogenesis of the malaria parasite *Plasmodium falciparum*: In: Shonhai, A., Blatch, G., Editors. *Heat shock proteins of malaria*, Springer New York; **p**.1-3.

Przyborski, J.M., Diehl, M., & Blatch, G.L. (2015). Plasmodial HSP70s are functionally adapted to the malaria parasite lifecycle. *Front. Mol. Biosci,* **2**: 34.

Ramakrishnan, G., Srinivasan, N., Padmapriya, P., & Natarajan, V. (2015). Homology-based prediction of potential protein-protein Interactions between human erythrocytes and *Plasmodium falciparum*. *Bioinfor. Biol. Insights*, **9**: **p**.BBI-S31880.

Riglar, D.T., Richard, D., Wilson, D.W., Boyle, M.J., Dekiwadia, C., Turnbull, L., Angrisano, F., Marapana, D.S., Rogers, K.L., Whitchurch, C.B., Beeson, J.G., Cowman, A.F., Ralph, S.A., & Baum, J. (2011). Super-resolution dissection of coordinated events during malaria parasite invasion of the human erythrocyte. *Cell Host Microbe,* **9**: 9-20.

Röhl, A., Wengler, D., Madl, T., Lagleder, S., Tippel, F., Herrmann, M., Hendrix, J., Richter, K., Hack, G., Schmid, A.B., Kessler, H., Lamb, D.C., & Buchner, J. (2015). Hsp90 regulates the dynamics of its co-chaperone Sti1 and the transfer of Hsp70 between modules. *Nat. Commun.*, **6**: 6655.

Rosano, G.L., & Ceccarelli, F.A. (2014). Recombinant protein expression in *E. coli*: anvances and challenges. *Front Microbiol.*, **5**: 172.

Rowe, J.A., Claessens, A., Corrigan, R.A., & Arman, M. (2010). Adhesion of *Plasmodium falciparum* infected erythrocytes to human cells: molecular mechanisms and therapeutic implications. *Expert Rev. Mol. Med.,* **11**: e16.

Rowe, J.A., Handel, I.G., Thera, M.A., Deans, A.M., Lyke, K.E., Koné, A., Diallo, D.A., Raza, A., Kai, O., Marsh, K., Plowe, C.V., Doumbo, O.K., & Moulds, J.M. (2007). Blood group O protects against severe *Plasmodium falciparum* malaria through the mechanism of reduced rosetting. *Proc. Natl. Acad. Sci. USA*, **104**: 17471-17476.

Rug, M., & Maier, A.G. (2011). The Heat shock protein 40 family of the malaria parasite *Plasmodium falciparum*. *IUBMB Life*, **63**: 1081-1086.

Rug, M., Prescott, S.W., Fernandez, K.M., Cooke, B.M., and Alan F., & Cowman, A.F. (2006.) The role of KAHRP domains in knob formation and cytoadherence of *P. falciparum*-infected human erythrocytes. *Blood,* **108**: 370-378

Russo, I., Babbitt, S., Muralidharan, V., Butler, T., Oksman, A., & Goldberg, D.E. (2010). Plasmepsin V licenses *Plasmodium* proteins for export into the host erythrocyte. *Nature,* **463**: 632-636.

Saibil, H. (2013). Chaperone machines for protein folding, unfolding and disaggregation. *Nat. Rev. Mol. Cell Biol.*, **14**: 630-642.

Saida, F., Uzan, M., Odaert, B., & Bontems, F. (2006). Expression of highly toxic genes in *E. coli*: special strategies and genetic tools. *Cur. Prot.Pept. Sci.*, **7**: 47-56.

Sargeant, T.J., Marti, M., Caler, E., Carlton, J.M., Simpson, K., Speed, T.P., & Cowman, A.F. (2006). Lineage-specific expansion of proteins exported to erythrocytes in malaria parasites. *Genome Biol.*, **7**: R12.

Scheufler, C., Brinker, A., Bourenkov, G., Pegoraro, S., Moroder, L., Bartunik, H., Hartl, F.U., & Moarefi, I. (2000). Structure of TPR domain-peptide complexes: critical elements in the assembly of the Hsp70Hsp90 multi-chaperone machine. *Cell*, **101**: 199-210.

Schmid, A.B., Lagleder, S., Gräwert, M.A., Röhl, A., Hagn, F., Wandinger, S.K., Cox, M.B., Demmer, O., Richter, K., Groll, M., Kessler, H., & Buchner, J. (2012). The architecture of functional modules in the Hsp90 co-chaperone Sti1/Hop. *EMBO J.l*, **31**: 1506-1517.

Shannon, P., Markiel, A., Ozier, O., Baliga, N. S., Wang, J.T., Ramage, D., Amin, N., Schwikowski, B. & Ideker, T. (2003). Cytoscape: A software environment for integrated models of biomolecular interaction networks. *Genome Res.*, **13**: 2498-504.

Sharma, Y.D. (1992). Structure and possible function of heat-shock proteins in *Plasmodium falciparum*. *Comp. Biochem. Physiol. B*, **102**: 437-444.

Sharma, YD., & Masison, D.C. (2009). Hsp70 structure, function, regulation and influence on yeast prions. *Protein Pept. Lett.,* **16**: 571-81.

Shi, H., Liu, Z., Li, A., Yin, J., Chong, A.G., Tan, K.S., Zhang, Y., & Lim, C.T. (2013). Life cycle-dependent cytoskeletal modifications in *Plasmodium falciparum* infected erythrocytes. *PLoS One,* **8**: e61170.

Shonhai, A. (2010). *Plasmodial* heat shock proteins: Targets for chemotherapy. *FEMS Immuno. Med. Microbiol.,* **58**: 61-74.

Shonhai, A. (2014). Role of Hsp70s in development and pathogenicity of *plasmodium* species: In: Shonhai, A., Blatch, G., Editors. *Heat shock proteins of malaria*, Springer New York; **p**.47-70.

Shonhai, A., & Blatch, G.L. (2014). Heat shock proteins of malaria: What do we not know, and what should the future focus be?: In Shonhai, A., Blatch, G., Editors. *Heat shock proteins of malaria*, Springer New York; **p**.207-211.

Shonhai, A., Boshoff, A., & Blatch, G.L. (2007). The structural and functional diversity of Hsp70 proteins from *Plasmodium falciparum*. *Protein Sci.*, **16**: 1803-1818.

Shonhai, A., Botha, M., de Beer, T.A.P., Boshoff, A., & Blatch, G.L. (2008). Structure-function study of *Plasmodium falciparum* Hsp70 using three dimensional modelling and in-vitro analyses. *Protein Pept. Lett.*, **15**: 1117-1125.

Shonhai, A., Maier, A.G., Przyborski, J.M., & Blatch, G.L. (2011). Intracellular protozoan parasites of humans: the role of molecular chaperones in development and pathogenesis. *Protein Pept. Lett.,* **18**: 143-157.

Sijwali, P.S. & Rosenthal, P.J. (2010). Functional evaluation of *Plasmodium* export signals in *Plasmodium berghei* suggests multiple modes of protein export. *PloS one*, ***5*:** e10227.

Silmon de Monerri, N.C., Flynn, H.R., Campos, M.G., Hackett, F., Koussis, K., Withers-Martinez, C., Skehel, J.M. & Blackman. M.J. (2011). Global identification of multiple substrates for *Plasmodium falciparum* SUB1, an essential malarial processing protease. Infect. Immun., **79**:1086-1097.

Smith. J.D., Rowe, J.A., Higgins, M.K., & Lavstsen, T. (2013). Malaria's deadly grip: cytoadhesion of *Plasmodium falciparum*-infected erythrocytes. *Cell Microbiol.,* **15**: 1976-1983.

Spielmann, T., & Gilberger, T.W. (2010). Protein export in malaria parasites: do multiple export motifs add up to multiple export pathways? *Trends Parasitol.,* **26**: 6-10.

Spielmann, T., & Gilberger, T.W. (2015). Critical steps in protein export of *Plasmodium falciparum* blood stages. *Trends Parasitol.,* **31**: 514-525

Spycher, C., Rug, M., Klonis, N., Ferguson, D.J., Cowman, A.F, Beck, H.P., & Tilley, L. (2006). Genesis of and trafficking to the Maurer's clefts of *Plasmodium falciparum*-infected erythrocytes. *Mol. Cell. Biol.*, **26**: 4074-85.

Stephens, L.L., Shonhai, A., & Blatch, G.L. (2011). Co-expression of the *Plasmodium falciparum* molecular chaperone, PfHsp70, improves the heterologous production of the antimalarial drug target GTP cyclohydrolase I, PfGCHI. *Protein Expr. Purif.*, **77**: 159-165.

Su, X.Z., Heatwole, V.M., Wertheimer, S.P., Guinet, F., Herrfeldt, J.A., Peterson, D.S., Ravetch, J.A., & Wellems T.E. (1995). The large diverse gene family var encodes proteins involved in cytoadherence and antigenic variation of *Plasmodium falciparum*-infected erythrocytes. *Cell*, **82.** 89-100.

Szklarczyk, D., Morris, J.H., Cook, H., Kuhn, M., Wyder, S., Simonovic, M., Santos, A., Doncheva, N.T., Roth, A., Bork, P. & Jensen, L.J. (2017). The STRING database in 2017: quality-controlled protein–protein association networks, made broadly accessible. *Nucleic acids Res.*, **p**.gkw937.

Tamez, P.A., Bhattacharjee, S., van Ooij, C., Hiller, N.L., Llinás, M., Balu, B., Adams, J.H., & Haldar, K. (2008). An erythrocyte vesicle protein exported by the malaria parasite promotes tubovesicular lipid import from the host cell surface. *PLoS Pathog,* **4**: e1000118.

Taschner, M., Kotsis, F., Braeuer, P., Kuehn, E.W., & Lorentzen, E. (2014). Crystal structures of IFT70/52 and IFT52/46 provide insight into intraflagellar transport B core complex assembly. J Cell Biol., **207**: 269-282.

Trager, W., & Jensen, J.B. (1976). Human malaria parasites in continuous culture. *Science*, **193**: 673-675.

Wegele, H., Wandinger, S. K., Schmid, A. B., Reinstein, J., & Buchner, J. (2006). Substrate transfer from the chaperone Hsp70 to Hsp90. *J. Mol. Biol.,* **356**: 802-811.

Weiss, G.E., Gilson, P.R., Taechalertpaisarn, T., Tham, W., de Jong, N.W.M., Harvey, K. L., Fowkes, F.J.I., Barlow, P.N., Rayner, J.C., Wright, G.J., Cowman, A.F., & Crabb, B. S. (2015). Revealing the sequence and resulting cellular morphology of receptor-ligand interactions during *Plasmodium falciparum* invasion of erythrocytes. *PLoS Pathog.*, **11**: 1-25.

Weng, H., Guo, X., Papoin, J., Wang, J., Coppel, R., Mohandas, N., & An, X. (2014). Interaction of *Plasmodium falciparum* knob-associated histidine-rich protein (KAHRP) with erythrocyte ankyrin R is required for its attachment to the erythrocyte membrane. *BBA Rev. Biomemb*, **1838**: 185-192.

WHO (2016). World Health Organisation World Malaria report http://www.who.int/malaria/publications/world-malaria-report-2016/en/pdf. Accessed January 2017.

WHO (2017). World Health Organisation World Malaria report. http://www.who.int/malaria/publications/world-malaria-report-2017/en/.pdf. Accessed January 2017.

Wuchty, S., (2011). Computational prediction of host-parasite protein interactions between *P. falciparum* and *H. sapiens*. *PLoS One*, ***6***: **p**.e26960.

Yamamoto, S., Subedi, G.P., Hanashima, S., Satoh, T., Otaka, M., Wakui, H., Sawada, K.I., Yokota, S.I., Yamaguchi, Y., Kubota, H., & Itoh, H. (2014). ATPase activity and ATP-dependent conformational change in the co-chaperone Hsp70/Hsp90-organizing protein (HOP). *J. Biol. Chem.*, **289**: 9880-9886.

Zhang, Y., Huang, C., Kim, S., Golkarama, M., Dixon, M.W.A., Tilley, L., Lib, J., Zhanga, S., & Sures S. (2015). Multiple stiffening effects of nanoscale knobs on human red blood cells infected with *Plasmodium falciparum* malaria parasite. *Proc. Natl. Acad. Sci. USA.*, **112**: 6068-73.

Zininga, T. (2015). Characterization of heat shock protein 70-z (PfHsp70-z) from P*lasmodium falciparium* (Doctoral dissertation). Available at http://univendspace.univen.ac.za/handle/11602/619. Accessed October 2016.

Zininga, T., Achilonu, I., Hoppe, H., Prinsloo, E., Dirr, H.W., & Shonhai, A. (2015a). Overexpression, purification and characterisation of the *Plasmodium falciparum* Hsp70-z (PfHsp70-z) protein. *PLoS One,* **10**: e0129445.

Zininga, T., Achilonu, I., Hoppe, H., Prinsloo, E., Dirr, H.W., & Shonhai, A. (2016). *Plasmodium falciparum* Hsp70-z, an Hsp110 homologue, exhibits independent chaperone activity and interacts with Hsp70-1 in a nucleotide-dependent fashion. *Cell Stress Chaperone.,* **21**: 499-513

Zininga, T., & Shonhai, A. (2014). Are heat shock proteins druggable candidates? *Am. J. Biochem. Biotechnol.*, **10**: 211-213.

Zininga, T., Makumire, S., Gitau, G. W., Njunge, J. M., Pooe, O. J., Klimek, H., Scheurr, R., Raifer, H., Prinsloo, E., Przyborski, J.M., Hoppe, H., & Shonhai, A. (2015b). *Plasmodium falciparum* Hop (PfHop) interacts with the Hsp70 chaperone in a nucleotide-dependent fashion and exhibits ligand Selectivity. *PLoS One,* **10**: e0135326.

Zuccala, E.S., & Baum, J. (2011). Cytoskeletal and membrane “remodeling” during malaria parasite invasion of the human erythrocyte. *Br. J. Haematol.*, **154**: 680-689.

Appendices

Appendix A: Supplementary data

A1. The NBD sequences and 3D models of PfHsp70-x/PfHsp70-1/hHsp70

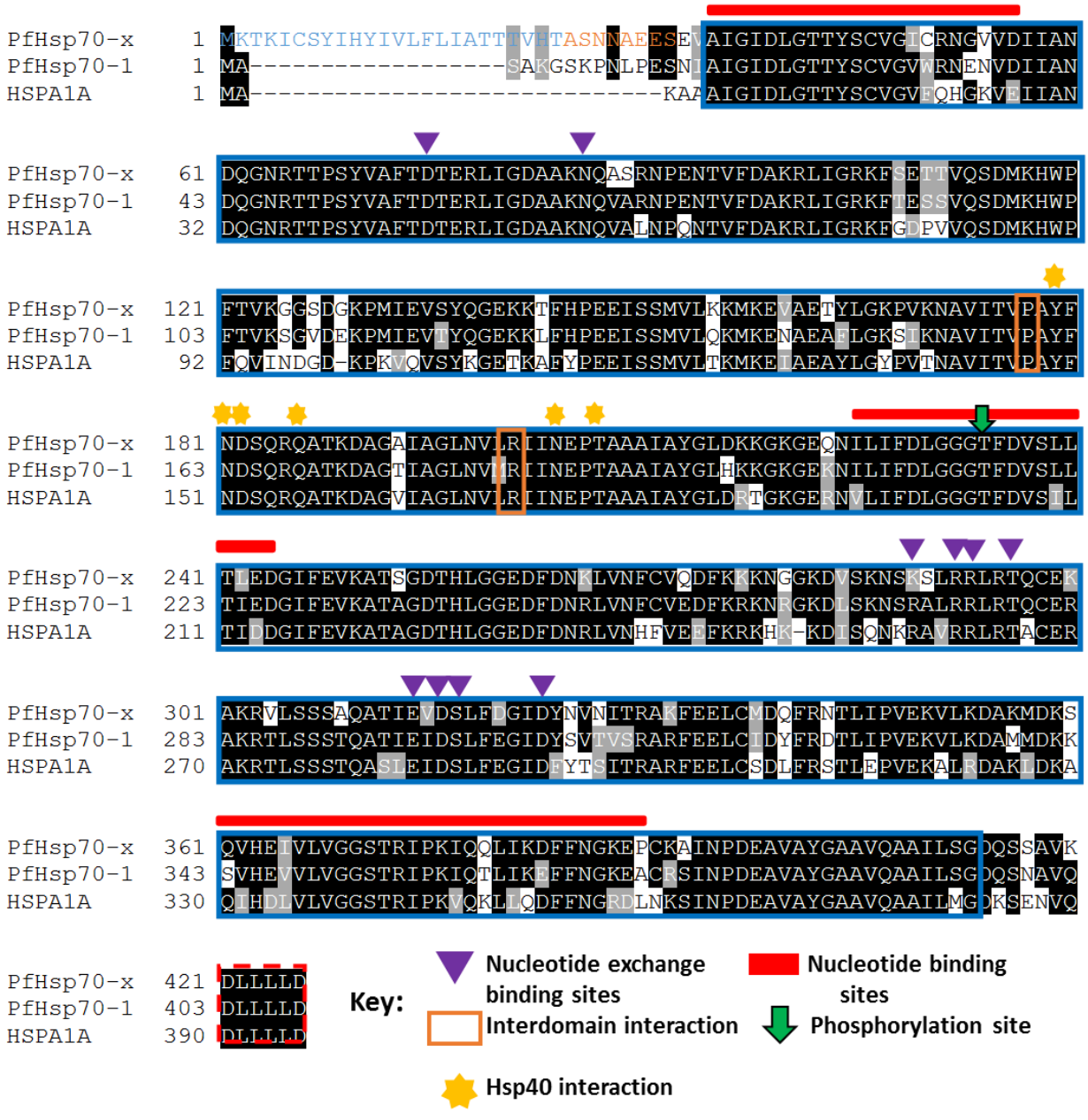

Figure A1. Multiple sequences alignment of nucleotide binding domain (NBD) Hsp70 homologues
Multiple sequence alignment of Hsp70 NBD of PfHsp70-x (PF3D7_0831700), PfHsp70-1 (PF3D7_0818900) and hHsp70 (NP_005336.3). PfHsp70-x N-terminal export signaling sequence (blue and orange letters) (Külzer *et al.*, 2012; Rhiel *et al.*, 2016). The white residues on black background represent identical residues; white on gray background represent similar residues while the black on white background show non-conserved residues. The MAFFT online ClustalW (http://www.ebi.ac.uk/Tools/msa/mafft/). The numbers on the left-hand side represent the position of the residues.

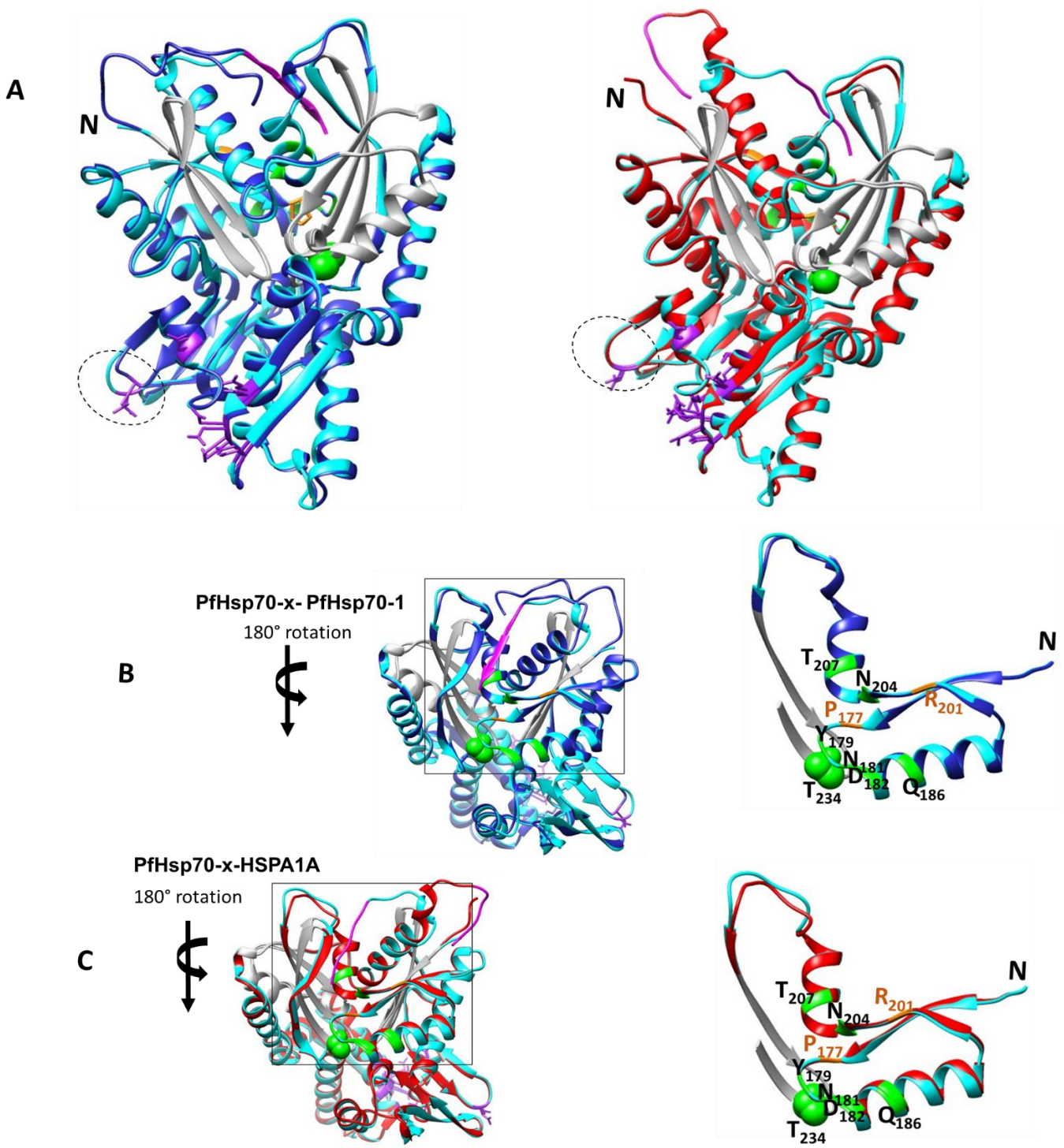

Figure A2. **Comparison of 3D models of the NBD of Hsp70 homologs**
Structural 3D models of the NBD of PfHsp70-x (cyan) was compared with that of PfHsp70-1 (medium blue) and hHsp70 (red). (**A**) The structural orientation and conformational differences in the ATPase activation and regulation of PfHsp70-x-PfHsp70-1 and PfHsp70-x-hHsp70. Sites implicated in nucleotide binding (grey) and phosphorylation (green sphere), NEF Bag2 binding (purple balls and sticks) and boxes show the linker. Hsp40 binding sites (green) and the phosphorylation site (green sphere) of (**B**) PfHsp70-x-PfHsp70-1 and (**C**) PfHsp70-x-hHsp70, boxes are zoomed in hsp40 binding sites. The models were generated by Phyre2 (www.sbg.bio.ic.ac.uk/phyre2) and visualized using Chimera (www.cgl.ucsf.edu/chimera; Pettersen *et al.,* 2004).

A2. The SBD sequences and 3D models of PfHsp70-x/PfHsp70-1/hHsp70

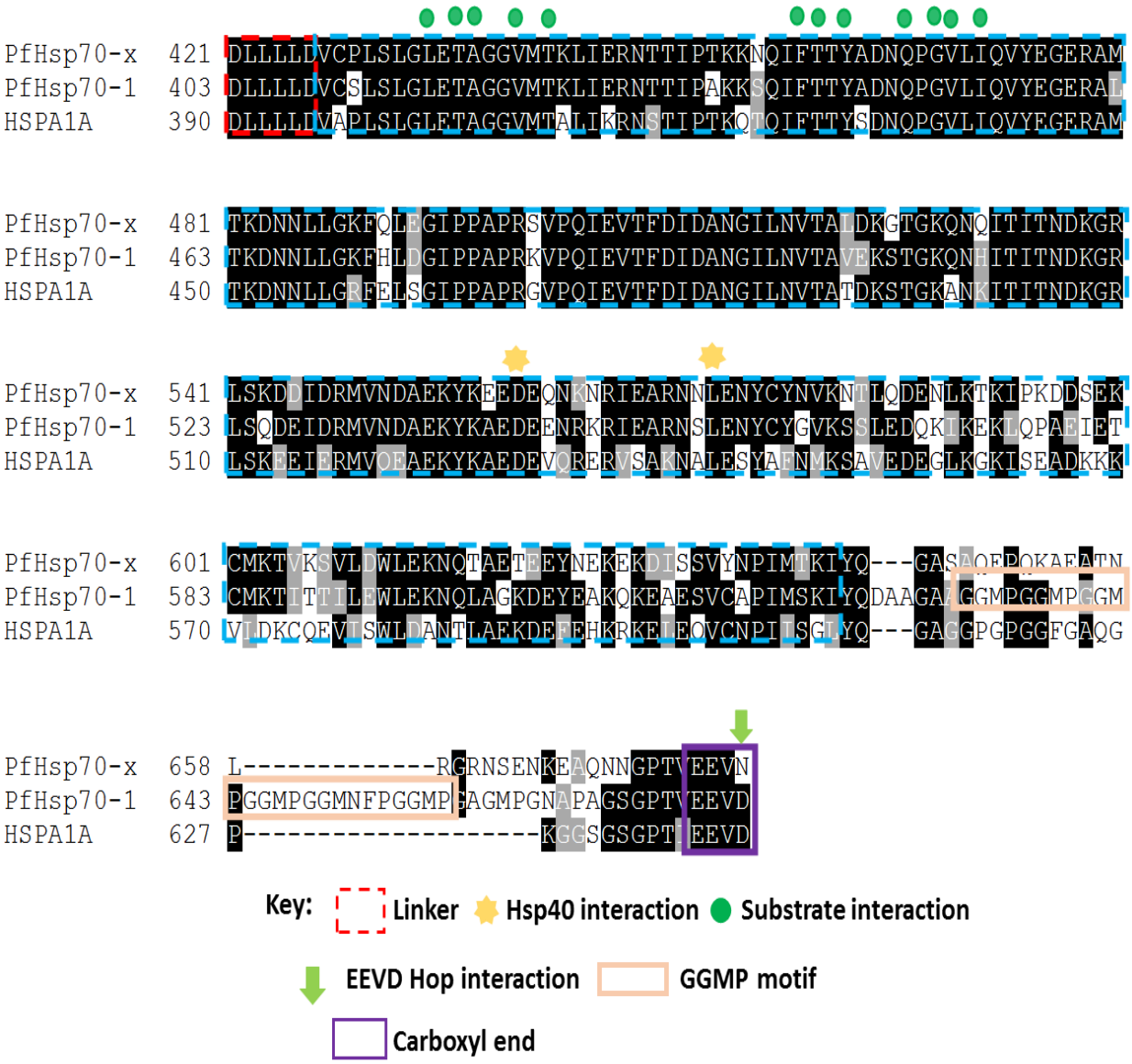

Figure A3. Multiple sequence alignment of substrate binding domain (SBD) Hsp70 homologues
Multiple sequence alignment of the SBD amino acid sequences of PfHsp70-x (PF3D7_0831700), PfHsp70-1 (PF3D7_0818900) and hHsp70 (NP_005336.3) were aligned, showing the linker, SBD and the carboxyl-terminal EEVD motifs with residues that interact with TPR domains, Hsp40s and substrate including the GGMP motif (Shonhai *et al.,* 2007). The regions of direct contact with substrates are highlighted including those that bind Hsp40. The white residues on black background represent identical residues; white on gray background represent similar residues while the black on white background show non-conserved residues. The MAFFT online ClustalW (http://www.ebi.ac.uk/Tools/msa/mafft/). The numbers on the left-hand side represent the position of the residues.

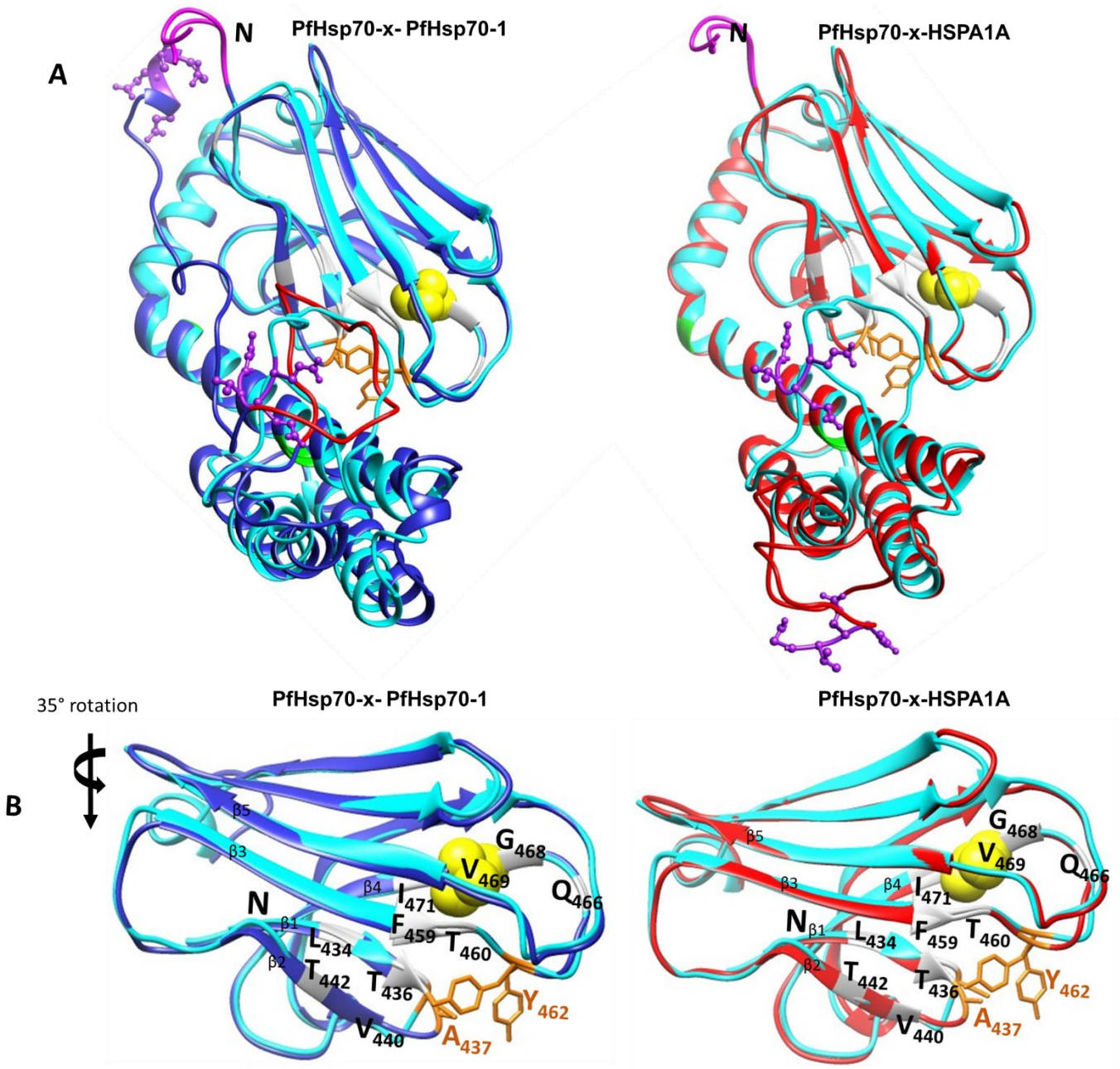

Figure A4. **Comparison of 3D models of the SBD of Hsp70 homologs**
The 3D models of PfHsp70-x was compared with that of PfHsp70-1 and hHsp70. (**A**) The structural orientation and conformational differences in the SBD of PfHsp70-x and PfHsp70-1 showing the substrate binding cavity and binding sites, Hsp40 binding site (green), the GGMP motif (red) and the carboxyl-terminal (purple ball and sticks). (**B**) The substrate binding cavity (β-sheets), hydrophilic pocket (yellow sphere), arch (orange) and substrate binding sites (grey) of PfHsp70-x-PfHsp70-1 and PfHsp70-x-hHsp70. The models were generated by Phyre2 (www.sbg.bio.ic.ac.uk/phyre2) and visualized using Chimera (www.cgl.ucsf.edu/chimera; Pettersen *et al.,* 2004).

A3. The amino acid sequences and 3D models of PfHop and hHop

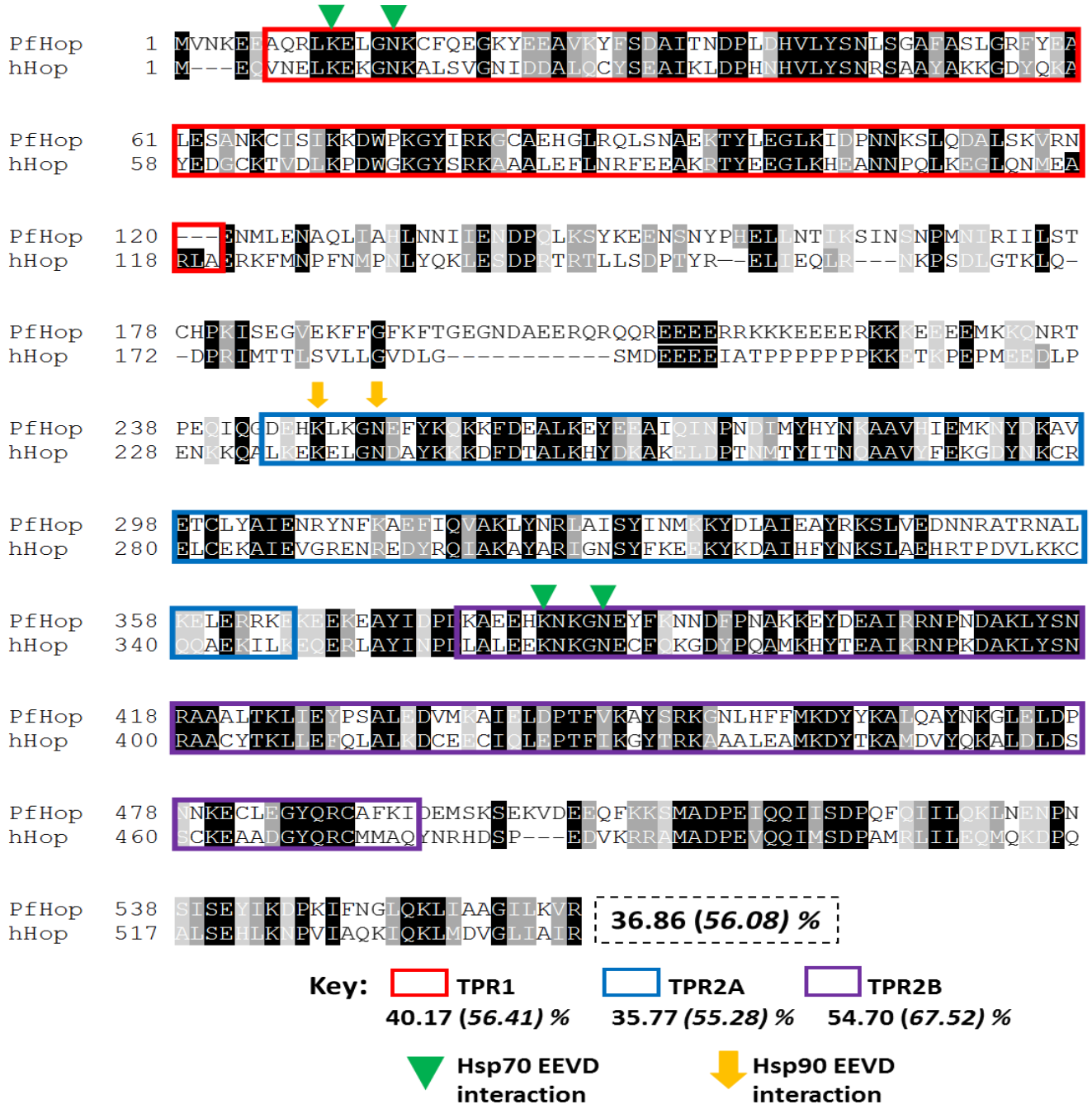

Figure A5. Pairwise sequence alignment of Hop homologues

Sequence alignment of Hop homologues, PfHop (PF3D7_1434300) and hHop (NCBI accession number; NP_006810.1) showing the TPR domains, respectively (Scheufler *et al.,* 2000, Gitau *et al.,* 2014). Residues for direct interaction of TPR1 with Hsp70, TPR2A with Hsp90 and TPR2B with Hsp70are highlighted (Gitau *et al.,* 2014). The numbers in brackets and italics represent the percentage identities between the proteins as well as their domain respectively, including their similarities. The white residues on black background represent identical residues; white on gray background represent similar residues while the black on white background show non-conserved residues. The MAFFT online ClustalW (http://www.ebi.ac.uk/Tools/msa/mafft/). The numbers on the left-hand side represent the position of the residues.

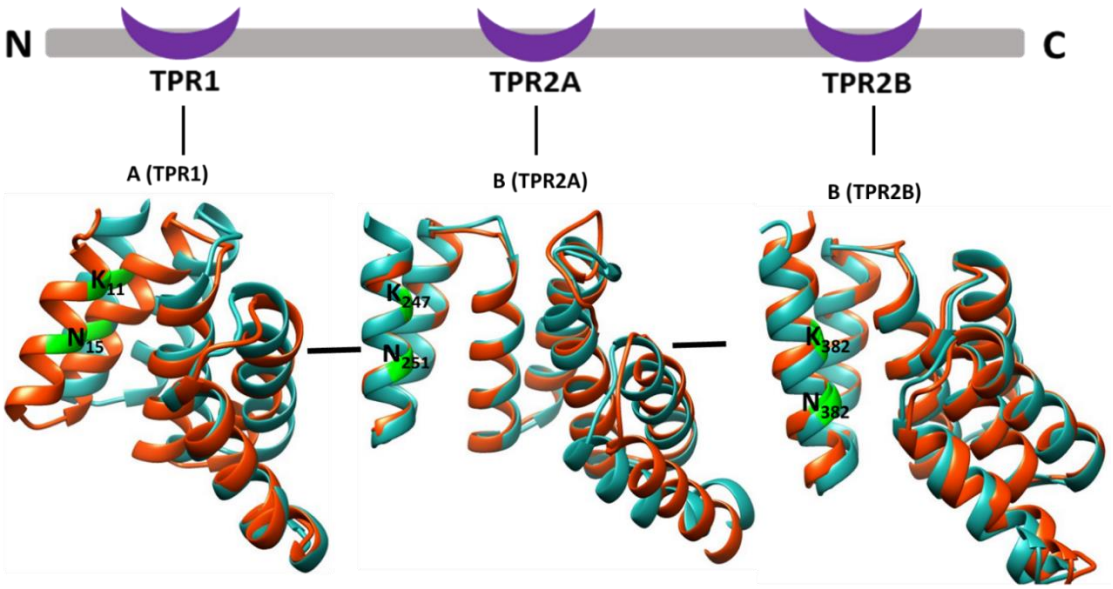

Figure A6. **Comparison of 3D models of Hop homologues**
The 3D models of PfHop (red) and hHop (light sea green) were compared. The models show the TPR domains of Hop homologs showing structural differences based on the folding orientation. (A) The KN sites of the TPR1, TPR2A and TPR2B are highlighted (green) that are involved in interaction with the carboxyl D residues of Hsp70 and Hsp90, respectively. The models were generated by Phyre2 (www.sbg.bio.ic.ac.uk/phyre2) and visualized using Chimera (www.cgl.ucsf.edu/chimera; Pettersen *et al.,* 2004).

A4. Bradford's assay standard curve

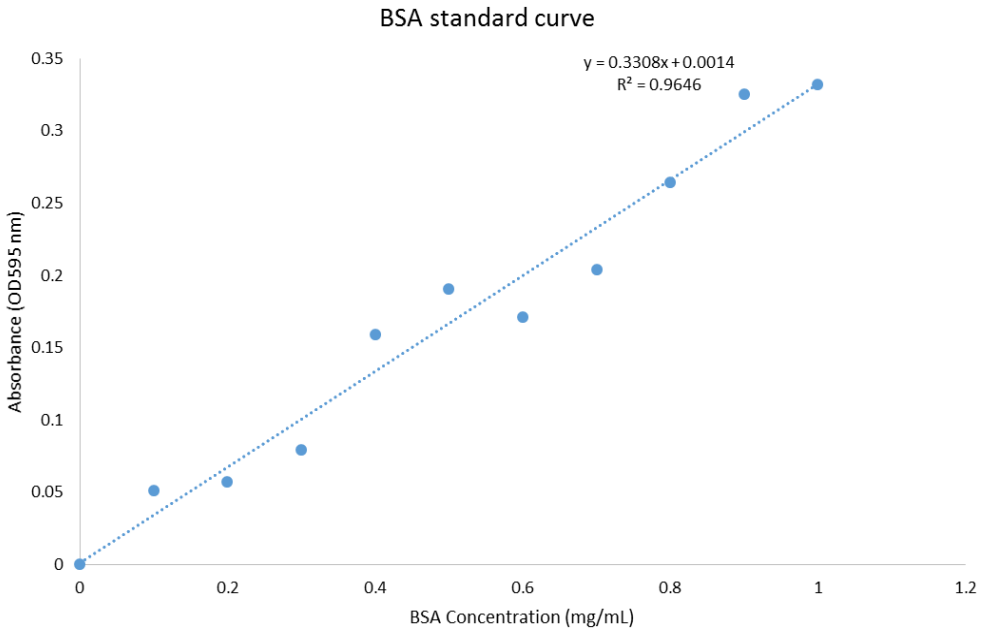

Figure C7. Brandford standard curve for protein concentration determination.
Bovine serum albumen (BSA) standards of concentration ranging from 0 to 1.0 mg/ml were prepared and absorbance was read at 595 nm using Spectramax M3 spectrometer. The linear equation: y = 0.3308x + 0.0014; R^2 = 0.9646 was used to calculate the protein concentration. The protein concentrations determined using Bradford's were confirmed using the Christoph-Leidig assay (Appendix B9).

A5. Interacting partners of PfHsp70-x

Table A5: The predicted chaperone functional interactors of PfHsp70-x

Protein PlasmoDB accession #	MW (KDa)	Protein description	Characterized localization	Scores/Reference
1. PF3D7_0708400	**86.16**	heat shock protein 90 (Hsp90)	cytosol	Zhang *et al.,* 2017; STRING
2. PF3D7_0113700	**46.98**	heat shock protein 40 (Hsp40), Type II	j-dots, membrane	Daniyan *et al.,* 2016; Jha *et al.,* 2017, STRING
3. PF3D7_0501100.1/2	**46.36**	heat shock protein 40 (Hsp40), Type II	j-dots, membrane	Zhang *et al.,* 2017; STRING
4. PF3D7_1232100	**81.48**	60 kDa chaperonin (CPN60)	cytosol	Zhang *et al.,* 2017; STRING
5. PF3D7_1015600	**62.55**	heat shock protein 60 (Hsp60), Chaperonin GroL	cytosol	Zhang *et al.,* 2017, STRING
6. PF3D7_1116800	**102.87**	heat shock protein 101 (Hsp101), ClpB2	PV/PVM	Charnuad *et al.,* 2017; Zhang *et al.,* 2017; STRING
7. PF3D7_1229500	**60.66**	T-complex protein 1 subunit gamma (CCT3)	cytosol	Zhang *et al.,* 2017,STRING
8. PF3D7_1357100	**48.95**	elongation factor 1-alpha	unknown	Zhang *et al.,* 2017, STRING
9. PF3D7_1015900	**48.67**	Enolase (ENO)	unknown	Zhang *et al.,* 2017; STRING
10. PF3D7_1436300	**112,40**	translocon component PTEX150	membrane	Charnuad *et al.,* 2017; Kulzer *et al.,* 2012
11. PF3D7_1471100	**33.41**	exported protein 2 (EXP2)	PVM	Charnuad *et al.,* 2017; Zhang *et al.,* 2017

The references are of reported interactions with PfHsp70-x (Charnuad *et al.,* 2017; Jha *et al.,* 2017; Külzer *et al.,* 2012; Zhang *et al.,* 2017).

A6. Direct interaction of PfHsp70-x with hHop using co-affinity chromatography

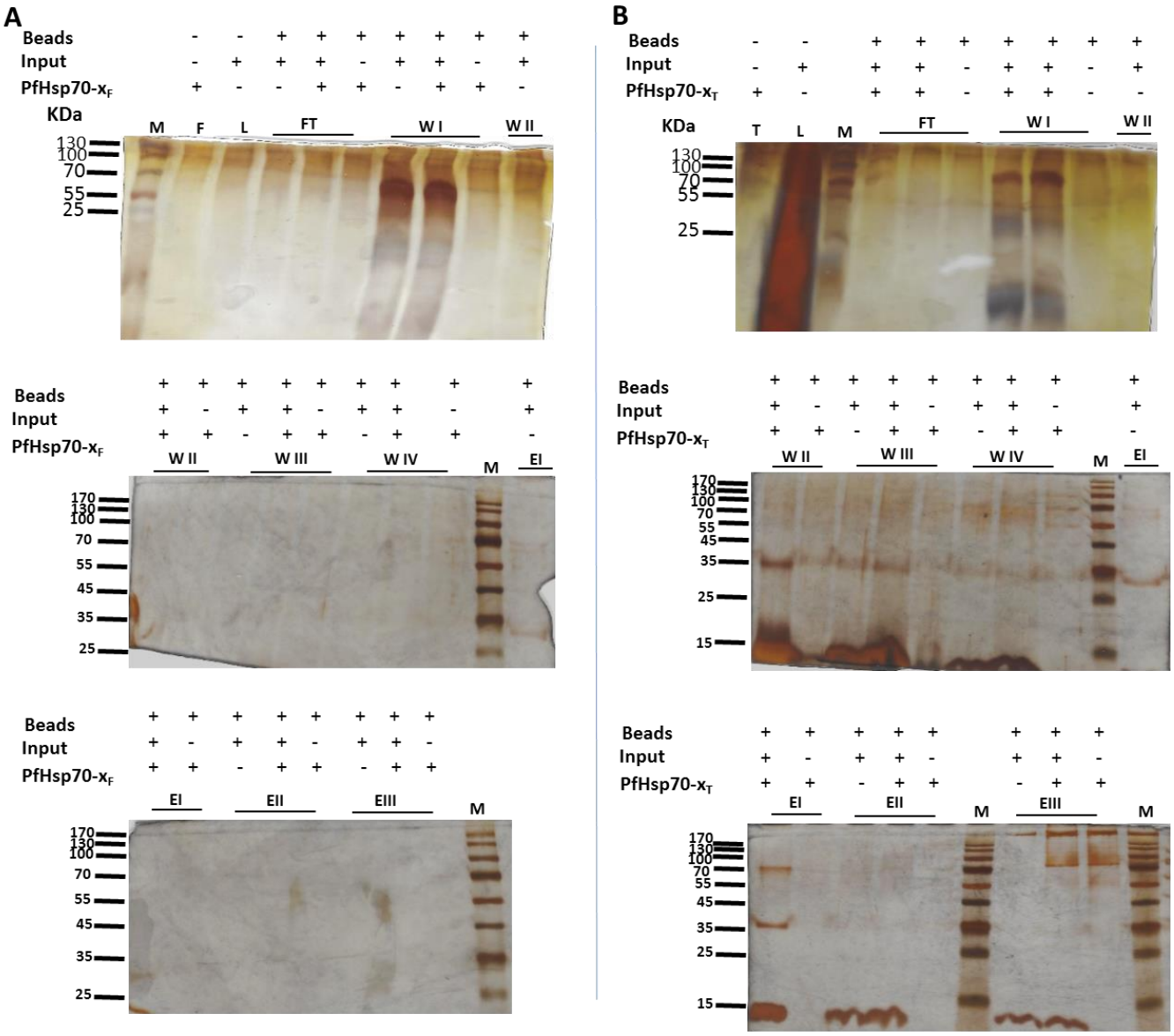

Figure A8: Investigating direct interaction of PfHsp70-x with hHop using co-affinity chromatography
Pulldown assay was conducted using recombinant full length PfHsp70-x (A) or truncated (EEVN minus) PfHsp70-x (B). Prey proteins in the cytosolic fraction of 3D7 parasite infected erythrocyte harvested from cultures grown under 37 °C. Prey protein was allowed to bind onto columns with recombinant PfHsp70-x proteins immobilized, respectively. The eluates were analyzed by silver staining. Lane M; marker, lanes F (full length) and T (truncated). Lane L is input, lane 2; beads without protein, lane 3; beads with antibody and input, lane 4; beads with input.

A7. Direct association of PfHsp70-x with hHop using immuno-affinity chromatography

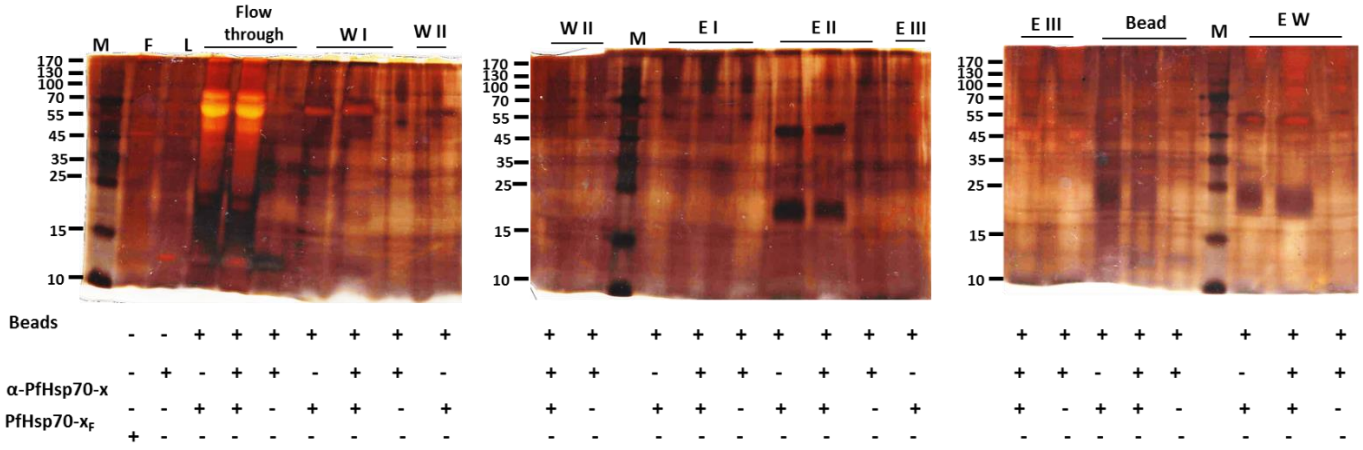

Figure A9: Investigating direct interaction of PfHsp70-x and hHop using immuno-affinity chromatography

Co-affinity chromatography was conducted from erythrocyte cytosolic fraction (input) harvested from cultures grown under normal temperature (37 °C) using antibodies against PfHsp70-x. The eluate and controls were analyzed by silver staining. Lane M; marker, F; PfHsp70-x, L; input, w; washes, E; elutions and EW; washes with water.

Appendix B: Methodolgy

B1. *E. coli* competent cells preparation

E. coli glycerol stocks of JM109 DE3 cells, XL1 blue cells and BL21 Star (DE3) cells were streaked on antibiotic free agar plates under flame. The flame conditions helps avoid contamination form aerobic microbial when using the continuous streaking method. The plates containing the cell lines were incubated for overnight at 37 ^{o}C. A single colony from the plate was picked, respectively, and transferred into 5 ml double strength yeast-tryptone broth (2 X YT media). The inoculum was allowed to grow in a shaking incubator at 37 ^{o}C for overnight. The overnight starter culture broth was transferred into 45 ml of fresh broth and incubated in an incubator at 37 ^{o}C shaking until absorbance was between 0.3 - 0.6 at optical density of 600 nm. The culture was collected in a 50 ml tubes and centrifuged at a speed of 5000 xg at a temperature of 4 ^{o}C for 10 minutes and the pellet was suspended on ice. The pellet cells were chemical treated with 10 ml of 0.1 M $MgCl_2$ to each tube and subsequent storage for 30 minutes on ice. The chemical suspension was centrifuged at 5000 xg at 4 ^{o}C for 10 minutes. The pelleted cells were resuspended with 10 ml 0.1 M $CaCl_2$ and incubated on ice for 5 hrs. The suspension mixture was centrifuged at 5000 xg at 4 ^{o}C for 10 minutes. The pellet was resuspended in 3 ml of 0.1 M $CaCl_2$ and 3 ml of 30 % glycerol and incubated on ice for 15 minutes. Following incubation, cell strains were aliquoted into labelled microcentrifuge tubes (eppendorf tube) and stored at -80 ^{o}C.

B2. Transformation into chemical competent cells

Competent cells from -80 ^{o}C freezer were retrieved and allowed to thaw on ice. PfHsp70x DNA was added into an eppendorf tube containing JM109 DE3 competent cells. pQE30 DNA was also added in a different tube as a positive control. Distilled water was added into another eppendorf tube as a negative control. The tubes were stored on ice for 30 minutes and heat shocked at 42 ^{o}C for 50 seconds. The tubes were placed back on ice and stored for 10 minutes. Pre-chilled broth was added into each eppendorf tube containing competent cells and DNA. The mixture was incubated for 1 hr at 37 ^{o}C with shacking at 100 rpm. The culture was streaked using a sterile cotton swab on the media plate containing 100ug/ml ampicillin. The plates were labelled and incubated for overnight at 37 ^{o}C.

B3. DNA extraction and restriction digestion analysis

Successful transformants were picked and inoculated into 2x YT broth containing ampicillin at final concentration of 100 µg/ml and incubated with shaking at 250 rpm at 37 ^{o}C. DNA extraction was done following the Zippy^{TM} Plasmid Miniprep kit (Zymo Research, USA) protocol. Briefly, the culture was added into a sterilized eppendorf tube and centrifuged for 60 seconds at 15000 xg. 7X lysis buffer from the kit was added and the solutions was thoroughly mixed and left to react for few minutes. The reaction was neutralized by adding neutralization buffer (yellow) and mixed thoroughly for complete neutralization. Once neutralized the mixture was centrifuged for 3 minutes at 15000 xg. The supernatant was carefully transferred into a Zymo-Spin^{TM} INN column to avoid disturbance of the cell debris in the pellet. The supernatant was collected by placing the column in the collection tube and centrifuged for 15 seconds. The flow through was decanted, and in the same collection tube, the column was washed with Endo-wash buffer. The column was extensively washed with Zyppy^{TM} wash buffer. The plasmid DNA was eluted with pre-warmed (50 ^{o}C) Zyppy^{TM} elution buffer in a sterile eppendorf tube. In order to confirm the DNA plasmid constructs, the plasmids were analyzed using restriction enzymes. The plasmid DNA were prepared as described in table below and analyzed on agarose gel electrophoresis.

Table B1: The samples will be prepared in this manner

Components	**Tube 1 Control (uncut)**	**Tube 2 *Bam* HI**	**Tube 3 *Hind* III**	**Tube 4 *Bam* HI & *Hind* III**
dH_2O	16 µl	15 µl	14 µl	13 µl
DNA	2 ng	2 ng	2 ng	2 ng
Buffer	2 µl	2 µl	2 µl	2 µl
R/Enzyme	--	1 µl	2 µl	2 µl & 1 µl
Loading dye	5 µl	5 µl	5 µl	5 µl

B4. Agarose gel electrophoresis

0.8 % agarose gel was prepared by dissolving 1.2 g in 150 ml TAE (1X) buffer, allowed to cool at room temperature. Once cooled, 10 µL of ethidium bromide was added and the gel contents were gently poured into the casting tray with a preplaced comb and allowed to solidify at room

temperature. The combs were removed from the solidified gel and the casting tray was placed in the electrophoresis chamber filled with TAE (1X) buffer.

B5. Solubility studies and purification of PfHsp70-x, hHop and hHsp70

Lysates were retrieved from the -80 ºC freezer and thawed on ice. 0.1 % (v/v) Polyethyleneimine (PEI) was added to the thawed lysate to solubilize any insoluble proteins. Additionally, PEI precipitates nucleic acids which may be protein-linked leaving the target protein in the supernatant. The lysate was sonicated and target protein was recovered in the supernatant by centrifugation at 5000 xg for 20 minutes at 4 ºC. The column was prepared using a small piece of cotton wool as a plug, and sterilized with 70 % ethanol. HisPur™ Nickel-charged nitrilotriacetic acid (Ni-NTA) (IMAC) beads (Thermo Scientific, USA) were added to the column, followed by the addition of distilled water to wash of the ethanol. The beads were equilibrated with lysis buffer. The supernatant was loaded onto the prepared HisPur™ Ni-NTA column and incubated at 4 ºC for four hours to allow binding of the His-recombinant proteins (PfHsp70-x/hHop/hHsp70) in the soluble cell extract. The supernatant was run through the column with the flow through being collected for analysis. The unbound proteins in the column were washed with wash buffer 1 (10 mM Tris pH 7.5; 300 mM NaCl, 1 mM EDTA and 25 mM Imidazole containing 1 mM PMSF) followed by wash buffer 2 (10 mM Tris pH 7.5; 300 mM NaCl, 1 mM EDTA and 80mM Imidazole containing 1 mM PMSF). The proteins bound to the column were then eluted with of elution buffer 1 (10 mM Tris pH 7.5; 300 mM NaCl, 1 mM EDTA and 250 mM Imidazole containing 1 mM PMSF), followed by elution buffer 2 (10 mM Tris pH 7.5; 300 mM NaCl, 1 mM EDTA and 500 mM Imidazole containing 1 mM PMSF). The washes and elutions were collected and prepared for SDS-PAGE and Western blot analysis including beads.

B6. Preparation of 12 % of sodium dodecyl sulphate-polyacrylamide resolving gel electrophoresis (SDS-PAGE) analysis

Running Gel	X 1	X 2	X 3	X 4	Stacking Gel	X 1	X 2	X 3	X 4
Bis (ml)	2.08	4.16	6.24	8.32	**Bis (ml)**	0.235	0.47	0.705	0.94
Tris pH 8.8 (ml)	1.25	2.5	3.75	5.0	**Tris pH 6.8 (ml)**	0.437	0.875	1.312	1.748
10 % SDS (ml)	0.05	0.1	0.15	0.2	**10 % SDS (ml)**	0.0175	0.035	0.0525	0.07
H_2O (ml)	1.58	3.16	4.74	6.37	**H_2O (ml)**	1.05	2.1	3.15	4.2
APS (ml)	0.025	0.050	0.075	0.1	**APS (ml)**	0.00875	0.017	0.026	0.03
TEMED (µl)	20	20	20	20	**TEMED (µl)**	20	20	20	20

B7. Concentration of proteins

The proteins were extensively dialyzed and concentrated using the Amicon® Ultra-15 10K centrifuge filter device (Merck, Germany) and dialysis buffer (300 mM NaCl, 10 mM Imidazole, 10 mM Tris-HCl, pH 7.5, glycerol 10 % (v/v), containing 1 mM PMSF) as previously described in Section 2.3.5. The recombinant proteins were subsequently concentrated with PEG (polyethyleneglycol) for 30 minutes and pipetted out of the tubing and stored at -20 ^{o}C. The eluted proteins was evaluated for purity using SDS-PAGE and further confirmed using various sets of antibodies by Western blotting (Appendix B10).

B8. Recombinant protein quantification using Bradford's assay

The Bradford assay (Sigma-Aldrich, USA), a method that uses the Bradford reagent to estimates the concentrate proteins at 595 nm absorption, was used. The assay was conducted using bovine serum albumin (BSA) protein as a standard following manufacturer's instructions. The assay is based on the association the dye, Brilliant Blue G, and the proteins in solution. Protein standards were prepared ranging from a concentration of BSA ranging from 0.1 – 1.4 mg/ml on a 96 well plate in individual wells. The Bradford's reagent was mixed with the protein standards. PBS buffer (137 mM NaCl, 27 mM KCl, 4.3 mM Na_2HPO_4 and 1.4

mM KH_2PO_4) was used as blank and added in the blanking wells. The protein sample(s) with the concentration ranging from approximately 0.1 – 1.4 mg/ml were prepared, mixed with Bradford's Reagent and incubated for approximately 30 seconds with shaking. The mixture was incubated for 5 – 45 minutes at room temperature followed by measuring the absorbance at 595 nm. The values of the BSA standard curve were compared with the absorbance of the protein to determine the range in which the protein fall in. To further confirmed the concentration of the protein the Christoph-leidig equation (Appendix B9) was used to calculate the concentration of the protein.

B9. Protein quantification using Christoph-leidig webtool

The concentrations of the proteins wwre determined as described by Zininga (2015) using webtool (http://christophleidig.de/tprot.html) with the formula below:

$A = c \times d \times \varepsilon$ ……Equation (1)

$m = n \times M$ ……Equation (2)

Where A= Absorbance at 280 nm

C= concentration (in mol/l)

D= cuvette length in (cm)

ε= extinction coefficient (in L/mol x cm)

m= mass (in g)

n= quantity (in mol)

M= molecular unit (in g/mol)

B10. Immunoblotting (Western blotting)

The expressed and purified proteins were resolved by 12 % SDS-PAGE as described above (Appendix B6). The SDS-PAGE gel was removed from the glass plates after completion of electrophoresis. The stacking gel was cut off to only leave the running gel. The gel, Whatman filter papers, two scotchbrite fibre pads and nitrocellulose/ immobilon®-P transfer membrane were immersed in Western transfer buffer and left to equilibrate at 8 °C for 30 minutes. The gel was prepared for transfer in a sandwich as follows: the filter paper was placed on a

scotchbrite pad; followed by the gel ensuring that there is no trapped air bubbles; nitrocellulose membrane was placed over the gel; followed by another filter paper on the membrane and another scotchbrite pad. The proteins were transferred to the nitrocellulose membrane at 100 volts for 1 hr. After transfer, the blot was removed from the sandwich, rinsed using the transfer buffer and stained with Ponceau stain to determine if transfer was successful followed by visualizing the band using chemiluminescence. The blot was washed off of the stain using TBS-Tween (TBST) and blocked for 1 hr in 10 ml of non-fat milk (5 %) in TBS on a rotary shaker set at 1 rpm. The membrane was washed 3 times for 10 minutes in TBST, followed by a 1 hr incubation with primary antibody. The unbound primary antibody was washed off the membrane 3 times, for each wash, 10 minutes with TBST. Following washes, the blot was incubated with the secondary antibody for 1 hr and washed 3 times using TBST.

B11. SDS-PAGE for silver stain analysis

The SDS-PAGE gel is removed cautiously from the gel casting plates and placed into the staining tray. The Pierce® Silver Stain Kit (Thermo Scientific, USA) was used for silver stain analysis of the SDS-PAGE gel using protocol as described by the manufacturer as follows:

1. The gel was wash for 5 minutes in ultrapure water. The water was replaced and washed for another 5 minutes.
2. After washing, the gel was fix in a solution of 30 % ethanol: 10 % acetic acid for 15 minutes. The fixing solution was replaced and fixed the gel for another 15 minutes.
3. Following fixing, the gel was wash for 5 minutes with 10 % ethanol. The ethanol solution was replaced and gel was washed for another 5 minutes.
4. The gel was washed for 5 minutes with ultrapure water. The water was replaced and washed for another 5 minutes.
5. The Sensitizer Working Solution was prepared by mixing 1 part of Silver Stain Sensitizer with 500 parts of ultrapure water.
6. After washes, the gel was incubated for exactly 1 minute in Sensitizer Working Solution, and then washed with 2 changes of ultrapure water for 1 minute each.
7. The Stain Working Solution was prepared by mixing 1 part of Silver Stain Enhancer with 50 parts of Silver Stain.
8. The gel was stained by incubating for 30 minutes in Stain Working Solution.

9. The Developer Working Solution was prepared by mixing 1 part of Silver Stain Enhancer with 50 parts of Silver Stain Developer.
10. The Stop Solution of 5 % acetic acid was prepare.
11. The gel was quickly wash with 2 changes of ultrapure water for 20 seconds each.
12. Immediately after washing, the Developer Working Solution (Step 9) was added onto the gel. The gel was incubated until the desired protein bands appeared (2 - 5 minutes).
13. Once the desired level of intensity was observed, the Developer Working Solution was replaced with the prepared Stop Solution (5 % acetic acid; Step 10).
14. The gel was washed with Stop Solution briefly. The Stop Solution was replaced and incubated for 10 minutes.

Appendix C: Additional materials

Table C1. Special chemical reagents

Name of reagents	Supplier
Acetic acid	Merck, Germany
Adenosine triphosphate (ATP)	Sigma-Aldrich, USA
Agarose	Merck, Germany
Ammonium persulphate	Sigma-Aldrich, USA
Ampicillin	Melford, UK
Bovine serum albumin	Melford, UK
Bromophenol blue	Merck, Germany
Calcium chloride	Merck, Germany
Chemiluminescence Western blotting kit	Amersham, USA
Nitrocellulose membrane	Thermo Scientific, USA
Immobilon®-P transfer Membrane	Merck, Germany
Coomasie brilliant blue R250	Merck, Germany
Ethidium bromide	Merck, Germany
Glacial acetic acid	Merck, Germany
Glycerol	Merck, Germany
Glycine	Merck, Germany
Glucose	Merck, Germany
Imidazole	Merck, Germany
Isopropyl-1-thio-D-galacopyranoside	Sigma-Aldrich, USA
GeneRuler 1 Kb DNA ladder	Thermo Scientific, USA
Lysozyme	Merck, Germany
Magnesium chloride	Merck, Germany
Methanol	Merck, Germany
Ni-chelating sepharose	Amersham, USA
Phenylmethylsufonyl fluoride	Merck, Germany
Polyacrylamide	Merck, Germany
Ponceau S	Sigma-Aldrich, USA
Restriction enzymes	Thermo Scientific, USA
Amicon® Ultra-15 10K centrifuge filter device	Merck, Germany
Snakeskin™ pleated dialysis tubing	Thermo Scientific, USA
Sodium chloride	Merck, Germany
Sodium dodecyl sulphate	Merck, Germany

Sodium hydroxide	Merck, Germany
TEMED	Sigma-Aldrich, USA
Tris-HCl	Merck, Germany
Tryptone	Oxoid, England
Tween 20	Melford, UK
Yeast	Merck, Germany
Page ruler prestained protein ladder	Thermo Scientific, USA
Nutrient agar	Merck, Germany